

Oxidative Addition of Amino Acids and Other Biologically Interesting Molecules to an Iridium Metal Center

By
Christopher P. Roy

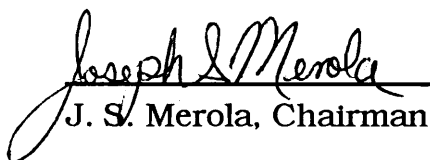
Dissertation submitted to the Faculty of the
Virginia Polytechnic Institute and State University
in partial fulfillment of the requirements for the degree of

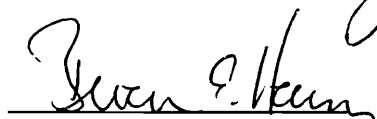
Doctor of Philosophy

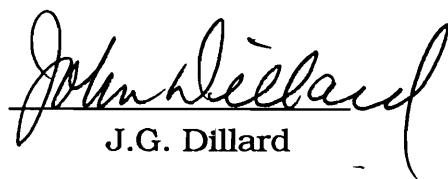
in

Chemistry

APPROVED


J. S. Merola, Chairman


B. E. Hanson


J.G. Dillard


M. R. Anderson


H.W. Gibson

October, 1993
Blacksburg, Virginia

**Oxidative Addition of Amino Acids and Other
Biologically Interesting Molecules to an Iridium
Metal Center**

By

Christopher P. Roy

Joseph S. Merola, Committee Chairman

Department of Chemistry

(ABSTRACT)

The oxidative addition of amino acids and other biologically interesting molecules to iridium(I) complexes was studied and the reactivity of the resulting hydrido chelate complexes was investigated. Oxidative addition of amino acids to $[\text{Ir}(\text{COD})(\text{PMe}_3)_3]\text{Cl}$ resulted in the formation of meridional tris trimethylphosphine Ir(III) hydride complexes, with the amino acid chelated to the metal center forming 5 membered rings. The majority of the naturally occurring amino acids were studied as potential oxidative addition reactants. The amino acids with reactive side chains did not form clean products. The amino acids without reactive side chains did form clean products which were characterized by ^1H NMR, ^{31}P NMR, ^{13}C NMR spectroscopy, C,H analyses, and single crystal X-ray diffraction. The studies went on to investigate other α amino acid compounds and attempts were made to form 6 membered ring complexes with β amino acids. The reactivity of these complexes was also studied. A number of reaction conditions were used in attempts to induce

the iridium amino acid complexes and various unsaturates, but the stability of the 5 membered ring system did not allow for insertion of unsaturates.

An attempt was made to synthesize coordinately unsaturated complexes of iridium with amino acids. A variety of reactions were tried with the coordinately unsaturated compound, $[\text{Ir}(\text{COD})(\text{DMPE})]\text{Cl}$, but amino acid products were not produced in these reactions. Rather, an interesting rearrangement product of $[\text{Ir}(\text{COD})(\text{DMPE})]\text{Cl}$ was formed and the crystal structure of $[\text{Ir}(\mu^1, \mu^3 - \text{COD})\text{DMPE}]\text{Cl}$ complex was solved. Other attempts to induce reactivity of hydrido amino acid - Ir complexes involved synthesizing N-methyl amino acid complexes. The treatment of $[\text{Ir}(\text{COD})(\text{PMe}_3)_3]\text{Cl}$ with N-methylphenylalanine or N-methylglycine formed the respective chelate hydrido complexes. The reactivity studies of these complexes were negative.

The insertion of an unsaturate was observed with 2-amino-4-pentenoic acid. This compound is an α -amino acid with a tethered olefin and when treated with $[\text{Ir}(\text{COD})(\text{PMe}_3)_3]\text{Cl}$ binds through three sites (O, N, C) to the metal center. The Ir-C bond formed supports the fact that the olefin has inserted into the Ir-H bond. The crystal structure of this complex was solved.

Several amino acid iridium complexes were tested for biological activity in NCI cancer and HIV assays. The complexes had no activity against cancer, but the phenylalanine complex did show moderate activity against HIV. The results prompted studies with other biologically

interesting molecules and a number of sulfur containing compounds were studied.

The formation of 4 membered ring systems was observed resulting from reactions of thiourea and analogs with $[\text{Ir}(\text{COD})(\text{PMe}_3)_3]\text{Cl}$. These compounds are to be studied for their reactivity with unsaturates.

*This dissertation is dedicated to my parents, who have been my so
supportive over all the years;
to my brothers (Bruce and Tom), who have been my idols all my
life and in trying to be like them, has made me who I am;
to my wife Janik, whose love and support have been my
strength;
and to God, for all the people He has touched my life with.*

Acknowledgements

I have to start with my advisor, Dr. Joseph Merola, he put up with me on road trips to ACS meetings, and all he asked was that I laugh at his jokes! I think I had it tougher. No, really, I have to thank Dr. Merola; he has been a good friend over the years and I have enjoyed working for him. (No, I'm not just saying it.) Dr. Brian Hanson for all that he has done. (and for having Rob Harris as a student, so I could share the grief.) Dr. Jim Tanko, never would have made it through the proposal without him. Dr. Mark Anderson , Dr. John Dillard and Dr. Harry Gibson for rounding out my committee. Special thanks go to Dr. Gibson for giving me someone my speed to guard in basketball.

All the people who have come and gone while I've been at Tech, Fola Ladipo, Joe Knorr, Hank Selnau, Trang Le and Kelly Matthews are all previous members of the Merola gang and made me smile when they were here. Rob Harris, Art Grieb, Rob Pafford, all the people in the "Merola, Hanson and Brewer groups" Yeah, thanks for all the chats Dr. Karen Brewer.

And finally my contemporaries, John Rimoldi, Carl Heltzel, Matt Sheridan, Kurt Neidigh, these guys have gone through it with me and we have cried and laughed together, and sometimes asked each other which one of those things we should do when we were clueless.

Table of Contents

Chapter 1. Literature Review	1
1.1 Intent of Thesis.....	1
1.2 Biological Importance of Metals.....	1
1.3 N-H Additions to Unsaturation.....	2
1.4 O-H Additions to Unsaturation.....	5
1.5 Biological Interest in Amino Acid Complexes.....	7
1.6 Ruthenium and Osmium Amino Acid Complexes.....	8
1.7 Platinum and Palladium Amino Acid Complexes.....	15
1.8 Rhodium and Iridium Amino Acid Complexes.....	30
1.9 References.....	35
Chapter 2. Oxidative Addition of Amino Acids.....	43
2.1 Introduction.....	43
2.2 Results and Discussion.....	44
2.2.1 References.....	75
2.2.2 Experimental.....	77
Chapter 3. Reactivity Studies of Oxidative Addition Products.....	103
3.1 Introduction.....	103
3.2 Results and Discussion.....	105
3.2.1 Experimental.....	112
3.2.2 Alternative Strategies to Amino acid reactivity.....	117
3.2.3 Experimental.....	124
3.2.4 N-substituted Amino Acids.....	129
3.2.5 Experimental.....	131
3.2.6 Reactivity Studies Exchange Reactions.....	136
3.2.7 Experimental.....	139
3.2.8 Insertion Reaction with 2-Amino-4-pentenoic acid.....	142
3.2.9 Experimental.....	149
3.3 Biological Assay Studies.....	152
3.4 References.....	157
Chapter 4. Oxidative Addition of Biologically interesting molecules....	158
4.1 Introduction.....	158
4.2 Results and Discussion.....	158
4.2.1 Experimental.....	166

4.3 References.....	172
Chapter 5. Conclusions and Future Goals.....	173
5.1 Conclusion.....	173
5.2 Future Goals.....	175
APPENDIX: X-ray Crystallographic Data.....	178
VITA.....	210

List of Illustrations

Figure 1.1	Possible Isomers of the enol ester.....	6
Figure 1.2	Cisplatin.....	8
Figure 1.3	Ruthenium tetrammine glycinate complex.....	8
Figure 1.4	Monodentate binding of histidine.....	11
Figure 1.5	Ruthenium bis amino acid complex.....	12
Figure 1.6	Schiff base complexes.....	12
Figure 1.7	C ₆ H ₆ -Ruthenium amino acid complex.....	13
Figure 1.8	C ₆ H ₆ -Ruthenium proline complex.....	14
Figure 1.9	Amino Acids with sulfur in side chain.....	17
Figure 1.10	Binding through S donor of amino acid.....	18
Figure 1.11	Palladium bis-methionine complex.....	19
Figure 1.12	Zwitterionic character of [Pd(NH ₃) ₂ (metH) ₂]Cl.....	19
Figure 1.13	Sulfur and nitrogen donation of cysteine.....	20
Figure 1.14	Nitrogen and oxygen donation to palladium.....	21
Figure 1.15	Ornithine.....	22
Figure 1.16	Twisted chair conformation of ornithine Pd complex.....	23
Figure 1.17	Histidine.....	23
Figure 1.18	Apical coordination of tyrosine.....	24
Figure 1.19	Palladium bis-serine complex.....	25
Figure 1.20	Facial arrangement of Pt(IV) complexes.....	27
Figure 1.21	[(NH ₃) ₅ (gly)Rh(III)] ion.....	31
Figure 1.22	Sulfur and nitrogen coordination to rhodium.....	31
Figure 1.23	Dimeric species of rhodium carbonyl.....	32
Figure 1.24	Monomeric species of rhodium carbonyl.....	32
Figure 2.1	[Ir(COD)(PMe ₃) ₃]Cl.....	43
Figure 2.2	General Structure of amino acids.....	44
Figure 2.3	Zwitterionic form of glycine.....	47
Figure 2.4	Initial ¹ H NMR spectrum glycine and [Ir(COD)(PMe ₃) ₃]Cl...48	48
Figure 2.5	Final ¹ H NMR spectrum glycine and [Ir(COD)(PMe ₃) ₃]Cl....51	51
Figure 2.6	Proposed amino acid iridium complex.....	52
Figure 2.7	Phosphorus NMR of iridium glycine complex.....	54
Figure 2.8	Carbon NMR of iridium glycine complex.....	55
Figure 2.9	Valine structure.....	56
Figure 2.10	Initial ¹ H NMR spectrum valine and [Ir(COD)(PMe ₃) ₃]Cl..57	57
Figure 2.11	Final ¹ H NMR spectrum valine and [Ir(COD)(PMe ₃) ₃]Cl....58	58

Figure 2.12 Proposed structure of valine iridium complex.....	60
Figure 2.13 X-ray crystal structure of [Ir(val)(H)(PMe ₃) ₃]PF ₆	62
Figure 2.14 Proline.....	63
Figure 2.15 Proposed structure of proline complex.....	64
Figure 2.16 X-ray crystal structure of [Ir(pro)(H)(PMe ₃) ₃]PF ₆	66
Figure 2.17 General structure of amino acid complexes.....	67
Figure 2.18 Methionine.....	68
Figure 2.19 Methionine chelate complex with palladium.....	69
Figure 2.20 Cysteine.....	70
Figure 2.21 Asparagine and aspartic acid.....	70
Figure 2.22 β-alanine.....	72
Figure 2.23 Palladium histidine complex.....	73
Figure 3.1 Water soluble unsaturates.....	111
Figure 3.2 Proposed formation of amino acid unsaturated complex...	118
Figure 3.3 Rearrangement of [Ir(COD)(DMPE)]Cl.....	122
Figure 3.4 X-ray crystal structure of rearranged COD product.....	123
Figure 3.5 Literature example of rearranged COD product.....	124
Figure 3.6 Amino acid with tethered olefin.....	142
Figure 3.7 Carbon NMR of 2-amino-4-pentenoic acid product.....	144
Figure 3.8 X-ray crystal structure of tridentate complex.....	146
Figure 3.3.1 Graph of Biological assay with phenylalanine complex....	155
Figure 3.3.2 Graph of Biological assay with tyrosine complex.....	156
Figure 4.1 Urea.....	159
Figure 4.2 X-ray crystal structure of thiourea complex.....	162
Figure 4.3 Sulfur containing compounds used in study.....	163
Figure 4.4 X-ray crystal structure of thioacetamide complex.....	165

List of Schemes

Scheme 1.1 Amino acid amination of olefin.....	3
Scheme 1.2 Nucleophilic attack of free amine on bound olefin.....	4
Scheme 1.3 Oxidative addition / Reductive elimination.....	5
Scheme 1.4 Nucleophilic attack of bound carbonyl.....	9
Scheme 1.5 Monodentate to bidentate binding of amino acids.....	26
Scheme 1.6 Results of study by Beck et al.....	34
Scheme 3.1 Proposed pathway for formation of esters.....	104
Scheme 3.2 Formation of ester product from reductive elimination.....	109

List of Tables

Table 2.1 Amino acids attempted and characterized.....68

Chapter 1. Literature Review

1.1 Intent of Thesis

The interaction of amino acids with metal centers is of importance not only from a biological point of view, but from the point of view of possible catalytic uses of the resulting complexes. The ability to form new organic fragments by reductively eliminating ligands from a metal center is an area of interest, as well as the use of the organometallic complexes as catalysts in hydrogenation of unsaturates. The intent of this research is to study the complexes resulting from the oxidative addition of amino acids and other biologically interesting molecules to iridium. Then, the reactivity of these complexes towards unsaturates is studied with a goal of developing catalytic activity. Finally, the biological activity of these complexes is explored.

1.2 Biological Importance of Metals

Metals play an important role in biological systems. The 1st row transition metals are involved in a variety of biochemical systems including oxygen transport, oxygen storage, electron transfer, and are also important in a variety of metalloenzymes¹. After the 1st row, excluding molybdenum in nitrogenase, bioinorganic systems do not utilize the second and third row transition elements in nature. This leads one to speculate on the biological chemistry of these heavier elements. The heavier metallic elements do attract a great deal of attention when it comes to biological activity due to their toxic effect on

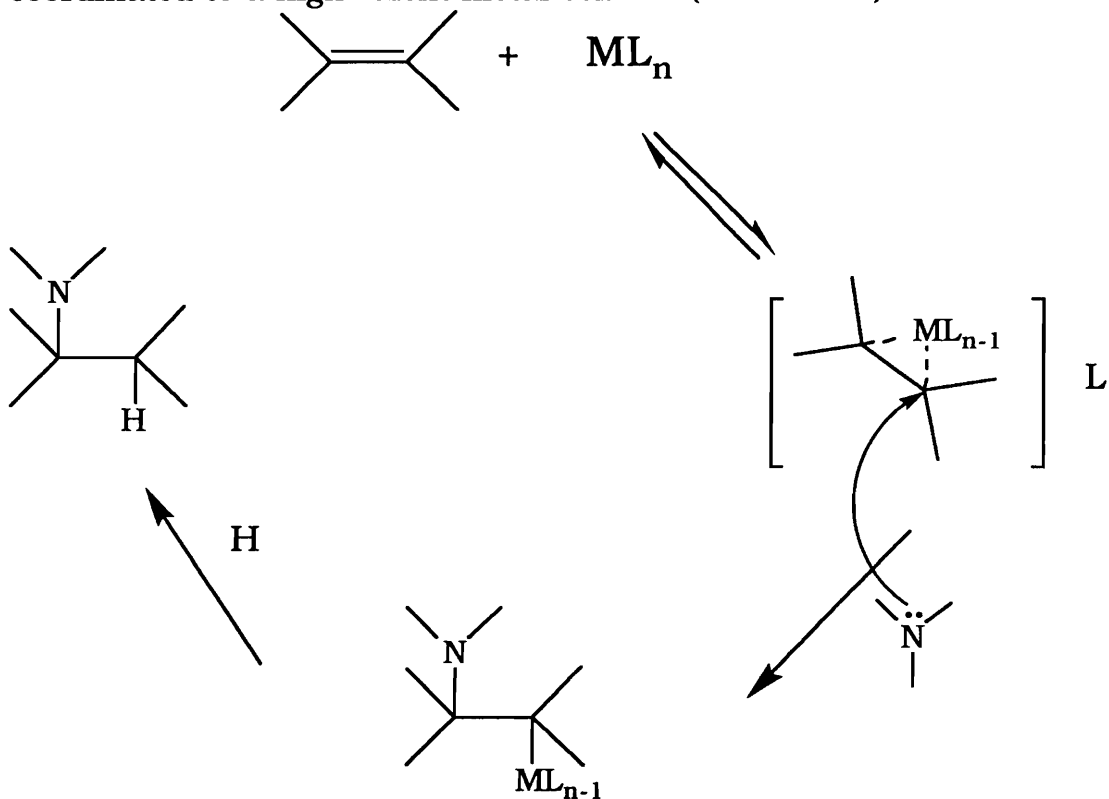
many organisms. The most notable of the toxic effects is the use of the platinum complex, cisplatin, $\text{Pt}(\text{NH}_3)_2(\text{Cl})_2$ as an anti-tumor agent. Cisplatin has had tremendous success in treating certain varieties of tumors.² This success has led to much interest in trying to understand the interaction of cisplatin and other platinum complexes with biological systems, in particular, the interaction with DNA.

There is actually very little known about the biological chemistry of the other platinum metals. This thesis deals with the chemistry of iridium, and the literature contains very little on the reactivity of iridium complexes with molecules of biological importance. Thus a goal of this thesis will be the determination of the biological importance of the iridium complexes.

1.3 N-H Additions to Unsaturation

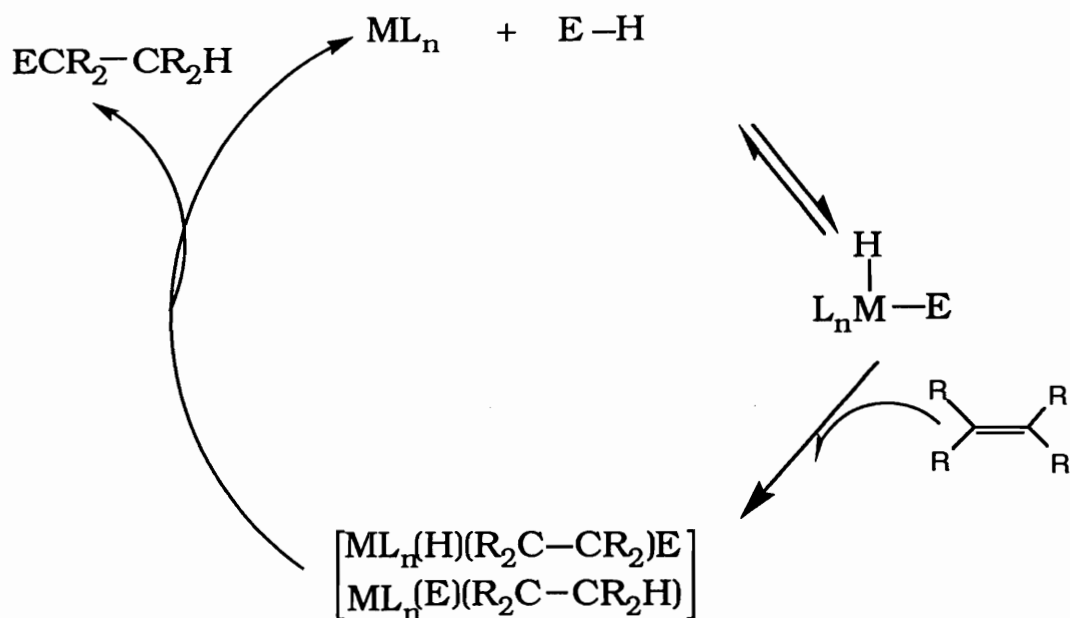
Another extremely important focus of the oxidative addition of amino acids to a metal center is the use of these complexes as catalysts for the amination and esterification of unsaturates. The work to be discussed in this thesis was preceded by that of Dr. Fola T. Ladipo who demonstrated that compounds with N-H and O-H functionalities could oxidatively add to iridium (equations 1.1 and 1.2).

substantial excess. The use of a transition metal to promote amination is based on nucleophilic attack of a free amine on the olefin which is coordinated to a high valent metal center.⁵ (Scheme 1.2)



Scheme 1.2. Nucleophilic attack of free amine on bound olefin

The approach that is of considerable interest is the oxidative addition of the N-H bond to the metal, olefin insertion into the M-H bond, and then reductive elimination of the aminated product. (where E-H is an amine) (Scheme 1.3)



Scheme 1.3. Oxidative addition / Reductive elimination

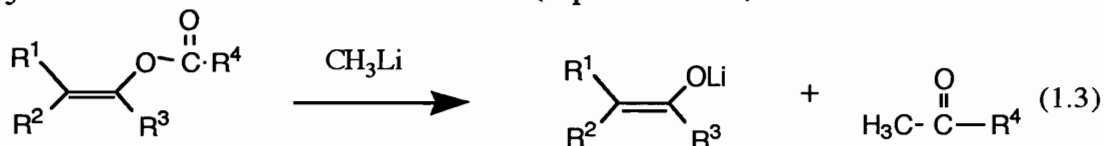
The activation of E-H bonds by transition metal complexes is known to be a key step in the catalytic functionalization of unsaturates. In some catalytic olefin hydroamination pathways, the oxidative addition of N-H bonds to a metal center may play an important role, but there are very few literature examples of the addition of N-H bonds to a metal.^{5a,b} In accordance there are even fewer examples of olefin insertion into a hydrido amido complex to effect catalytic amination.

1.4 O-H additions to unsaturates

Another area of catalytic interest is the use of metal carboxylates as possible catalysts for the hydro carboxylation of unsaturates. Since amino acids have both the potential for functionalization at the amine

terminus and the carboxylato terminus a short discussion of metal carboxylate chemistry is necessary. Amino acid complexes could feasibly be used to form enol esters.

The formation of enol esters as intermediates is very important in organic synthesis.⁸ One important application of enol esters is their easy conversion to lithium enolates. (equation 1.3)



In spite of their utility in organic synthesis there are very few general methods for the stereospecific generation of enolates. The existing methods consist of the following: treatment of aldehydes or ketones under acidic or basic conditions with the appropriate acid anhydride or chloride⁹, the palladium-promoted acetoxylation of olefins¹⁰, and the catalyzed addition reaction of carboxylic acids to alkynes¹¹.

One of the advantages of using a transition metal complex as a catalyst is the potential for selective formation of the G, E, or Z isomers of the enol ester. (Figure 1.1)

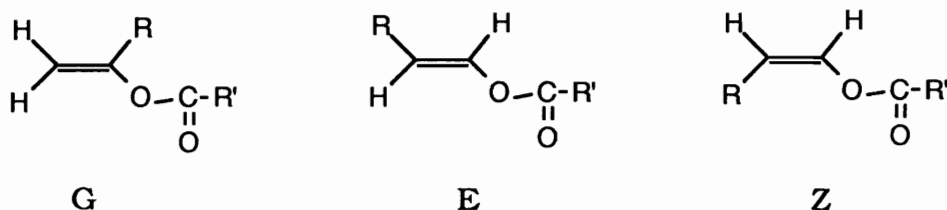


Figure 1.1 Possible isomers of the enol ester

A proposed scheme for the activity of these carboxylato-metal complexes would follow a pathway similar to that described for the amine complexes; oxidative addition of the O-H bond to the metal, insertion of the unsaturate and then the reductive elimination of the enol ester product.

1.5 Biological Interest in Amino Acid Complexes

The study of amino acid complexes is of interest not only for their potential catalytic uses, but for their possible biological uses. The previous description is only a brief overview of possible uses for amino acid complexes as amination or esterification catalysts. The chiral centers of these amino acids also make them potential candidates for use as asymmetric hydrogenation catalysts.

The main part of the literature review will discuss the kinds of complexes, binding modes and results derived from past research of amino acids and platinum metals. The review will focus on the platinum metals due to the intense number of studies that have been done with those metals and amino acids over the years. For a complete review see *Amino acids and Peptides* edited by R.W. Hay and K.B. Nolan.^{11a} These reviews give a up to date listing of what has been done in this field over the past year and are published annually.

Interest in the interaction of platinum metals with biologically important molecules began about 25 years ago when Rosenberg et al.

published their discovery that certain platinum complexes exhibit anti-cancer activity.¹² The most famous of these complexes is cisplatin.(Figure 1.2)

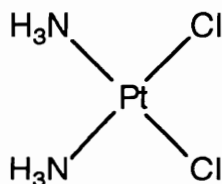


Figure 1.2. Cisplatin [Cis-diamminedichloroplatinate]

A variety of groups started looking at platinum metal complexes with a variety of ligands in order to develop better anti-tumor agents.

1.6 Ruthenium and Osmium Amino Acid Complexes

Not all the research that has been done is devoted to studying biological uses of complexes of amino acids. Ru and Os complexes were studied for their ability to promote hydrolysis of the bound amino acid ester.¹³⁻¹⁶ With simple amino acids Ru(III) can bind through the NH₂ and COO⁻ donor centers to form chelate complexes. An example of this is the [Ru(III)(gly)(NH₃)₄] complex. (Figure 1.3)

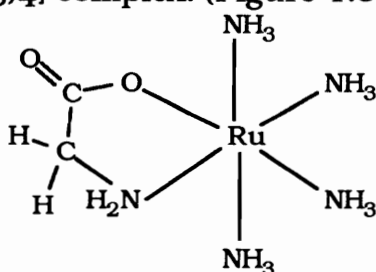
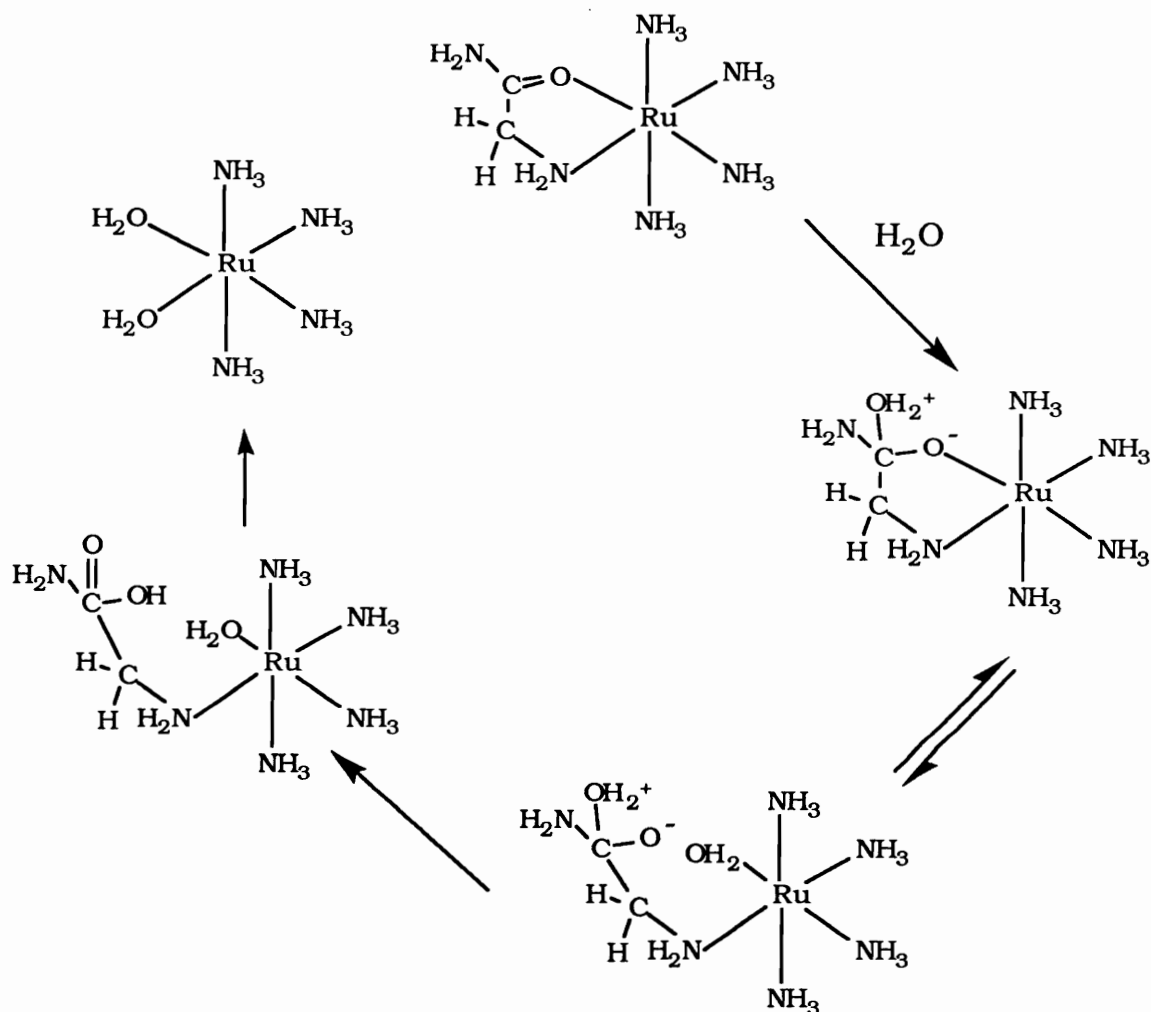


Fig. 1.3 Ruthenium tetraammine glycinate complex

Hydrolysis of the amino acid derivative is made easier by chelation of the amino acid derivative through the amino nitrogen and the carboxylate oxygen. The carbonyl group is then made more susceptible toward nucleophilic attack due to its attachment to the metal ion.¹⁷ (Scheme 1.4)

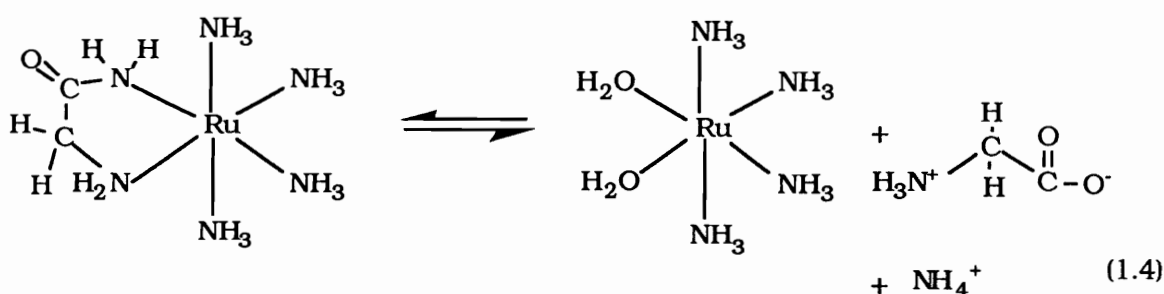


Scheme 1.4 Nucleophilic attack on carbonyl attached to metal

The reactivity of the kinetically inert ammine Co(III) amino acid complexes have been studied by Buckingham and Sargeson.^{18,19} The

analogous Ru(III) complexes are also inert and were prepared by Taube and co-workers.^{20,21,22} By studying the inert Ru(III) metal systems, the properties and structures for the complexes have been determined. The intermediates and mechanisms of metal ion promoted hydrolysis can also be defined by studying these systems.

The chemistry of Ru(III) complexes of amino acid and derivatives shows significant derivations from the chemistry of the analogous Co(III) complexes. The Ru(III) chelated glycineamide complex undergoes parallel hydrolysis and aquation in acidic solution (equation 1.4) as compared to the Co(III) complexes which are stable at acidic pH.²³



The pentammine Ru(III) bound metalloproteins can be used as probes by binding to the imidazole group of histidine. These "probes" are used to facilitate the kinetic and thermodynamic studies of long-range electron transfer²⁴ in cytochrome c^{25,26} azurin²⁷ and myoglobin²⁸. Further work done by Schuger et al. showed that Ru(III) binds to *l*-histidine preferably to the N3 of the imidazole ring. Thus a monodentate

mode of binding of the amino acid to the Ru metal center is observed.²⁹
(Figure 1.4)

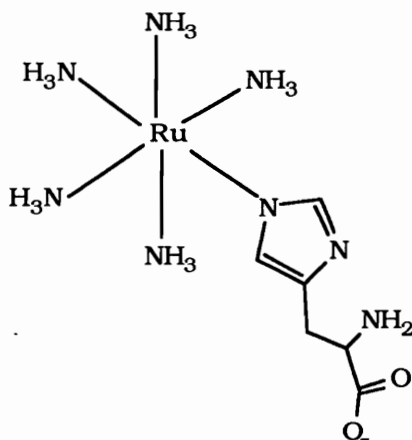


Figure 1.4 Monodentate binding of histidine

Another series of studies dealing with ruthenium as undertaken by Sheldrick and Exner³⁸ examining the reaction of [RuCl₂(PPh₃)₂] with α -amino acids. The complexes were formed by refluxing [RuCl₂(PPh₃)₃] and the respective amino acid in methanol in the presence of NaHCO₃. These complexes have the general structure shown with bidentate amino acidate ligands where the carboxyl oxygen of one ligated amino acid is trans to the amine of the other amino acid. (Figure 1.5)

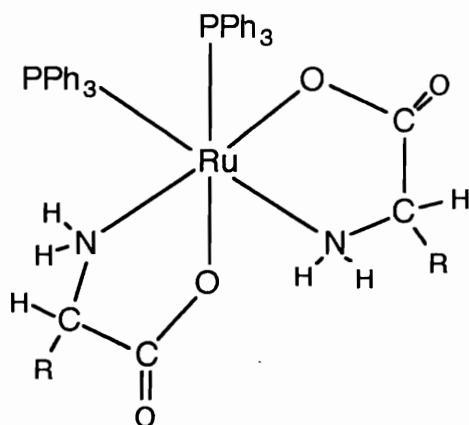


Figure 1.5 Ruthenium bis amino acid complex

Sheldrick also found that when glycine or *l*-alanine were added to the Ru(III) complex in acetone the Schiff base complexes were formed. (Figure 1.6) In the case of glycine the phosphines are trans to one another, with alanine the phosphines are trans to the ammine nitrogens.

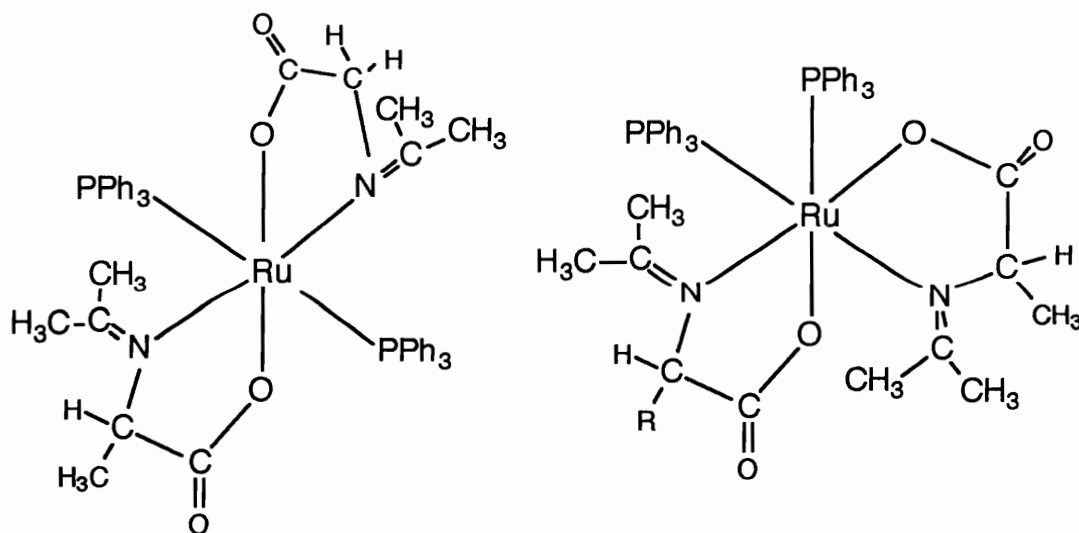


Figure 1.6 Schiff base complexes

A series of complexes of the type $[\text{RuCl}(\text{aaH})(\text{PPh}_3)_2]$ (aaH = glycine, *l*-serine, *l*-hydroxyproline, *l*-allohydroxyproline where prepared by Saito et al.³⁹ These novel complexes led to the above work of Sheldrick since only elementary analytical data was presented for only one of the synthesized complexes. Interest in these complexes is due to their potential use as homogeneous catalysts for the hydrolysis of amino acid esters.^{40,41,42}

Ruthenium complexes have also been studied as potential antitumor compounds. The primary work has been done on Ru(II) complexes that contain amino acid ligands.⁴³ The results that led to this work dealt with $[\text{RuCl}_2(\text{DMSO})]$,⁴⁴ this compound showing activity towards lung cancer similar to that of cisplatin. In the cases of B16 melanoma and MCa mammary cancer, Ru(II) derivatives exhibit greater activity than that of cisplatin. The preparation of complexes of type $[\eta^6\text{-C}_6\text{H}_6\text{Ru}(\text{aa})\text{Cl}]$ (aa = *l*-alanine or *l*-alanine methyl ester) (Figure 1.7) was reported by Sheldrick et al.⁴⁵ These complexes were prepared by stirring $[\eta^6\text{-C}_6\text{H}_6\text{RuCl}_2]$ in water with 2 equivalents of amino acid.

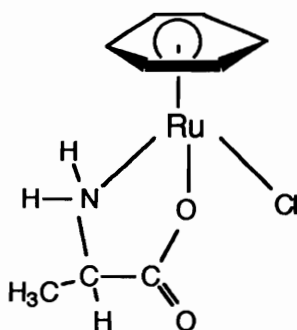


Figure 1.7 C_6H_6 -Ruthenium amino acid complex.

These complexes have been found to have significant activity against the P388 form of leukemia, in particular the $[\eta^6\text{-C}_6\text{H}_6\text{Ru}(\text{proline})\text{Cl}]$ complex.⁴⁶ (Figure 1.8)

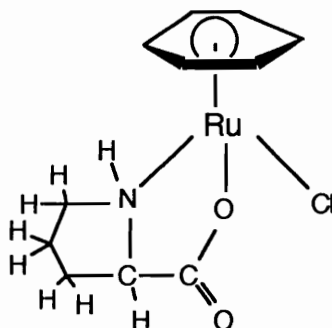


Figure 1.8 $[\eta^6\text{-C}_6\text{H}_6\text{Ru}(\text{proline})\text{Cl}]$ complex

Other studies that have been done with ruthenium include the work by Taube and co-workers directed towards trying to understand the binding of imidazole to the metal center.^{30,31} This work is mentioned because of its relation to the complexes that Ru forms with *l*-histidine. The variety of work presented here with Ru and amino acids has been directed towards a discussion of biological and catalytic uses of these compounds. There is much more that needs to be done with this particular metal and molecules of biological importance.

Very few osmium-amino acid complexes have been characterized. The work of Hanker et al. suggested the formation of OsL_4 complexes (*L* = aspartic acid, glutamic acid, glycine), but no analytical data were presented in the paper.³² Farooq et al. have measured stability constants for a number of Os(IV) amino acid complexes.³³ OsO_4 has been found to react with amino acids in water³⁴, and in solutions

buffered³⁵ to pH 7 at room temperature. These reactions yielded black solids that were insoluble and were not characterized. In the case where OsO₄ reactions were attempted at higher temperatures the amino acids were oxidized.³⁶

In a study done by Griffith et al. reactions were carried out with OsO₄ and amino acids whose α -amino group was unreactive. The reactive sites were limited to any donors on side chains³⁷ of the acid. These complexes were formed by stirring a solution of OsO₄ in aqueous acetone or chloroform with the amino acid. The products of these reactions were characterized by IR, Raman and C,H,O analysis.

It is clear that ruthenium and osmium chemistry of amino acids has received very little attention. The work that has been done has focused on ruthenium complexes for their use as hydrolysis catalysts, homogenous catalysts and certainly the most researched area is the use of these complexes as anti-cancer and anti-tumor agents. The work on osmium is almost non-existent. The work that has been done is plagued with problems as far as characterization of the products. The need for more studies with amino acids and these two metals is very apparent.

1.7 Platinum and Palladium Amino Acid Complexes

The work that has been done on the synthesis of amino acid complexes of palladium and platinum is extensive. This is understandable due to the extreme interest in cisplatin as an anti-tumor agent,⁴⁷ This discovery started a rush of activity in trying to understand the chemistry of platinum with amino acids. The interest

specifically in amino acid complexes of these two metals is aroused by a number of factors. The first of these factors is the need for an analog of cisplatin that is as effective as the drug, but with fewer side effects, such as nausea, vomiting, ototoxicity, neurotoxicity and renal damage.⁴⁸⁻⁵⁰ The second of these factors is the need for a complex that has increased water solubility for the purpose of intravenous administration, and chemical stability for formulation developments.⁵¹⁻⁵⁴ The third is the desire to develop complexes that have anti-tumor efficiency and are target specific.

The high requirement and uptake of important nutrients, such as amino acids, by tumor cells,^{55,56} has been exploited to produce selective cytotoxic effects towards specific tumor tissues. This specificity and the resulting cytotoxic effects are required for enhanced activity of the already existing compounds. For this reason of enhanced specificity, a number of groups have focused their attention on Pd and Pt amino acid complexes.

As stated before the amount of work done with Pd/Pt and amino acids far outmeasures the efforts with the other platinum metals. The studies with palladium have focused mainly on amino acids which contain sulfur donor atoms in addition to the nitrogen and oxygen donor centers. (Figure 1.9)

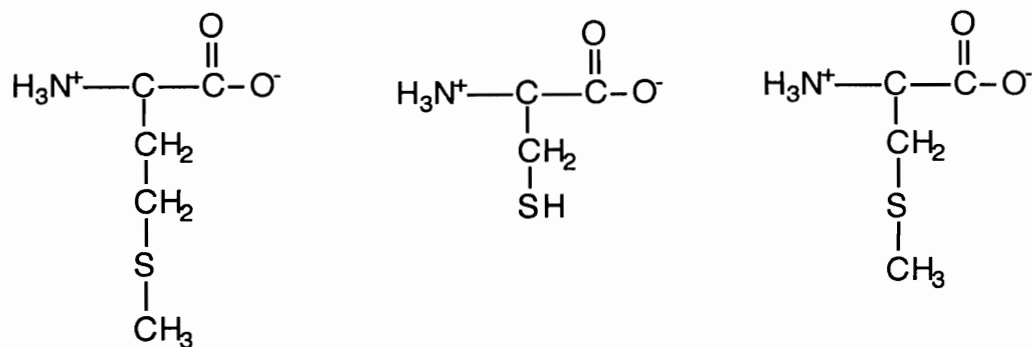


Figure 1.9 Amino acids that contain sulfur in their side chain
(Methionine, Cysteine, S-methyl cysteine)

These types of systems are of particular interest due to the preferential binding of palladium by 'soft' donors such as sulfur.⁵⁷

The earliest work done on palladium and amino acids was done by Ackerfeldt and Lovgren.⁵⁸ Their work demonstrated that Pd(II) ions could be used for the quantitative estimation of cysteine and related thiols in solution.

McAuliffe et al. studied the formation of [PdCl₂Met] (met = methionine) and through inspection of the IR spectrum of the complex suggested that the binding of the amino acid to the metal was through both the S and N centers.⁵⁹ Later crystallographic studies performed by Stephenson et al. showed that McAuliffe was correct in his analysis. The methionine bound the metal preferentially through the S and N donor centers.⁶⁰ (Figure 1.10)

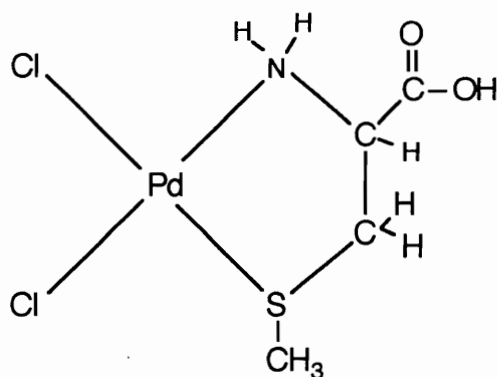


Figure 1.10 Preferential binding through the S donor atom

Chernova et al. synthesized a variety of palladium/methionine complexes.⁶¹ These complexes widely varied in their formulas: $[\text{Pd}(\text{MetH})_2]\text{Cl}_2$, $[\text{Pd}(\text{Met})_2]$, $[\text{Pd}(\text{MetH})\text{Cl}_2]$, $[\text{Pd}(\text{Met})(\text{H}_2\text{O})]\text{Br}$, $[\text{Pd}(\text{Met})(\text{H}_2\text{O})]\text{Cl}$, and $[\text{Pd}(\text{NH}_3)(\text{MetH})_2]\text{Cl}_2$. The IR spectra of these complexes showed considerable variation and Chernova was able to show that $[\text{Pd}(\text{MetH})\text{Cl}_2]$ contains coordination through both the N and S donors, which is consistent with the structure found by Stephenson. $[\text{Pd}(\text{MetH})_2\text{Cl}_2]$ shows bands in its IR spectrum consistent with both ionized and unionized carboxyl groups. $[\text{Pd}(\text{Met})_2]$ shows the carboxyl group to be ionized but not coordinated. (Figure 1.11)

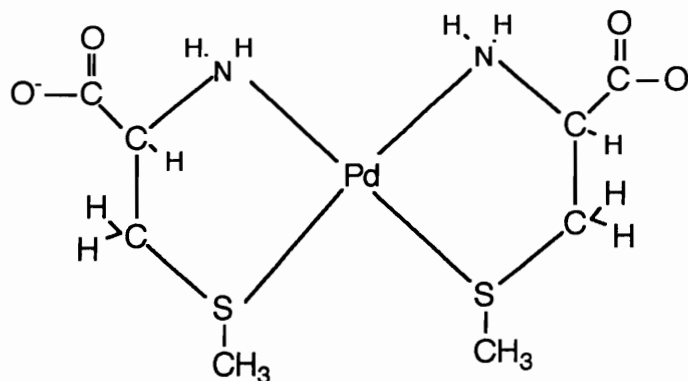


Figure 1.11 [Pd(Met)₂]

The [Pd(Met)(H₂O)]Cl complex shows no Pd-Cl band and the spectrum shows the methionine to be terdentate, with indications that the compound is polymeric. Finally, the [Pd(NH₃)₂(MetH)₂]Cl complex gives a spectrum that shows that binding only occurs through the sulfur group of the amino acid and the rest of the acid exists as a zwitterion. (Figure 1.12)

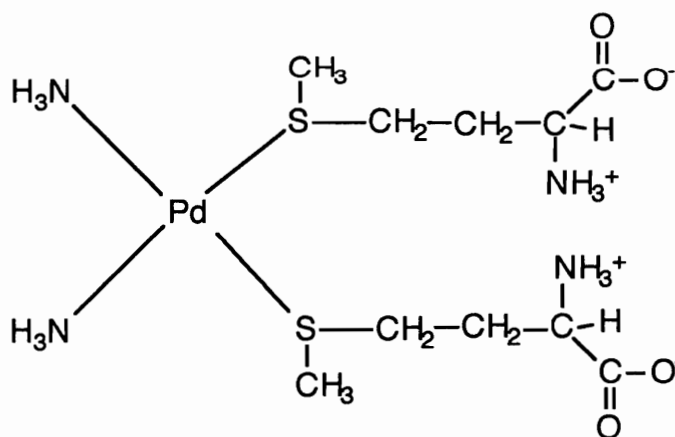


Figure 1.12 Zwitterionic character of [Pd(NH₃)₂(MetH)₂]Cl

Vicol et al. managed to synthesized several other Pd(II) complexes.⁶² Starting with the [Pd(Met)Cl₂] complex, Vicol managed to produce the following complexes: [Pd(NH₃)(Met)Cl], [Pd(Met)Cl₂]₂, [Pd(Met)₂]Cl₂, [Pd(Met)(NH₃)₂]₂, [Pd(MetH)(NH₃)₂][PdCl₄], [Pd(MetH)(NH₃)₂]Cl₂, and [Pd(MetH)₂(NH₃)₂][PdCl₄]. All of these complexes showed characteristics of square planar, d⁸ ions in the IR spectra, but showed extreme variations in their metal ligand binding.

Chanrasekhoran et al. prepared cysteine complexes of both platinum and palladium.⁶³ Their IR spectra gave sufficient information to deduce that cysteine coordinates through the thiol sulfur and the carboxylate oxygen donors. These metal complexes are square planar with the amino group protonated.

Levason and McAuliffe also prepared palladium complexes with *l*-cysteine.⁶⁴ Two complexes were isolated corresponding to [Pd₂(Cys)₃Cl] x 2H₂O and [Pd(CysHCl₂)]. The IR spectra of these compounds showed unionized carboxyl groups, suggesting that nitrogen and sulfur act as the donors to the metal. (Figure 1.13)

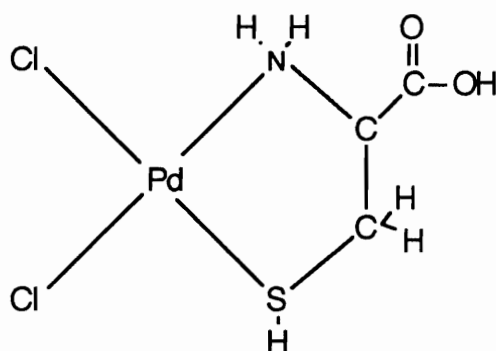


Figure 1.13 Nitrogen and sulfur donation of cysteine

Corresponding to this work are the studies done by Pnematikakis and Hajilidis in preparing cysteine and cystein methyl ester complexes with Pd(II) and Pt(II).⁶⁵ The reaction of $K_2[PdCl_4]$ and $PdCl_2$ with cysteine at ratios of 1:1 or 1:2 (M:L) gave products whose spectra showed that binding modes are pH and pH dependent. Proton NMR studies on these compounds showed that the binding occurs through the sulfur and nitrogen donors in both the 1:1 and 1:2 cases.⁶⁶

Pd(II) and amino acids that do not contain a sulfur atom have not been studied in the detail of sulfur containing amino acids. The following is a synopsis of the work that has been done with Pd(II) and other amino acids.

Wilson and Martin have recorded the CD spectra for a number of *l*-amino acids with Pd(II).⁶⁷ The spectra indicate that 2 nitrogen and 2 oxygen donors surround the metal when the ligands are N-methyl alanine, *l*-valine and *l*-glutaminc acid with a molar ratio of 1:2 (M:L). (Figure 1.14)

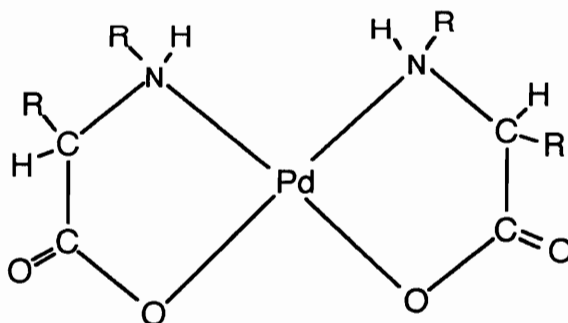


Figure 1.14 Nitrogen and oxygen donation to palladium

Wilson and Martin found some very interesting results on the binding modes of ornithine. Ornithine, $\text{H}_2\text{N}(\text{CH}_2)_3\text{CH}(\text{NH}_2)\text{COOH}$ (Figure 1.15) has 3 potential donor sites but acts as a bidentate ligand towards Pd(II).

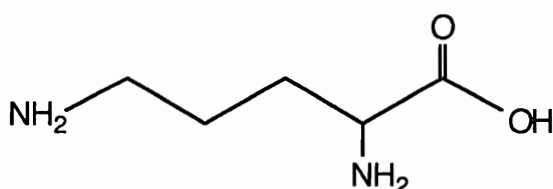


Figure 1.15 Ornithine

Wilson and Martin discovered that in solution equal amounts of 5- and 7- membered rings were formed.⁶⁸ The five membered ring results from coordination of the carboxyl group and the α -amino group, the seven membered ring arises from coordination of the α and δ amino groups. The formation of the larger ring is competitive with the formation of the smaller ring due to the preference of Pd(II) for nitrogen donors. Nakayama et al. solved the crystal structure of $[\text{Pd}(\ell\text{-orn})_2]$ and found that two 7-membered rings were arranged around the metal with the chelates in a twisted chair conformation.⁶⁹ (Figure 1.16)

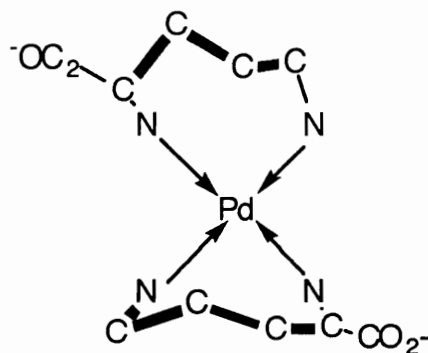


Figure 1.16 Twisted chair configuration of ornithine complex

Another interesting amino acid to consider as a ligand is *l*-histidine. (Figure 1.17) This amino acid has four potential donor centers, COO^- , NH_2 , and the two imidazole nitrogens.

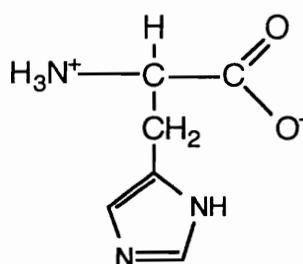


Figure 1.17 Histidine has four donor centers

Chernoval et al. showed that in all bis histidine-Pd(II) complexes they synthesized the complexes are square planar with coordination occurring through the amino nitrogen and through the imidazole nitrogen when the ligand is bidentate.⁷⁰ There was no evidence for any coordination through the carboxylate group.

The crystal structures of several other amino acid complexes of Pd(II) have been solved. $[\text{Pd}(\text{pro})_2]$ was determined to be square planar around the palladium center and the proline ions were found to be cis

to one another.⁷¹ The structures of $[\text{Pd}(\text{II})(l\text{-tyr})_2] \cdot 1/2 \text{H}_2\text{O}$ and $[\text{Pd}(\text{II})(l\text{-val})_2]$ were also determined to be square planar complexes by Jarzab et al.⁷² Sabat et al. also did a study on the possible apical coordination of tyrosine to Pd(II).⁷³ (Figure 1.18)

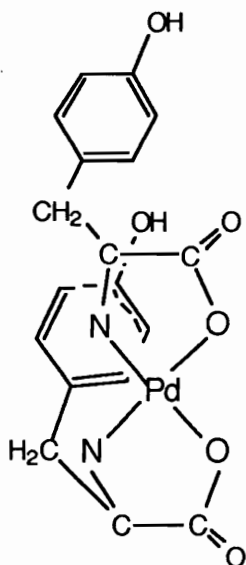


Figure 1.18 Apical coordination of tyrosine

They determined that the Pd-C interatomic distances between one tyrosine ring and the metal suggested direct interaction between the aromatic ring and the metal ion. It also indicated that the second aromatic side chain may interact with an adjacent Pd(II) ion.

The structure of $[\text{Pd}(l\text{-ser})_2]$ has been determined by Vagg et al.⁷⁴ Bakakim et al. solved the structure of $[\text{Pd}(\text{cis-gly})_2] \cdot 3\text{H}_2\text{O}$. These structures were also determined to be square planar as the majority of the Pd(II) amino acids complexes follow that coordination geometry. (Figure 1.19)

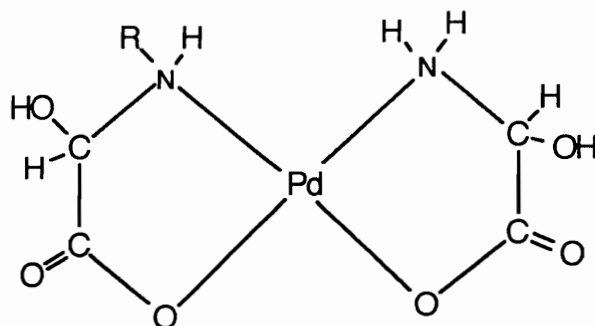


Figure 1.19 Palladium bis-serine complex

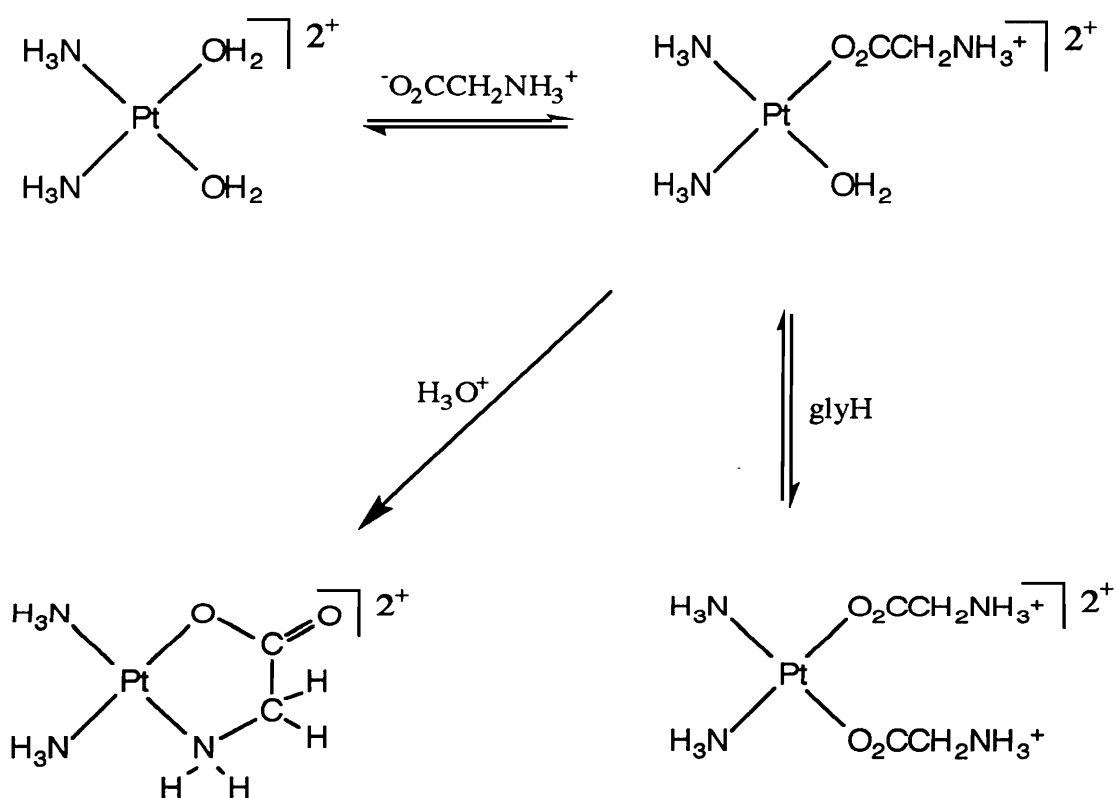
There are a number of reviews that cover the work that has been done with platinum and amino acids,^{76a,b,c} The studies of palladium and platinum chemistry with amino acids are very similar, an overview of the work that has been done with platinum will be presented here.

In complexes platinum can be found as either Pt(II) or Pt(IV). Pt(II) forms square planar, four coordinate complexes similar to palladium. In order to maintain planar coordination amino acids may bind through either of their donor centers, the nitrogen of the amino group or the oxygen of the carboxylate. It was originally thought that when an amino acid binds to Pt(II) it did so in a monodentate fashion through the nitrogen donor.^{77,78} The CD spectroscopy of Martin and Wilson on palladium compounds suggested that amino acids bind in a bidentate coordination scheme {N,O}.⁷⁹ X-ray crystallography has shown on numerous amino acid Pt complexes that {N,O} is possible, with cis coordination being more frequent than trans.^{80, 81}

Monodentate coordination through the nitrogen atom is often thought to be the case with platinum (II) complexes⁸¹. X-ray structures have shown that the nitrogens of two amino acids bound unidentately

can be trans⁸² or cis⁸³ to each other while the carboxyl groups remain protonated.

Appleton et al.^{84,85} did work using ¹⁵N and ¹³⁵Pt NMR spectroscopy which showed that an amino acid such as glycine could initially bind unidentately through the oxygen. The chelate ring {N,O} will close if the solution is allowed to stand for several hours, if heated, or if the pH is increased.[Scheme 1.5]



Scheme 1.5 Monodentate to bidentate binding of amino acids

Appleton attributes this monodentate to bidentate transformation to differing rates of reaction. The monodentate O-bound glycine complexes

were found to be metastable even though they easily rearranged to the thermodynamically stable {N,O} chelate complex. If the length of the amino acid is increased, complexes with monodentate O-binding are found to be kinetically stable, and the {N,O} chelated species are thermodynamically favored.⁸⁶

There have been a few studies that involve the formation of Pt(IV) - amino acid complexes. $[\text{PtCl}_6]^{2-}$ will react with amino acids, but the reaction is very slow and the products are insoluble.⁸⁷ The reactions of $(\text{Me})_3\text{Pt(IV)}$ ion with amino acids on the other hand, have provided useful information about Pt(IV) complexes. These complexes are octahedral and prefer to be in a facial arrangement in terms of the methyl groups arrangement in the octahedron.^{88,89} (Figure 1.20)

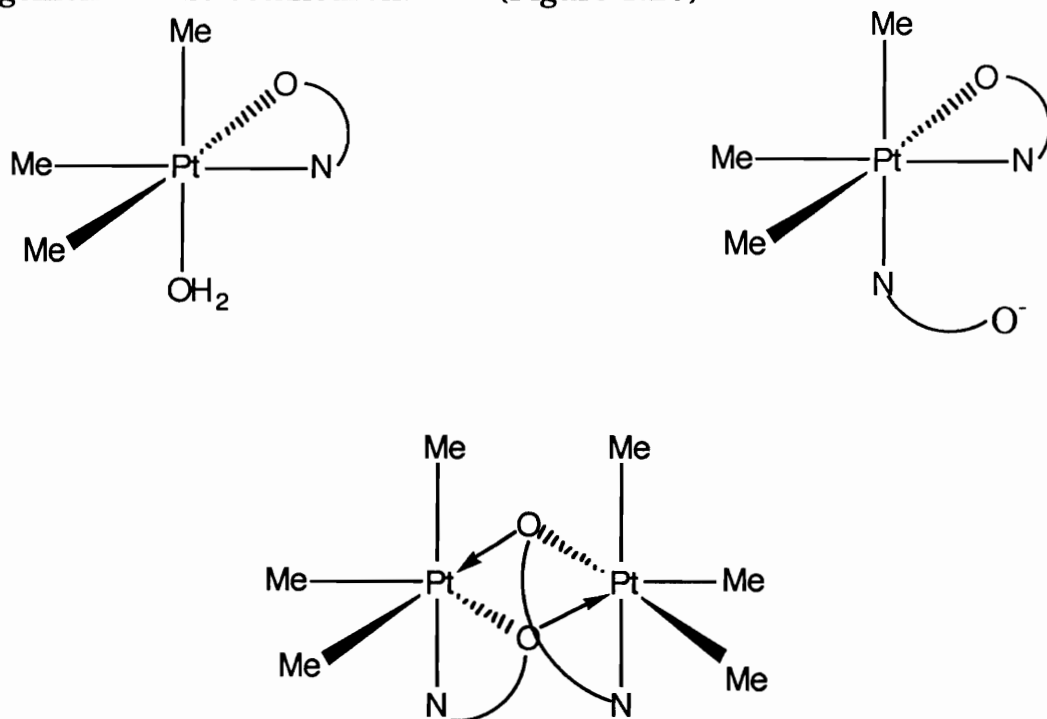


Figure 1.20 Facial arrangement of Pt(IV) complexes

When simple amino acids are complexed with $(\text{Me})_3\text{Pt(IV)}$ several different forms of the complex can be made. These forms consist of the dimeric species, $[(\text{Me})_3\text{Pt(aa)}]_2$, $[(\text{Me})_3\text{Pt(aa)H}_2\text{O}]$, in addition to bis-aa, and tris-aa complexes. The amino acids bind unidentately through the N-donor or bidentately {N,O}. The formation of $[(\text{Me})_3\text{Pt(gly)L}]$ where L is a monodentate ligand can lead to the formation of enantiomeric species and by varying the temperature the formation of one species can be favored.⁹⁰

The use of an amino acid with an asymmetric carbon in the reaction with the Pt(IV) complexes leads to the production of diastereoisomers.⁹¹ The diastereoisomers result from the two chiral centers present on the amino acid (the α -carbon and the β -carbon of the side chain) on attachment to the metal diastereoisomers are formed. Platinum(IV) complexes can also be synthesized by oxidizing the corresponding Pt(II) complex with chlorine in the presence of HCl.^{92,93}

Most of the work that has been done with platinum and amino acids is similar to that of palladium, and similarly focuses on the amino acids where a sulfur donor is contained in the side chain. Again, this is due to the 'soft' donor (sulfur) being a preferred binding site for both palladium and platinum. Methionine, which has 3 potential coordination sites, NH_2 , COO^- , and the sulfur atom, only uses two of these donors { NH_2 , S} to form six-membered chelate rings with Pt(II).^{94,95} In the case of S-methyl-*l*-cysteine there is one less methylene group in the side chain and now the {N,S} chelation forms a more stable 5-membered ring with the platinum center.

Platinum(IV) also coordinates strongly to sulfur donors and a variety of isomeric forms of methionine complexes with Pt(IV) have been isolated. These complexes have been synthesized by the oxidation of [PtCl₂(Met)] with chlorine in the presence of HCl.^{96,97} The binding in all complexes is chelation through the nitrogen and sulfur donors. The chemistry of Pt with sulfur donating amino acids is almost identical to palladium in all respects and has been covered thoroughly in the previous section on palladium-amino acid complexes.

Both palladium(II) and platinum(II) preferentially bind to nitrogen over oxygen. Thus compounds with other N donors would be expected to form {N,N} chelate complexes. Amino acids such as *l*-histidine, with the imidazole nitrogens form {N,N} chelate products with Pt(II) just as with Pd(II).⁹⁸ In the case of asparagine and glutamine, which have side-chain amide nitrogens the formation of "platinum blue" complexes, is observed. Platinum "blue" complexes contain limited chains with Pt-Pt interaction and variable oxidation states, Pt^{II,III,IV}.⁹⁹

As expected the chemistries of platinum and palladium with amino acids are quite similar. Quite often palladium complexes are studied instead of (or as well as) the platinum analogs. The work that has been done with these two metals is quite extensive, the studies that have been presented here are more of an overview of the types of complexes that have been formed. These studies also characterize the typical binding modes and structures of the amino acid-Pd/Pt complexes that have been synthesized over the years.

1.8 Rhodium and Iridium Amino Acid Complexes

The two metals which are of most relevance to this thesis are rhodium and iridium. The work that has been done with these metals will be discussed in more detail but there are a very limited number of studies with amino acids and these two metals.

Compared with Pt and Pd almost nothing has been done with rhodium and iridium complexes of amino acids. The electroanalytical studies done by Farooq suggest that Rh(III) complexes with amino acids are stable.¹⁰⁰ The binding of N and O donors to form chelates is suggested for most amino acids with no involvement of side chain donors, contrasting with the complexes made with the sulfur donation of methionine to palladium and platinum. RhCl₃ reacts with glycine in the solid form to produce a species that has either -NH₂ or COO⁻ monodentate coordination.¹⁰¹ Chelation of both NH₂ or COO⁻ occurs in several species including [RhL₃] [L= amino acids] but the yield of these products is very low.

The studies done by Rajca et al. demonstrated that RhCl₃ reacts with amino acids in H₂O/ethanol solutions to form H[Rh₂L₂Cl] species with {N,O} chelation.¹⁰² These compounds were determined to be efficient catalysts in homogeneous hydrogenation of some aromatic compounds. This is one of the few examples of a platinum metal - amino acid complex being studied for its hydrogenation catalyst capabilities.

The possibility for monodentate carboxylate coordination was demonstrated by the work of Chatterjee with [(NH₃)₅(gly)(Rh)(III)] ion.¹⁰³

(Figure 1.21) This is prepared by heating an aqueous solution of $[(\text{NH}_3)_5\text{Rh}(\text{III})\text{ClO}_4]$ with a five-fold excess of glycine at 90°C for 3 hours. On reduction in volume of the solution, crystals of the glycine complex separate out.

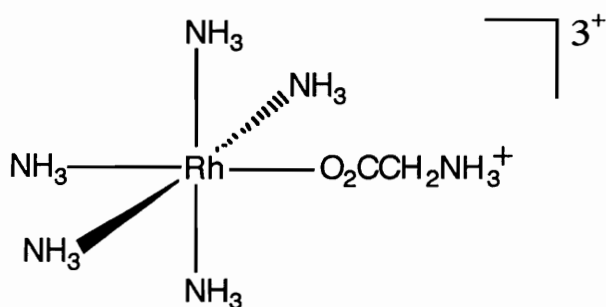


Figure 1.21 $[(\text{NH}_3)_5(\text{gly})(\text{Rh})(\text{III})]$ ion

The stable tetraaceto rhodium (II) ion can react with amino acids containing a sulfur group to form monomeric square planar Rh(II) complexes that have {S,N} chelation.¹⁰⁴ (Figure 1.22)

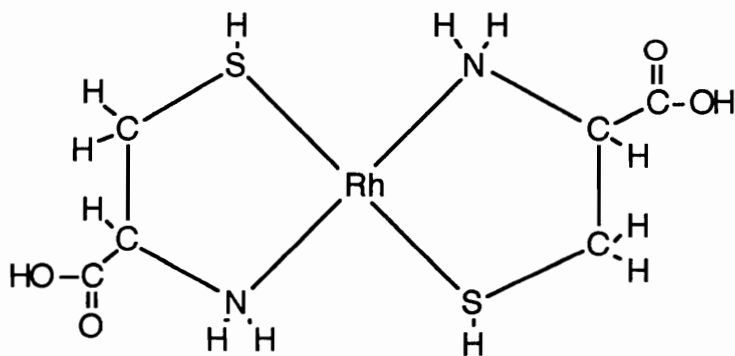


Figure 1.22 Sulfur and nitrogen coordination to rhodium

The $[\text{Rh}(\text{L})_2]$ complexes can be made with cysteine and penicillamine, each having a thiol sulfur that can donate to the metal. These $[\text{Rh}(\text{L})_2]$ complexes are of the few mononuclear Rh(II) complexes isolated.

The work done by Singh et al. demonstrates that Rh(I) amino acid complexes can also be isolated.¹⁰⁵ These complexes are stabilized by carbonyl ligands. The compounds are synthesized by reaction of a solution of $[(\text{OC})_2\text{Rh}(\eta\text{-Cl})_2\text{Rh}(\text{CO})_2]$ in benzene with an excess of amino acid ion. [glycine, *l*-alanine, β -alanine, *l*-leucine, *l*-histidine, *l*-tryptophan, *l*-phenylalanine, sarcosine] These compounds are dimeric in the solid state and have the structure shown in Figure 1.23.

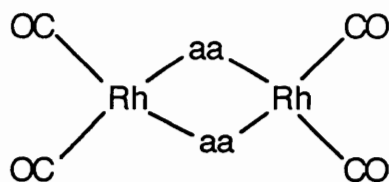


Figure 1.23 Dimeric species of rhodium carbonyl

In solution they are monomeric and the amino acid chelates to the metal center. (Figure 1.24)

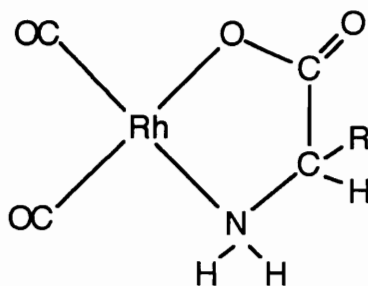
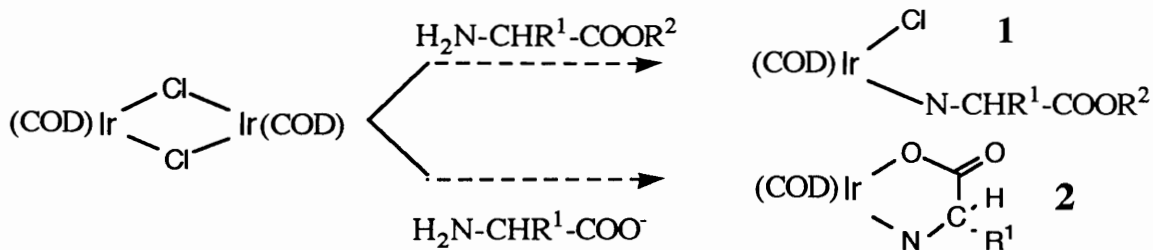


Figure 1.24 Monomeric species of rhodium carbonyl

These carbonyl complexes are reactive and the CO ligands can be exchanged with PPh_3 or AsPh_3 .

Complexes with iridium and amino acids are not even mentioned in most reviews. The few studies that have been done have not been done in any detail. In fact, after thorough investigation of the literature, the only amino acid complexes of iridium that were found were those made by Beck et al.¹⁰⁶

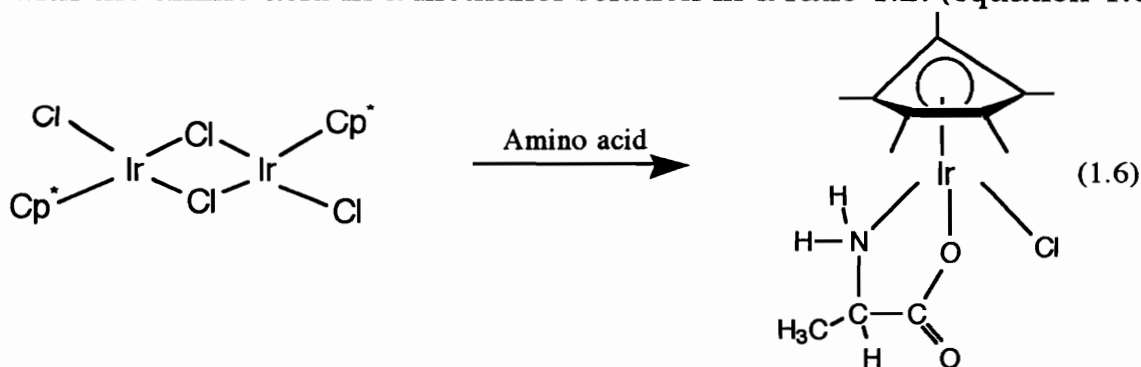
In this study Beck made amino acid complexes of both Ir(I) and Ir(III) oxidation states. In the case of Ir(I) complexes, the reaction of $[(\text{COD})\text{Ir}(\text{Cl})]_2$ with an amino acid anion resulted in a 5-membered chelate compound. If the amino acid was in its ester form, instead of the protonated carboxylate, the resulting complex had the unidentate ligand bound through the amine terminus. (Scheme 1.6)



1	2
R ¹ R ²	R ¹
H -CH ₃ -CH(CH ₃) ₂	-CH ₃ -CH ₂ Ph -CH(CH ₃) ₂ -CH ₂ CH(CH ₃) ₂ -Ph

Scheme 1.6 Results of study done by Beck et al.¹⁰⁶

The Ir(III) complexes were made by reacting Cp*(Cl)Ir(η-Cl)₂Ir(Cl)Cp* with the amino acid in a methanol solution in a ratio 1:2. (equation 1.6)



The Ir(III) complexes were made with the following amino acids: glycine, *l*-valine, *l*-phenylalanine, *l*-tryptophan, *l*-proline, and phenylglycine.

It is surprising that so many studies on palladium and platinum have been done while almost none exist with the remaining platinum

metals. As the author was scanning through review articles and literature sources a quote from Kozlowski and Pettit in Studies in Inorganic Chemistry really put the importance of the research presented in this thesis in perspective.¹⁰⁷

.....there should soon be more systematic studies of the interaction of platinum metals with amino acids and peptides including iridium, amino acid complexes of which are virtually unknown.

Even the studies that have been done do not mention the formation of oxidative addition products of amino acids. The compounds that will be discussed in this thesis are the result of oxidative addition to an iridium center. The literature makes no mention of amino acid - hydride complexes. The complexes that the Merola group is interested in are hydride complexes, the novel complexes that will be discussed are the first examples of platinum metal hydride amino acid compounds.

1.9 References

¹Cotton, F.A.; Wilkinson, G.; Advanced Inorganic Chemistry 5th ed.; John Wiley and Sons; New York, New York; 1988.

²a) Sherman, S.E.; Lippard, S.J.; *Chem Rev.*, **87**, 1987 (1153-81).

b) Lippard, S.J., ed.; Platinum, Gold, and other Metal Chemotherapeutic Agents, ACS Symposium Series, **209**, 1983.

- ³Patai, S.; The Chemistry of the Amino Group, Interscience Publishing Co., New York, New York, 1968.
- ⁴Barton, D.; Ollis, W.D.; Comprehensive Organic Chemistry, Interscience Publishing Co., New York, New York, 1982.
- ⁵Trost, B.M.; Verhoeven, T.P.; *Comp. Organomet. Chem.*; **8**, 1982 (892).
- ^{5a} Roundhill et al., *J Amer. Chem. Soc.*, **106**, 1984, (5014). ^{5b}Roundhill, D.M., Hedden, D., *Inorg. Chem.*, **25**, 1986, (9-15).
- ⁶Parshall, G.W.; In Wiley: New York, 1980.
- ⁷Khan, R.C.; Martell, A.E.; In Academic : New York Vol. 2, 1974 (45).
- ⁸Larock, R.C.; Oertle, K.; Beatty, K.M.; *J. Amer. Chem. Soc.*; **102**, 1980 (1966).
- ⁹Bedoukian, P.Z.; *J. Amer Chem. Soc.*; **66**, 1944 (1325-27).
- ¹⁰Kitching, W.; Rappaport, Z.; Winstein, S.; Youngs, W.G.; *J. Amer. Chem, Soc.*; **88**, 1966 (2054-55).
- ¹¹Bach, R.D.; Woodward, R.A.; Anderson, T.J.; Glick, M.D.; *J. Org. Chem.*; **47**, 1982 (3707-3717).
- ¹²Rosenberg, B.; Van Camp, L.; Trosko, J.E.; Mansour, V.H.; *Nature*, **222**, 1969 (385).
- ¹³Hay, R.W.; Morris, P.J.; Metal Ions in Biological Systems Vol.5, Sigel, H. ed.; Marcell Dekker Co.; New York, New York, 1976.
- ¹⁴Satchill, D.P.N.; Satchill, R.S.; *Annual Rep. Prog. Chem. Sect. A : Phys. Inorg. Chem.*. **75**, 1978 (75).
- ¹⁵Sigel, H.; Martin, R.B.; *Chem, Rev.*, 1982 (385).

- ¹⁶Buckingham, D.A.; Addison, A.W.; Cullen; W.R.; Dolphin, D; James., B.R., Eds.: Biological Aspects of Inorganic Chemistry ; Wiley and Sons, New York, 1977.
- ¹⁷Ilan, Y.; Kfir,A.; *Inorg. Chem.*, **26**, 1987 (2872).
- ¹⁸Buckingham, D.A.; Addison, A.W.; Cullen; W.R.; Dolphin, D; James., B.R., Eds.: Biological Aspects of Inorganic Chemistry ; Wiley and Sons, New York, 1977.
- ¹⁹Buckingham, D.A.; Clark; C.; *Inorg. Chem.*, **25**, 1986 (3478).
- ²⁰Taube, H.; *J. Amer. Chem Soc.*, **102**, 1980 (4275-9).
- ²¹Diamond, S.E.; Taube, H.; *J. Amer. Chem. Soc.*, **97**, 1975 (5921-3).
- ²²Ilan, Y.; Taube, H.; *Inorg. Chem.*, **22**, 1983 (1655-64).
- ²³Ilan, Y.; Kfir,A.; *Inorg. Chem.*, **26**, 1987 (2872).
- ²⁴Gray, H.B., *Science*, 1986 (948).
- ²⁵Nocera, D.G.; Winkler, J.R.; Yocum, K.M.; Bordignon. E.; Gray, H.B.; *J. Amer. Chem. Soc.*, **106**, 1984 (5145).
- ²⁶Isied, S.S.; Kuehn, C.; Worosila, G.J.; *J. Amer. Chem. Soc.*, **106**, 1984 (1722-6).
- ²⁷Gray, H.B.; *Chem. Soc. Rev.*, **15**, 1986 (17).
- ²⁸Crutchley, R.J.; Ellis, W.R.; Gray, H.B.; *J. Amer. Chem. Soc.*, **107**, 1985 (5002).
- ²⁹Krogh-Jespersen, K.; Westbrook, J.D.; Potenza, J.A.; Schugar, H.J.; *J. Amer. Chem. Soc.*, **109**, 1987 (7025).
- ³⁰Tweedle, M.F.; Taube, H.; *Inorg. Chem.*, **21**, 1982 (3361).
- ³¹Sundberg, R.J.; Bryan, R.F.; Taylor, J.F.; Taube, H.; *J. Amer. Chem. Soc.*, **96**, 1974 (387).

- ³²Seligman, A.M.; Wasserkrug, H.L.; Deb., C.; Hanker, J.S.; *J. Histochem. Cytochem.*, **16**, 1958 (220).
- ³³Poddar, S.N.; Biswas, D.K.; *Sci. Culture*, **31**, 1965 (189).
- ³⁴Bahr, G.F.; *Exp. Cell. Res.*, **7**, 1954 (221).
- ³⁵Hake, T.; *Lab. Invest.*, **14**, 1965 (1208-12).
- ³⁶Nylasi, J.; Orsos, P.; *Acta. Chim. Acad. Sci. Hung.*, **75**, 1973 (267-72).
- ³⁷Nielsen, A.J.; Griffith, W.P.; *J. Chem. Soc., Dalt. Trans.*, 1979 (1084).
- ³⁸Sheldrick, W.S.; Exner, R.; *Inorg. Chim. Acta.*, **175**, 1990.
- ³⁹Saito, Y.; Takita, K.; Inoue, N.; Shinoda, S.; *Inorg. Chim. Acta.*, **65**, 1982 (L21-L23).
- ⁴⁰Saito, Y.; Shinoda, S.; Yamaguchi, Y.; *Inorg. Chem.*, **18**, 1979.
- ⁴¹Saito, Y.; Shinoda, S.; Yamaguchi, Y.; *J. Organomet. Chem.*, **121**, 1976 (93).
- ⁴²Rapoport, H.; Buckley, T.F. III; *J. Amer. Chem. Soc.*, **103**, 1987 (6157).
- ⁴³Sheldrick, W.S.; Heeb, S.; *Inorg. Chim. Acta.*, **168**, 1990 (93).
- ⁴⁴James, B.R.; Ochai, E.; Rempel, G.C.; *Inorg. Nucl. Chem. Lett.*, **7**, 1971 (975-6).
- ⁴⁵Sheldrick, W.S.; Heeb, S.; *Inorg. Chim. Acta.*, **168**, 1990 (93).
- ⁴⁶Sheldrick, W.S.; Heeb, S.; *Inorg. Chim. Acta.*, **168**, 1990 (93).
- ⁴⁷Rosenberg, B.; Van Camp, L.; Trosko, J.E.; Mansour, V.H.; *Nature*, **222**, 1969 (385).
- ⁴⁸Prestayko, A.W.; D'Aoust, J.C.; Issel, B.F.; Cook, S.T.; *Cancer Treat. Rep.*, **63**, 1979 (17).
- ⁴⁹Van Hoff, D.D.; Schilsky, R.; Reichert, C.M.; *Cancer Treat. Rep.*, **63**, 1979 (1439).

- ⁵⁰Krakoff, J.H.; *Cancer Treat. Rep.*, **63**, 1979 (1523).
- ⁵¹Rose, W.C.; Schurig, J.E.; Huffalen, J.B.; Bradner, W.T.; *Cancer. Treat. Rep.*, **66**, 1982 (135).
- ⁵²Lee, F.H.; Canetta, R.; Issel, B.T.; Lenaz, L.; *Cancer Treat. Rev.*, **10**, 1983 (39).
- ⁵³Harrap, K.R., 'Platinum Analogous Criteria for Selection' in F.M. Muggia, Ed. Cancer Chemotherapy, Vol.1; Martin Nijhoff, Boston, 1983.
- ⁵⁴Hacker, M.P.; Khokhar, A.R.; Brown, D.B.; McCormack, J.J.; Karkoff, J.H.; *Cancer Res.*, **45**, 1985 (4748-53).
- ⁵⁵Wallach, D.F.H.; *J. Mol. Med.*, **1**, 1976 (97).
- ⁵⁶Williams, D.R.; *Chem. Rev.*, **72**, 1972 (203).
- ⁵⁷Pettit, C.; Bezer, M.; *Coord. Chem. Rev.*, **61**, 1985 (97-114).
- ⁵⁸Akerfeldt, S.; Lovgren, G.; *Anal. Biochem.*, **8**, 1964 (223-8).
- ⁵⁹McAuliffe, C.A.; *J. Chem. Soc. A*, 1967 (641-2).
- ⁶⁰Stephenson, N.C.; McConnell, J.T.; Warren, Z.; *Inorg. Nucl. Chem. Lett.*, **5**, 1967 (553).
- ⁶¹Chernova, N.N.; Kurskii, I.G.; Shukov, V.V.; *Russ. J. Inorg. Chem.*, **23**, 1978 (239).
- ⁶²Vicol, O.; Hurdue, N.; Scheider, I.A.; *J. Inorg. Nucl. Chem.* **41**, 1979 (309).
- ⁶³Chandraskhoran, M.R.; Udapa, M.; Aravamnden, G.; *Inorg. Chim Acta.*; **7**, 1973.
- ⁶⁴Levason, W.; McAuliffe, C.A.; *Inorg. Nucl. Chem. Lett.*, **13**, 1977 (123).
- ⁶⁵Pneumatikakis, G.; Hajilidis, N.; *J. Inorg. Nucl. Chem.*, **41**, 1979 (429).
- ⁶⁶Allain, A; Kozlowski, H.; *Acta Crystallogr.*, **25**, 1980 (2246).

- 67 Wilson, E.W.; Martin, R.B.; *Inorg. Chem.*, **10**, 1971,(1197-202).
- 68 Wilson, E.W.; Martin, R.B.; *Inorg. Chem.*, **10**, 1971,(1197-202).
- 69 Nakayama, Y.; Matsumoto, K.; Ooi, S.; Kuroya, H.; *J. Chem Soc. Chem. Comm.*, 1973 (170).
- 70 Chernova, N.N.; Strukov, V.; Avetikyan, G.; *Russ. J. Inorg. Chem.*, **25**, 1980 (872).
- 71 Ito, T.; Marumo, I.; Saiton, Y.; *Acta Crystallogr. Sect. B* , **27**, 1971 (1062).
- 72 Jarzab, T.C., Hare, C.R.; Lange, D.A.; *Cryst. Struct. Comm.*, **3**, 1973 (395).
- 73 Sabat, M.; Jezowska, M.; Koslowski, H.; *Cryst. Struct. Comm.*, **3**, 1973 (399).
- 74 Vagg, R.S.; *Acta Crystallogr. Sect. B*, **35**, 1979 (34).
- 75 Bakakin, V. et al.; *Zh. Strukt. Khim.*, **20**, 1979 (544).
- 76a) Hartley, F.S.; in The Chemistry of Platinum and Palladium, Applied Science, London, 1973. b) Laurie, S.H.; Wilkinson, G. ed.; Comprehensive Coordination Chemistry, Pergamon Press, Oxford, 1987. c) Pickert, L; Weinstein, S., ed.; Chemistry and Biochemistry of Amino acids, Peptides an Proteins, Dekker, New York, 1982.
- 77 Hartley, F.S.; in The Chemistry of Platinum and Palladium, Applied Science, London, 1973 (205).
- 78 Volstein, L.; *Koord. Khim.*, **1**, 1975 (595).
- 79 Wilson, E.W.; Martin, R.B.; *Inorg. Chem.*, **9**, 1970 (521).
- 80 Sabat, M.; Jezowska, M.; Koslowski, H.; *Inorg. Chim. Acta.*, **37**, 1974 (L511).

- ⁸¹Hartley, F.S.; in The Chemistry of Platinum and Palladium, Applied Science, London, 1973 (205).
- ⁸²Baidina, J.A.; Borisov, S.V.; *Zh. Strukt. Khim.*; **22**, 1981 (183).
- ⁸³Baidina, J.A.; Borisov, S.V.; Podberzka, N.V.; *Zh. Strukt. Khim.*, **21**, 1980 (185).
- ⁸⁴Appleton, T.G.; Hall, J.R.; *J. Chem. Soc. Chem. Comm.*, 1983 (911).
- ⁸⁵Appleton, T.G.; Hall, J.R.; Ralph, S.F.; *Inorg. Chem.*, **24**, 1985 (673).
- ⁸⁶Appleton, T.G.; Hall, J.R.; Ralph, S.F.; *Austr. J. Chem.*, **39**, 1986 (1347).
- ⁸⁷Volstein, L.; *Koord. Khim.*; **1**, 1975 (595).
- ⁸⁸Appleton, T.G.; Hall, J.R.; Lampart, L.; *Inorg. Chim. Acta.*, **29**, 1978 (89).
- ⁸⁹Appleton, T.G.; Hall, J.R.; Jones, T.G.; *Inorg. Chim Acta.*, **32**, 1979 (127).
- ⁹⁰Appleton, T.G.; Hall, J.R.; Lampart, L.; *Inorg. Chim. Acta.*, **29**, 1978 (89).
- ⁹¹Appleton, T.G.; Hall, J.R.; Jones, T.G.; *Inorg. Chim Acta.*, **32**, 1979 (127).
- ⁹²Mogolevkina, M.F. et al.; *Koord. Khim.*, **5**, 1979 (1866).
- ⁹³Mogolevkina, M.F. et al.; *Koord. Khim.*, **11**, 1985 (1381).
- ⁹⁴Freeman, H.C.; Golomb, J.; *J. Chem. Soc. Chem. Comm.*, 1970 (1523).
- ⁹⁵Warren, R.C.; McConnel, J.F.; Stephenson, N.C.; *Acta Crystallogr. B26*, 1970 (1402).
- ⁹⁶Mogolevkina, M.F. et al.; *Koord. Khim.*, **5**, 1979 (1866).
- ⁹⁷Mogolevkina, M.F. et al.; *Koord. Khim.*, **11**, 1985 (1381).

- ⁹⁸Kozłowski, H.; Matczak-Jon, E.; *Inorg. Chim Acta.*, **32**, 1979 (143).
- ⁹⁹Larent, J.P.; Charlson, A.J.; *Inorg. Chim. Acta.*, **66**, 1982 (L9).
- ¹⁰⁰Farooq, O.; Ahmad, N.; *J. Electroanal. Chem.*, **53**, 1974 (461).
- ¹⁰¹Kazbanov, V.I. et al.; *Zh. Neorg. Khim.*, **27**, 1982 (2037).
- ¹⁰²Rajca, I.; *Pol. J. Chem.*, **55**, 1981 (775).
- ¹⁰³Chatterjee, C.; Bali, A.; *Bull. Chem. Soc. Jpn.*, **60**, 1987 (1210).
- ¹⁰⁴Pneumatikakis, G.; Psaroulis, P.; *Inorg. Chim Acta.*, **46**, 1980 (97).
- ¹⁰⁵Dowerah, P.; Singh, M.; *J. Chem. Res.*, **13**, 1979 (38).
- ¹⁰⁶Beck, W.; Wanjack, I.; Polborn, H.; Kramer, R.; *Chem. Ber.*, **123**, 1990 (767).
- ¹⁰⁷Kozłowski, H.; Petitt, L.D.; *Studies in Inorg. Chem.*, **11**, 1991 (530-545).

Chapter 2. Oxidative Addition of Amino Acids

2.1 Introduction

While the complexes of amino acids with platinum and palladium metals have been studied in considerable detail, there has been much less effort directed toward those of the remaining platinum metals. The binding of amino acids to an iridium center has been demonstrated by Beck et al.¹ The work done by Beck and the initial studies conducted by Ladipo supported the proposal that reactions of amino acids would react with the iridium center that is used in the Merola Group, $[\text{Ir}(\text{COD})(\text{PMe}_3)_3]\text{Cl}$. (Figure 2.1)

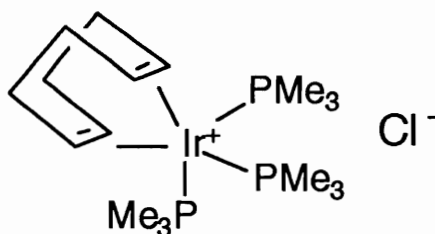
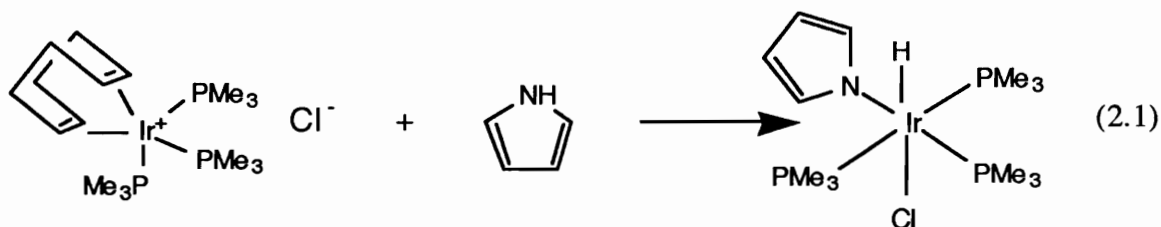
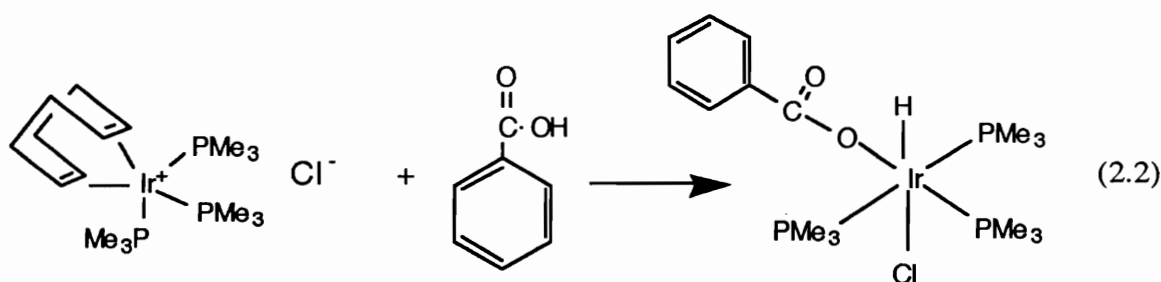


Figure 2.1 $[\text{Ir}(\text{COD})(\text{PMe}_3)_3]\text{Cl}$

Ladipo showed that compounds that contained an amine could oxidatively add to the iridium center to form amino-hydrido complexes.² In the case of pyrrole the following addition was seen. (Equation 2.1)



Dr. Ladipo also did work with the oxidative addition of carboxylic acids to the iridium center. In the case of benzoic acid the formation of a complex that underwent an O-H oxidative addition was identified.³ (equation 2.2)



It is obvious from the work done by Dr. Ladipo that N-H and O-H additions are feasible with the iridium system used in the Merola group. It became of interest to see what would happen if we attempted to add a compound that had both an amine and a carboxylic acid. Nature had supplied us with a source of compounds with these functionalities: amino acids.

2.2 Results and Discussion

α -Amino acids which are of the general structure: (Figure 2.2)

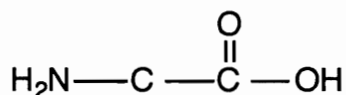
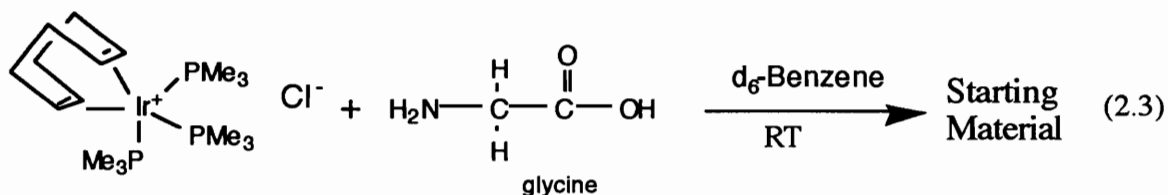


Figure 2.2 General structure of α -amino acids

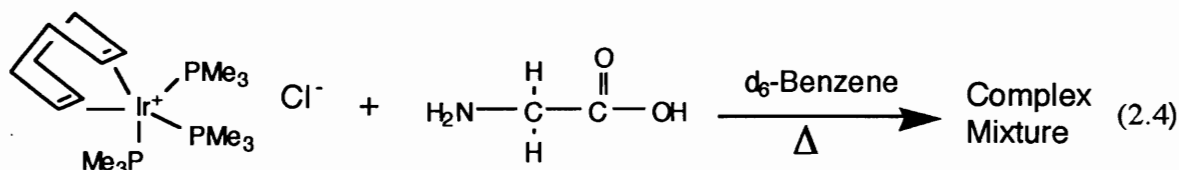
have both amine and carboxylic acid functionalities. Both groups have the capability of oxidatively adding to the metal center and it was of interest to us to examine just how these compounds would add.

From the literature it is known that amino acids have a number of possible binding modes.⁴ The potential to bind through the N terminus, the O terminus, or the ability to chelate to the metal center to form metallacycles have all been demonstrated. It is also important to point out at this time that there are very few examples of amino acid-iridium complexes in the literature, but out of all the examples shown, there are no examples of platinum metal-amino acid hydride complexes. Such hydride complexes could have some very interesting catalytic uses and this thesis reports the first examples of amino acid hydride iridium complexes.

The initial attempts to add the amino acids oxidatively to the metal center were done in benzene at room temperature (equation 2.3) with glycine, the simplest amino acid. NMR studies of this reaction indicated that after days of sitting at room temperature no reaction had occurred.



When the same reaction was attempted with heating, (equation 2.4) a complex NMR spectrum was obtained, indicating a variety of products had formed.



A number of problems were associated with these initial attempts to add the amino acid to the metal. The first of these problems is the insolubility of the amino acid in most organic solvents. Thus, in the initial attempts with glycine and [Ir(COD)(PMe₃)₃]Cl in benzene the interaction of the amino acid and the iridium center was minimal. The heating of the reaction mixture presents another problem when attempted in benzene. It has been demonstrated in the Merola group that C-H activation of benzene occurs on heating of [Ir(COD)(PMe₃)₃]Cl in a benzene solution.⁵ In the case of glycine in d₆-benzene with [Ir(COD)(PMe₃)₃]Cl the possibility of competition between the oxidative addition of glycine and benzene could account for the complex mixture of products observed in the ¹H NMR spectrum.

The problem of solubility is easily overcome by attempting the reaction in D₂O. Since water is an excellent solvent for most amino acids. Surprisingly, water is also an excellent solvent for the [Ir(COD)(PMe₃)₃]Cl complex.^{5a} In solution the amino acid exists in zwitterionic form. (Figure 2.3)

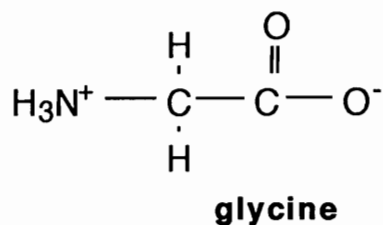


Figure 2.3 Zwitterionic form of glycine

Therefore, the next set of NMR studies was done in D₂O because of the enhanced solubility of the reactants in that medium. This enhanced solubility is readily apparent in the initial ¹H NMR spectrum (Figure 2.4) The spectrum clearly shows the resonances due to the [Ir(COD)(PMe₃)₃]Cl complex: The resonance at δ 1.5 ppm is due to the protons of the trimethylphosphines of the fluxional complex. The signals at 2.1 ppm and 2.4 ppm the broad singlet at 3.3 ppm correspond to the protons of the attached 1,5-cyclooctadiene. The resonances at 2.2 and 2.4 are due to the aliphatic protons on coordinated COD. The singlet resonance at 3.3 ppm corresponds to the olefinic protons of the cyclooctadiene. The presence of glycine in solution is also clear from the spectrum. The singlet at 3.5 ppm is the resonance due to the protons on the α- carbon.

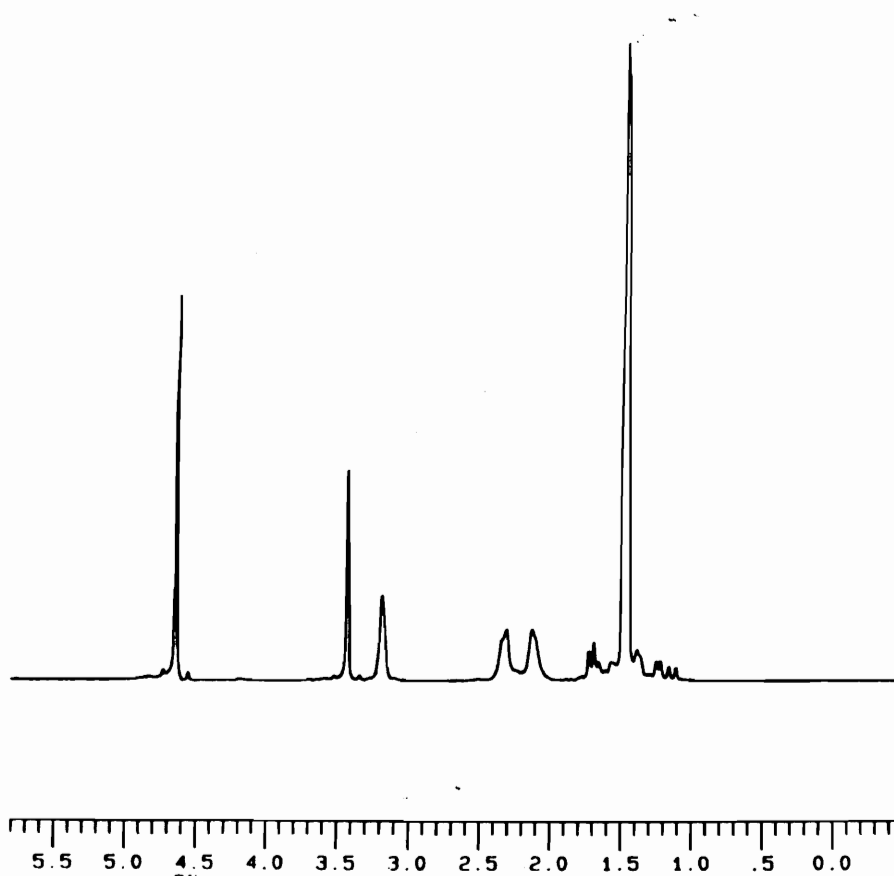
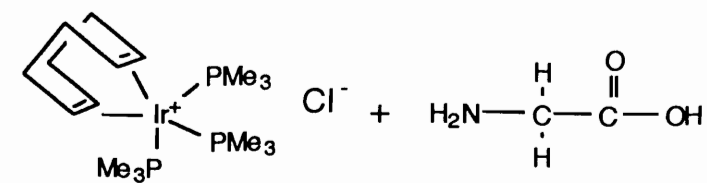


Figure 2.4 Initial ^1H NMR spectrum of glycine with $[\text{Ir}(\text{COD})\text{PMe}_3]_3\text{Cl}$ in D_2O (270MHz)

If the reaction tube is allowed to sit at room temperature for days, no reaction occurs. On heating to 50°C, again no reaction can be observed as indicated by ¹H-NMR spectroscopy. If the solution is then heated and allowed to remain at 100°C for 18 hours, a reaction does occur resulting in the final NMR spectrum shown in Figure 2.5. In this spectrum the resonances of the trimethylphosphine are a virtual triplet and a doublet indicative of a meridional arrangement of phosphines in the octahedron. The virtual triplet results from the set of phosphines trans to one another, the methyl protons are coupled to the phosphorous to which they are bound and then coupled to the phosphorous trans to that phosphorous arising from communication through the metal center. The doublet corresponds to the methyl protons of the cis phosphine in which the protons are only coupled to the phosphorous that is attached to the methyl groups. From the spectrum it is obvious that the 1, 5-cyclooctadiene resonances are no longer observed, showing that the cyclooctadiene has been lost in the oxidative addition of the amino acid. The free cyclooctadiene resonance is not seen due to the insolubility of COD in water. The resonance at 3.5 ppm corresponding to the methylene protons of glycine is still seen since an excess of amino acid was used in the study. A new resonance shifted upfield from the methylene protons of the excess amino acid corresponds to the methylene protons of the *bound* amino acid. A resonance occurs at -19.09 ppm corresponding to a hydride. The chemical shift is consistent with a hydride that is trans to an electronegative atom such as N or O; a further upfield shift would indicate a hydride being trans to chlorine.⁶ An

interesting result of the ^1H NMR studies is the observance of the hydride in the spectrum. This observation supports evidence that will be presented later on the mechanism of formation of the complexes. The hydride resonance gives a great deal of information about the structure of the amino acid complex.

The fact that the resonance is a quartet signifies that the hydride is cis to three phosphines, confirming the meridional arrangement of the phosphines in the octahedron.

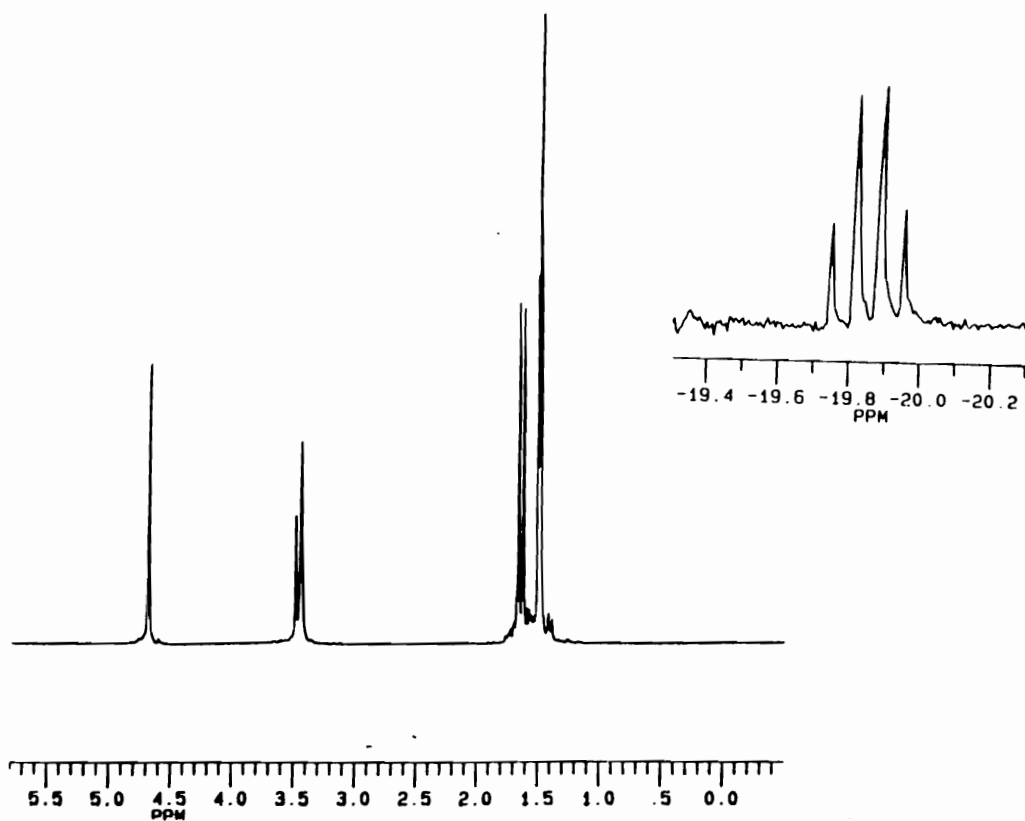
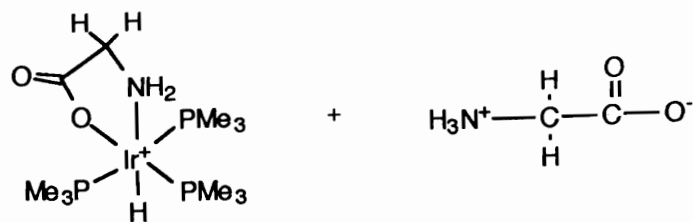


Figure 2.5 Final ^1H NMR spectrum of the glycine study in D_2O
(270 MHz)

The binding mode of glycine was determined to involve chelation through both the N-terminus and the O-terminus to the iridium metal center. After inspection of the $^1\text{H-NMR}$ data it was proposed that the structure of the amino acid product was: (Figure 2.6)

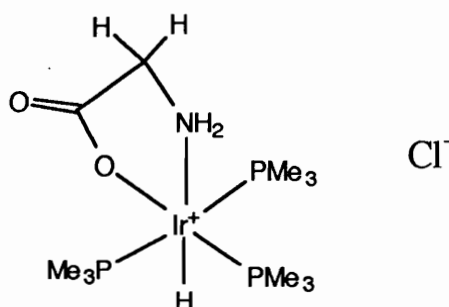
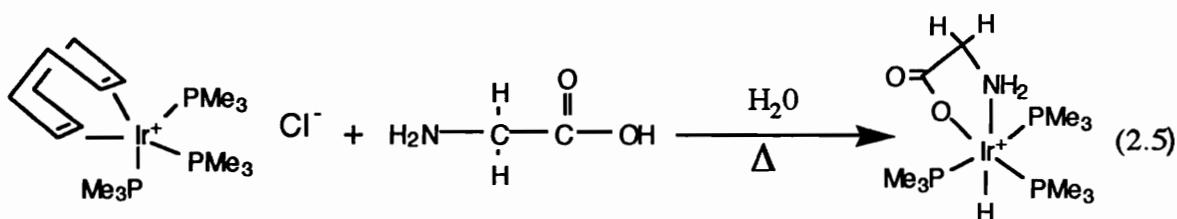


Figure 2.6 Proposed amino acid iridium complex

Additional information was needed in order to determine whether this structure was correct. The $^1\text{H-NMR}$ data supported the proposed structure. The reaction was so clean that a preparative scale reaction of glycine with the $[\text{Ir}(\text{COD})(\text{PMe}_3)_3]\text{Cl}$ complex was attempted. (equation 2.5)



The reaction mixture was allowed to stir in H₂O at 100°C for 18 hours. The solvent was then removed in vacuo to yield product and excess amino acid. The fact that the amino acids have limited solubility in most organic solvents allowed for rather simple isolation of the product. The iridium complex was soluble in methylene chloride while the amino acid was not. The product was extracted with methylene chloride and filtered from the excess amino acid using cannula techniques. Then by removing the solvent in vacuo pure product was obtained in 95% yield.

The ³¹P NMR data also supports that the complex has a meridional arrangement of phosphines in the octahedron. (Figure 2.7) The resonances observed for the phosphines are a triplet and doublet. The triplet is indicative of the cis PMe₃ coupling to the two mutually trans phosphines. The doublet is indicative of the trans phosphines coupling to each other by communication through the metal. The ¹³C NMR data also supports the structure proposed. (Figure 2.8) The phosphine region of the ¹³C NMR spectrum shows resonances of a doublet and virtual triplet. The virtual triplet is indicative of trans phosphines; the carbon couples to both the phosphorous it is bound to, and the phosphorous trans to it. The doublet is indicative of the methyls of cis phosphine which only exhibits coupling due to the carbon and the phosphorous to which it is bound. The resonance at 42 ppm is due to the CH₂ backbone of the amino acid and the resonance at 187 ppm corresponds to the carboxyl group carbon.

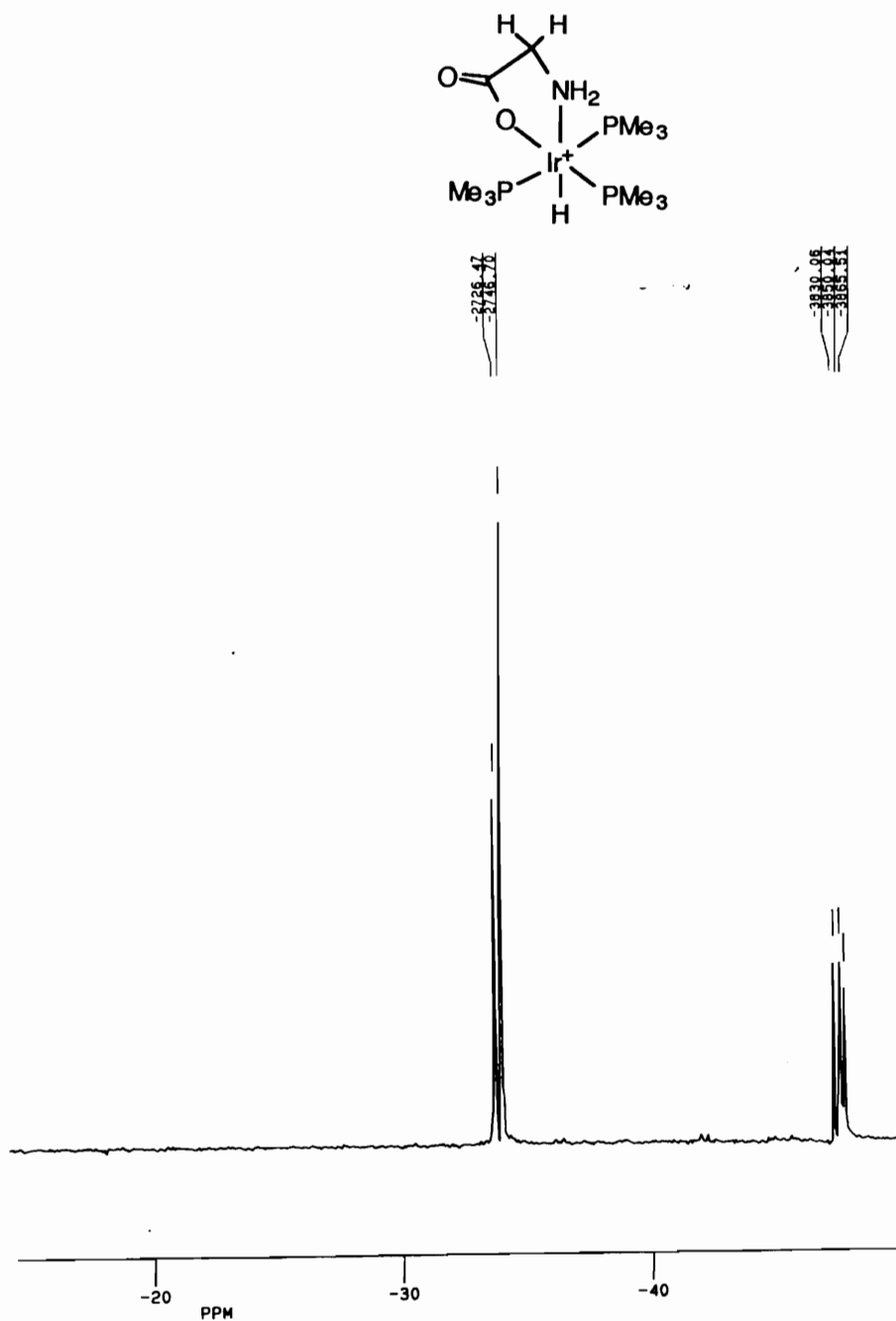


Figure 2.7 Phosphorus-31 NMR spectrum of $[\text{Ir}(\text{COD})(\text{gly})(\text{PMe}_3)_3]\text{Cl}$ in CDCl_3 (80 MHz)

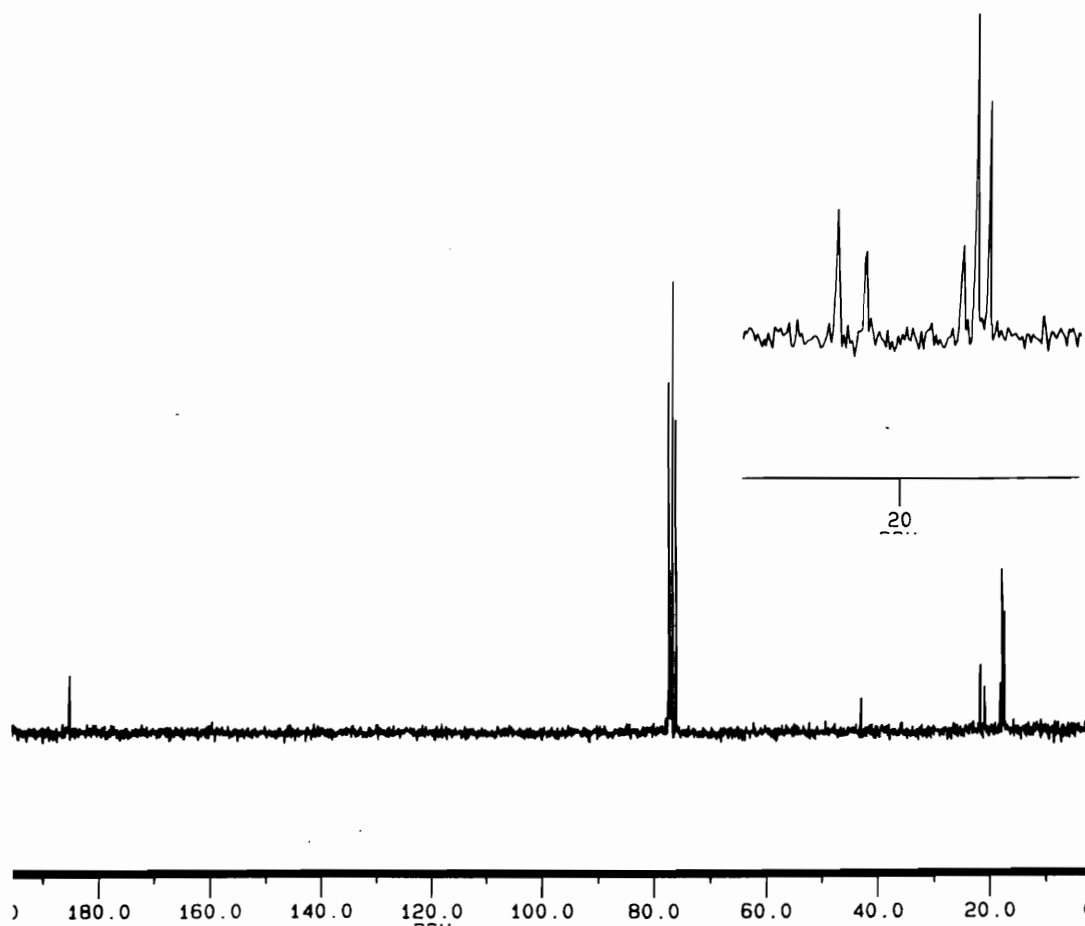
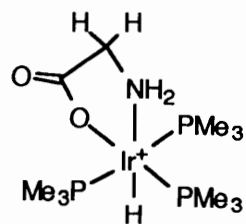


Figure 2.8 Carbon-13 NMR spectrum of [Ir(gly)(H)(PMe₃)₃] in CDCl₃ (50 MHz)

The next step involved study of the reaction of a chiral amino acid with $[\text{Ir}(\text{COD})(\text{PMe}_3)_3]\text{Cl}$. The choice was completely arbitrary, but *l*-valine became the next amino acid of the study. (Figure 2.9)

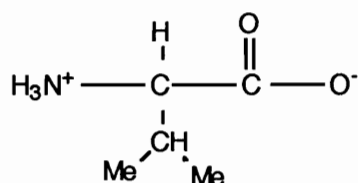


Figure 2.9

Valine

The isopropyl group of *l*-valine gives it a distinctive NMR "marker" in determining its binding to the metal. The NMR study is quite similar to that carried out with glycine in that the starting complex and the amino acids are easily discerned. The free amino acid resonances are easily observed in D_2O . (Figure 2.10) The resonances at 0.82 ppm correspond to the diastereotopic methyl protons of the isopropyl group. The multiplet partially obscured by COD resonances at 2.1 ppm is due to the methine proton of the isopropyl moiety, and the doublet at 3.53 ppm is the resonance for the methine proton of the α -carbon. The resonances of the $[\text{Ir}(\text{COD})(\text{PMe}_3)_3]\text{Cl}$ complex protons are identical to those described for the glycine ^1H NMR study.

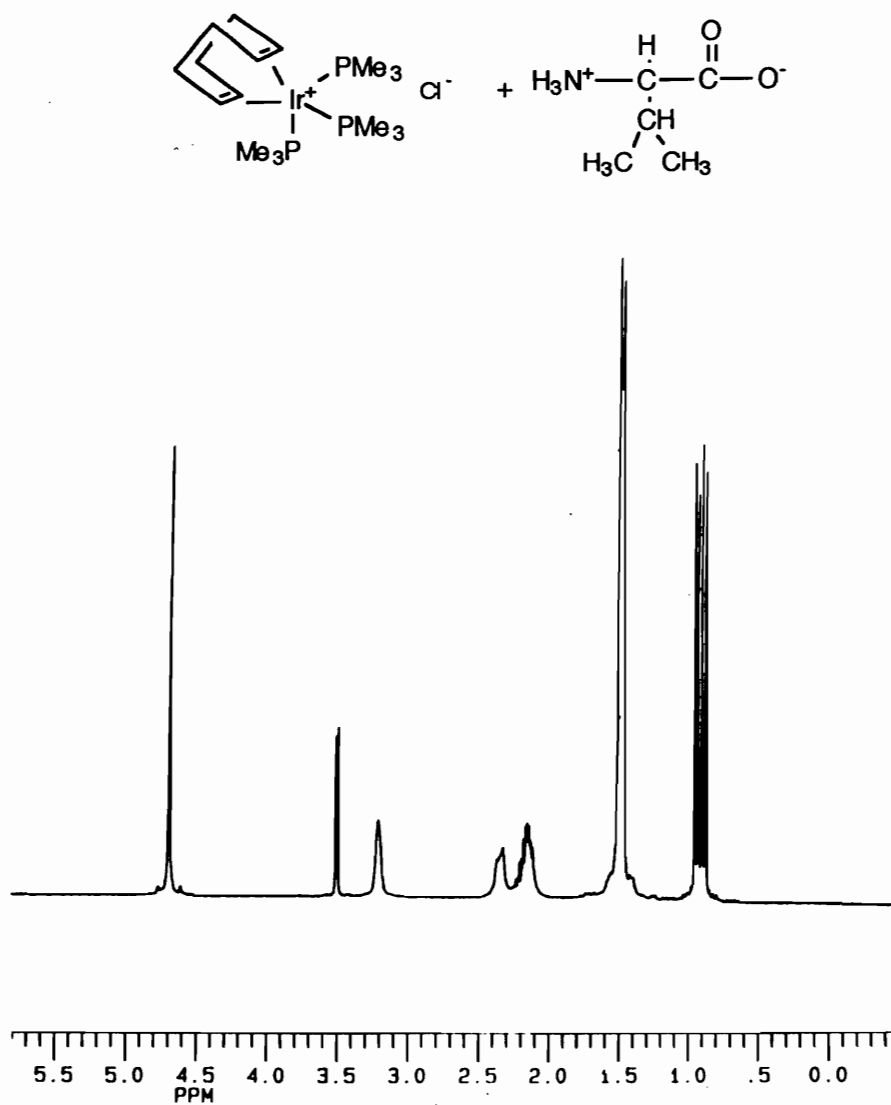


Figure 2.10 Initial ^1H NMR spectrum of valine and $[\text{Ir}(\text{COD})(\text{PMe}_3)_3]\text{Cl}$ in D_2O (270 MHz)

On heating the solution at 100°C overnight, the following ^1H NMR spectrum is obtained. (Figure 2.11)

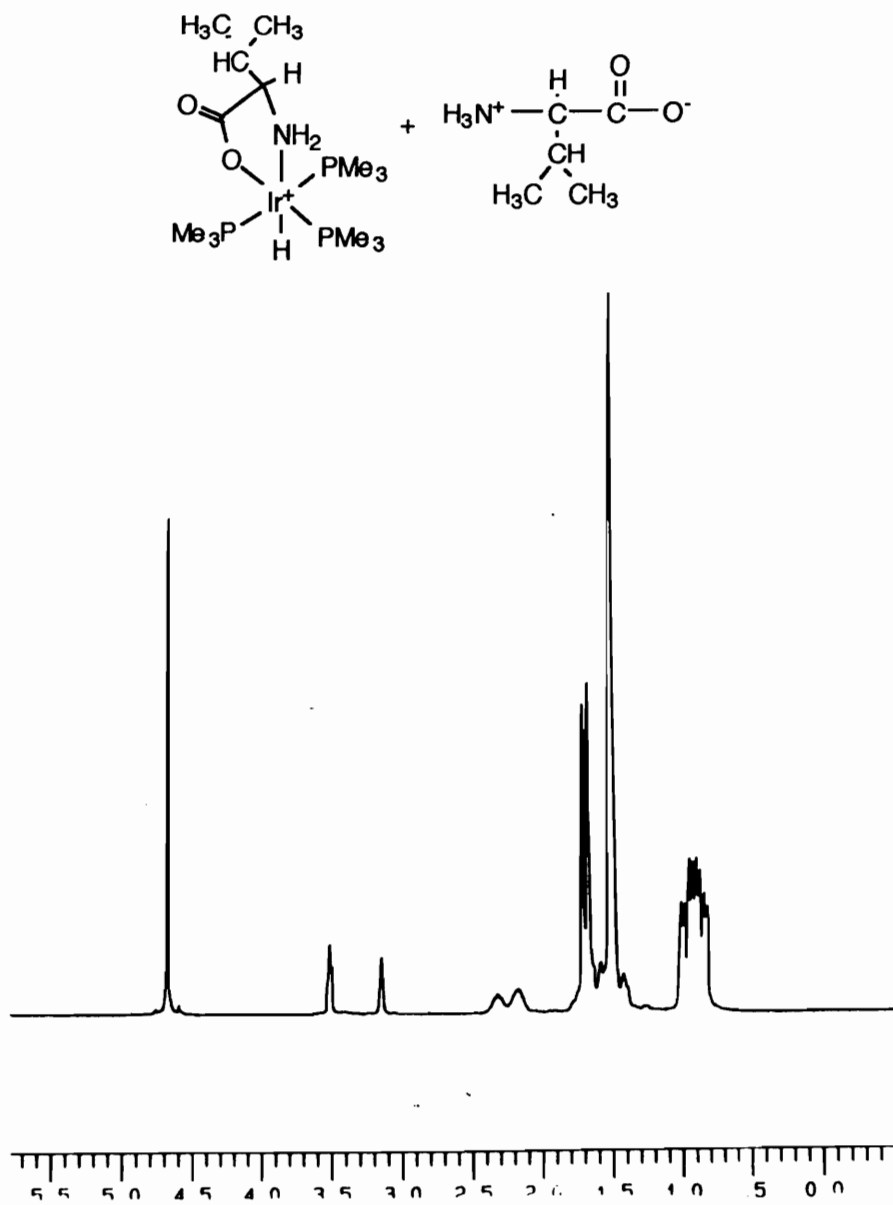


Figure 2.11 Final ^1H NMR spectrum of valine and $[\text{Ir}(\text{COD})(\text{PMe}_3)_3]\text{Cl}$ in D_2O (270 MHz)

In the ^1H -NMR spectrum shown (Figure 2.11) the virtual triplet and doublet resonances of the methyl protons on the phosphorous again indicate the meridional arrangement of the phosphines in the octahedron. The isopropyl methyl groups of the bound valine molecule are now two distinct sets of doublets, one shifted upfield and the other shifted downfield, bordering the original resonances of the free valine isopropyl methyl protons. The methine proton resonance of the isopropyl group of the bound valine is a multiplet shifted downfield slightly, and the methine proton of the α -carbon remains a doublet shifted slightly upfield from its free amino acid counterpart. The hydride resonance of the *l*-valine product is again a quartet shifted upfield to -19.71 ppm. This resonance supports the meridional arrangement of phosphines in the octahedron and the fact that the hydride is trans to an electronegative atom such as N or O.

A preparative scale synthesis of the *l*-valine product was undertaken using the same conditions as that of the NMR study. On workup the complex was easily removed from excess amino acid by extraction with methylene chloride. The solution was removed in vacuo to yield clean $[\text{Ir}(\textit{l}\text{-val})(\text{H})(\text{PMe}_3)_3]\text{Cl}$. (Figure 2.12)

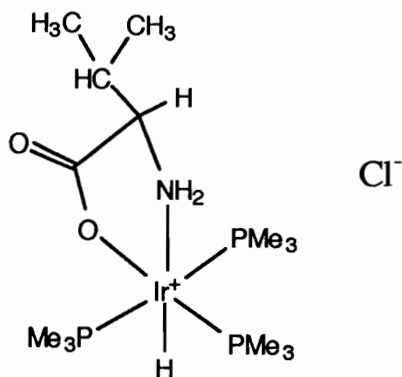


Figure 2.12 $[\text{Ir}(\text{val})(\text{H})(\text{PMe}_3)_3]\text{Cl}$

In order to unambiguously determine the structure of the hydrido iridium amino acid compounds, a crystal structure was desired. Crystals were grown of the valine chloride complex by using a two solvent method. The complex was dissolved in methylene chloride and then ether was layered over the top of the solution. The slow diffusion of ether forced the growth of crystals over a period of days. On removal of the crystals from the solvent they became opaque and were not usable for X-ray diffractometry. This behavior is not uncommon for salts which have a large size mismatch between the cation and anion. In order for a crystal lattice to form properly, solvent molecules are often incorporated in voids caused by cation/anion size mismatch. When crystals are removed from solvent, the solvent in the lattice evaporates and the crystal lattice decomposes. The problem may sometimes be overcome by exchange of the smaller anion for a larger one, closer in size to the cation. Hexafluorophosphate, PF_6^- , can often fulfill that role. The PF_6^- salt of the valine complex was made by treatment of an aqueous solution of the chloride complex with K^+PF_6^- . The PF_6^- salt immediately precipitated

from the solution and was removed from the aqueous solution using cannula filtration techniques.

The PF_6^- salt was then dissolved in methylene chloride and ether was layered over the top. The slow diffusion of ether into the methylene chloride layer caused the slow growth of crystals over a period of days. The solvent removal had no effect on the crystals and the structure was solved for the $[\text{Ir}(\ell\text{-val})(\text{H})(\text{PMe}_3)_3]\text{PF}_6^-$ salt. (Figure 2.13)

$[(\text{Me}_3\text{P})_3\text{Ir}(\text{H})(\ell\text{-val})]\text{PF}_6$ crystallizes in the tetragonal space group $P4_3$ with $a = 14.327(3)\text{\AA}$, $c = 14.397\text{ \AA}$, $V = 2955.3(16)\text{\AA}^3$ and $d_{\text{calcd}} = 1.534\text{ Mg/m}^3$ for $Z = 4$. The resulting ORTEP plot is shown in Figure 2.13. The solid state structure of the complex confirmed the structure assigned by spectroscopy: an octahedral arrangement of ligands with the three PMe_3 groups arranged meridionally around the metal. The Ir-O distance of $2.126(10)\text{\AA}$ is comparable to that of the η^1 -benzoate Ir ($2.123(7)\text{\AA}$) complex reported by Ladipo.⁶ The lengths of the coordinated and uncoordinated C-O bonds are in line with those reported by Ladipo. The Ir-N bond length of $2.190(11)\text{\AA}$ is considerably longer than that of the indole - iridium complex prepared by Ladipo. This lengthening of this bond is the result of chelation and the strong trans influence of the hydride. The relatively short Ir-P distance for the PMe_3 trans to the carboxylate oxygen ($2.252(4)\text{\AA}$) compared to the mutually trans PMe_3 bond lengths of $2.345(4)\text{\AA}$ and $2.349(4)\text{\AA}$ indicates that the carboxyl group does not exert as strong a trans influence as PMe_3 . The hydride was not found in this experiment. It would be located in the open position trans to the nitrogen atom of the chelate ligand.

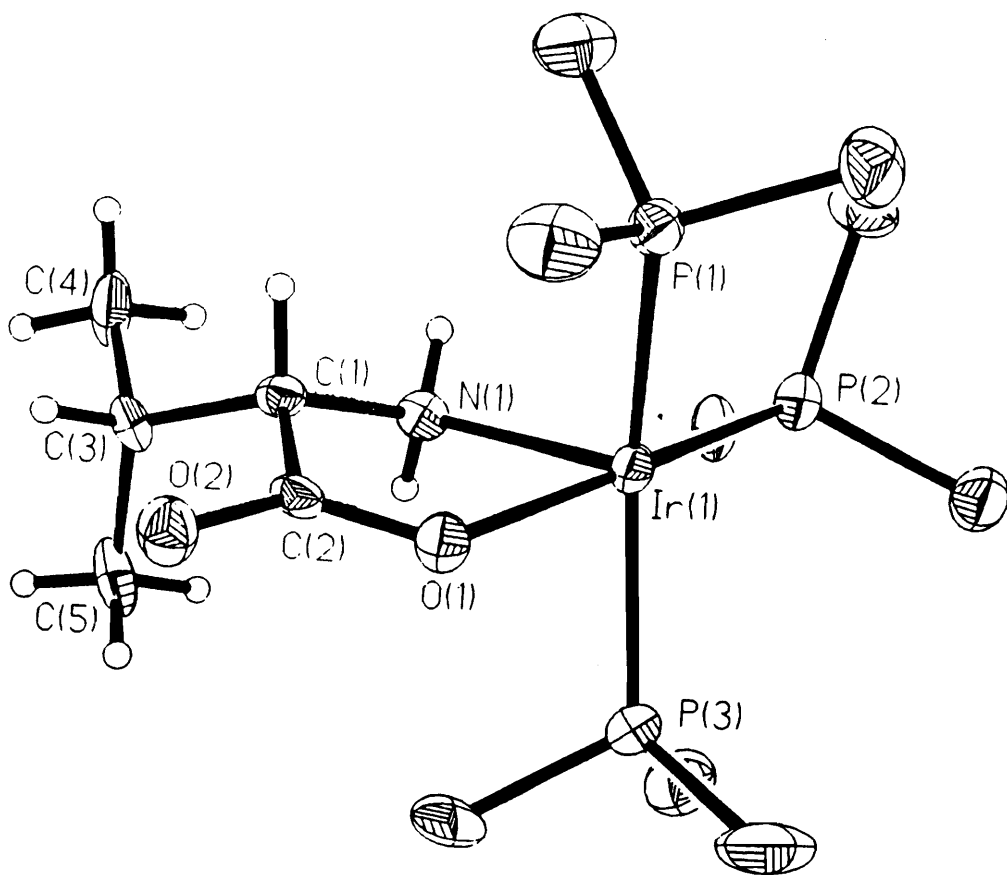


Figure 2.13 ORTEP plot of $\text{Ir}(\text{val})(\text{H})(\text{PMe}_3)_3$

A number of complexes of naturally occurring amino acids were prepared in D₂O studies similar to those described previously. One of the more interesting amino acids that was used in this study was *l*-proline. (Figure 2.14) This naturally occurring amino acid is the only one that has a ring containing its amine group.

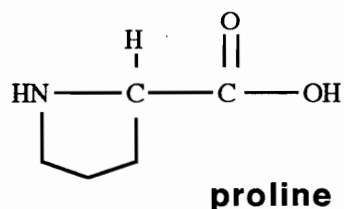
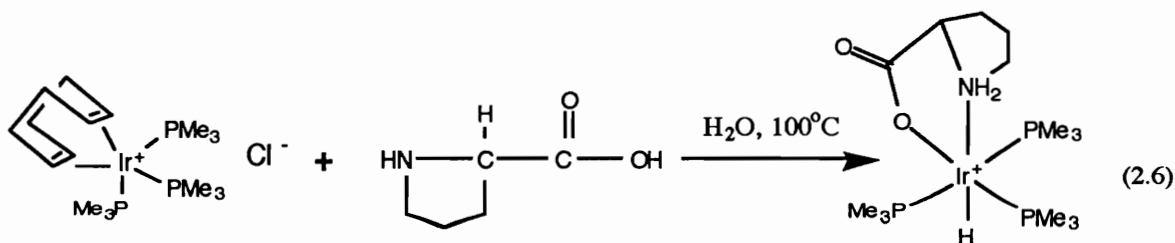


Figure 2.14

A preparative scale reaction between proline and [Ir(COD)(PMe₃)₃]Cl (equation 2.6) was carried out using reaction conditions and work-up identical to those used in the glycine and valine experiments.



The ¹H-NMR spectrum of the proline product displayed three resonances of doublets in the methyl phosphine region, indicating that there was no longer a plane of symmetry running between the trans phosphines.

The hydride resonance still remained a quartet at -20.33 ppm giving evidence for a hydride being cis to three phosphines, which would correspond to a meridional arrangement of phosphines in the octahedron. Examination of the structure of the proline complex explained the variations observed for the trimethyl phosphine resonances (Figure 2.15)

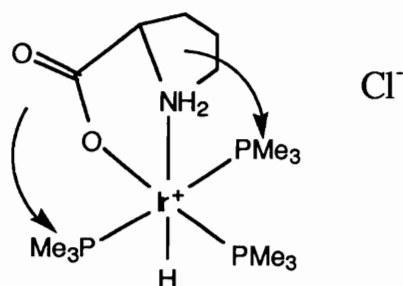


Figure 2.15 Structure of proline complex

The arrangement of the phosphines and the chelating side group causes an inequivalence in the environment of the trans phosphines. This makes all three sets of phosphines inequivalent and gives rise to the three sets of doublets in the ¹H-NMR spectrum.

A structure of [Ir(pro)(H)(PMe₃)₃]PF₆ was obtained, (Figure 2.16) The PF₆⁻ salt of the proline product was synthesized in a manner analogous to that of the valine complex.

$[(\text{Me}_3\text{P})_3\text{Ir}(\text{H})(\ell\text{-pro})]\text{PF}_6$ crystallizes in the monoclinic space group $P2_1$ with $a = 10.824(2)\text{\AA}$, $b = 20.021(4)\text{\AA}$, $c = 11.856(2)\text{\AA}$, $V = 2562.1(7)\text{\AA}^3$, and $d_{\text{calcd}} = 1.764 \text{ Mg/m}^3$ for $Z = 4$. The solid state structure of $(\text{Ir}(\text{pro})(\text{H})(\text{PMe}_3)_3)\text{PF}_6$ confirmed the structure assigned by spectroscopy: an octahedral arrangement of ligands about the iridium with the three PMe_3 ligands arranged meridionally around the metal. The Ir-N bond length for this compound $(2.211(7)\text{\AA})$ was predicted to be longer than the valine complex because of the added steric congestion at the nitrogen atom. This prediction was correct with the Ir-N bond length of the valine complex being shorter at $2.190(11)\text{\AA}$. Of course this difference in bond lengths seems insignificant when experimental error is taken into account. The Ir-O bond of $2.118(7)\text{\AA}$ is consistent with the length reported for the valine complex. The O-Ir-N bond angle in both cases is very close in value. This bond angle for the valine complex is $77.6(4)^\circ$ as compared to $79.8(3)^\circ$ for the proline complex. The hydride was not located in this experiment, but would be located in the open coordination site trans to the amino group.

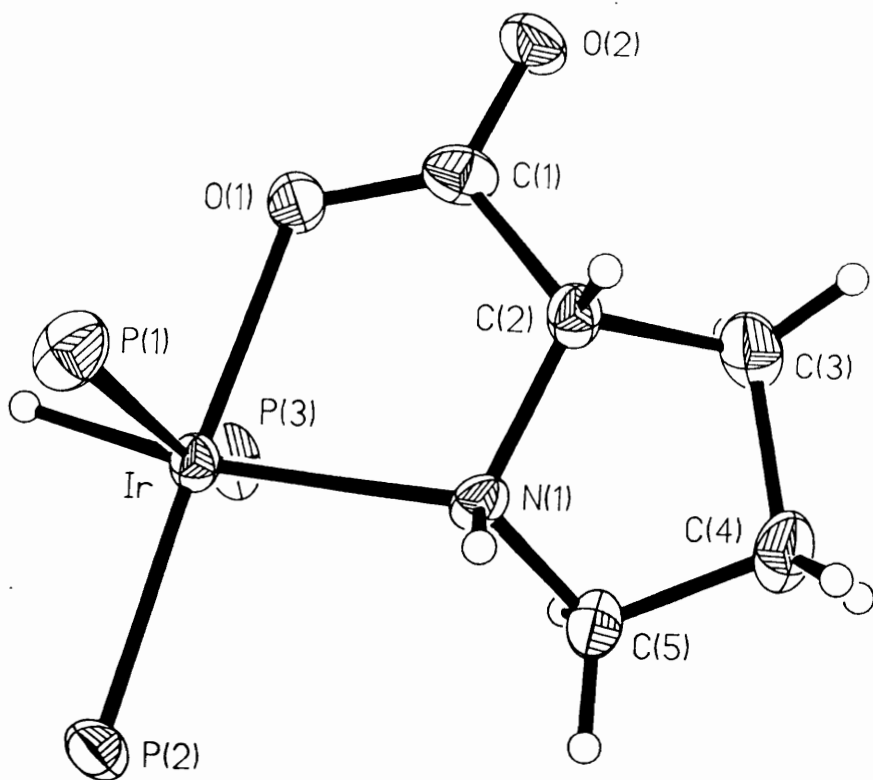


Figure 2.16 ORTEP plot of [Ir(pro)(H)(PMe₃)₃]Cl

(methyl groups on PMe₃ ligands omitted for clarity)

The study went on to investigate reaction with a number of the common amino acids and all were prepared in preparative scales or at least characterized by $^1\text{H-NMR}$ studies. The common amino acids that have no side functionalities such as sulfur, or another nitrogen functionality gave clean products in the $^1\text{H-NMR}$ studies and were synthesized in preparative quantities. All of these complexes gave 5-membered iridacycles that were formed by binding the metal through the nitrogen terminus and the oxygen terminus of the amino acids. The complexes were all hydride complexes and the phosphines were always arranged meridionally around the octahedron. (Figure 2.17)

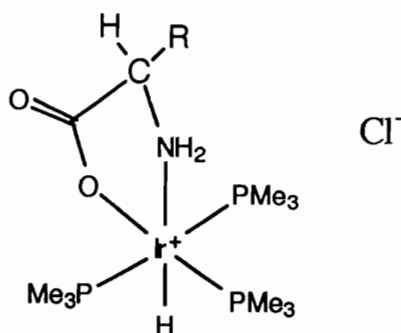
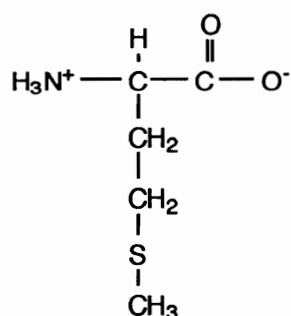


Figure 2.17 General structure of amino acid complexes made

Table 2.1 Naturally Occurring Amino Acids Products Characterized

Amino Acid Reaction attempted	Ir product Characterized
glycine	C, H analysis, H NMR, P NMR, C NMR
l-valine	C, H analysis, H NMR, P NMR, C NMR
l-proline	C, H analysis, H NMR, P NMR, C NMR
l-alanine	C, H analysis, H NMR, P NMR, C NMR
l-tyrosine	C, H analysis, H NMR, P NMR, C NMR
l-tryptophan	C, H analysis, H NMR, P NMR
l-serine	C, H analysis, H NMR, P NMR, C NMR
l-threonine	C,H analysis, H NMR, P NMR
picolinic acid	H NMR
pipecolic acid	H NMR
l-histidine	H NMR

There are a number of naturally occurring amino acids that have more functionalities that may bind to the metal center and these compounds were introduced into the study as well. The first of these amino acids studied was *l*-methionine. (Figure 2.18)

**Figure 2.18** Sulfur containing amino acid (methionine)

This amino acid has a sulfur that could indeed bind to the metal and form a six-membered ring with the amine chelating to the metal. There are a number of examples of the formation of six-membered ring systems

with platinum metals and methionine,⁸ A recent example of this is the reaction of K_2PtCl_4 and methionine to form the chelate complex shown in Figure 2.19.⁹

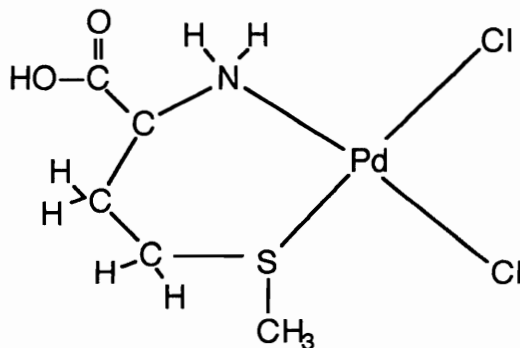
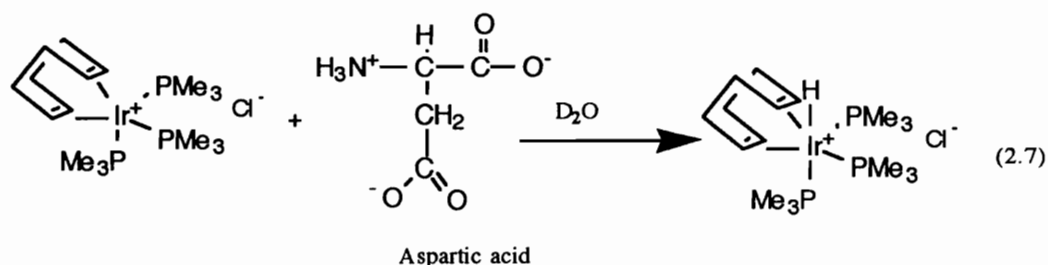


Figure 2.19 Methionine chelate complex

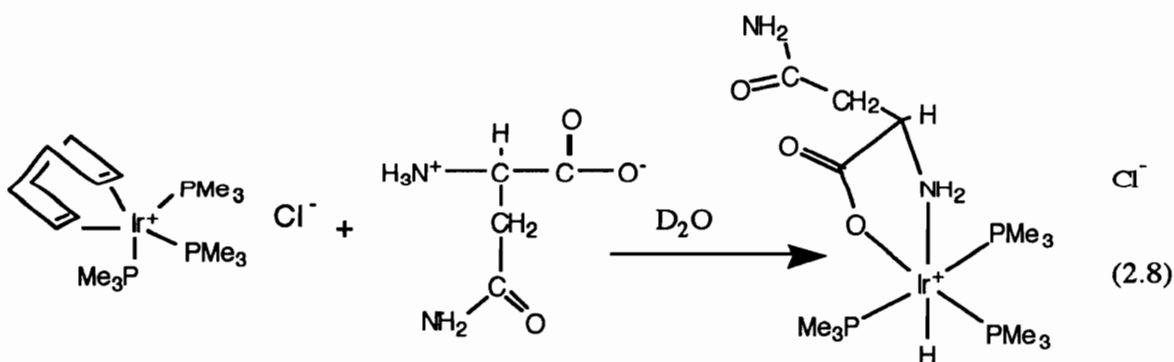
In the case of the reaction between methionine and $[Ir(COD)(PMe_3)_3]Cl$ the ¹H NMR study showed a complex mixture of products being formed. This indicates that a number of binding modes could be observed between the amino acid and the metal center. The reaction was not attempted on a preparative scale due to the complexity of the NMR spectrum of the products of the preliminary study.

The other amino acid that was studied which contained a sulfur atom with potential to bind to the metal center was cysteine.(Figure 2.20)

In the reaction between aspartic acid and $[\text{Ir}(\text{COD})(\text{PMe}_3)_3]\text{Cl}$, the initial NMR spectrum on addition of aspartic acid showed the formation of protonated $[\text{Ir}(\text{COD})(\text{PMe}_3)_3]\text{Cl}$.^{5a}(equation 2.7)



On heating the reaction mixture a complex mixture of products was observed. Again, the additional carboxylic acid functionality must be playing some role in binding to the metal center. On the other hand, the asparagine reaction was clean and the ^1H -NMR study showed the expected resonances for the formation of a meridional hydride amino acid metallocycle product.(equation 2.8)



The formation of the 5-membered ring system is favored over the 6-membered ring system based on two reasons. The first of these reasons is the fact that 5-membered ring systems are more stable in metallocycle systems.¹⁰ The second possible reason is the failure to form 6-

membered ring systems with β -alanine. The most important factor is the lowered basicity of the nitrogen of the amide group. (Figure 2.22)

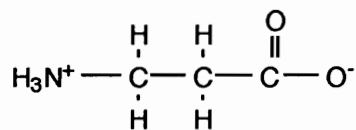


Figure 2.22 Chelation of β -alanine will form a six membered ring system.

The reaction between this amino acid and the metal center gave a complex mixture of products. This along with the difficulty in obtaining a clean product with salicylic acid (another acid that would form a 6-membered ring on chelation) led us to believe that formation of cyclic systems of 6 members or more was difficult.^{10a} Since the formation of 6-membered rings was difficult the conclusion followed that asparagine has also bound through the amine nitrogen and the carboxylic acid to form the 5-membered ring system.,

l-Histidine is another interesting amino acid This acid has an imidazole ring which contains nitrogen that is quite basic. The work done by Caubet et al. showed that histidine does indeed bind to Pd through the imidazole nitrogen and the amine nitrogen.¹¹ (Figure 2.23)

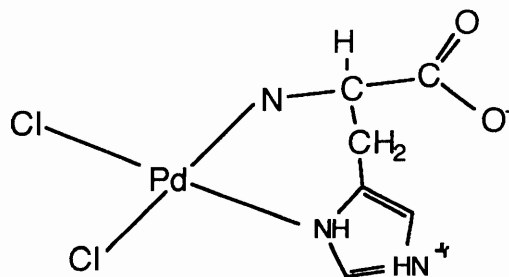
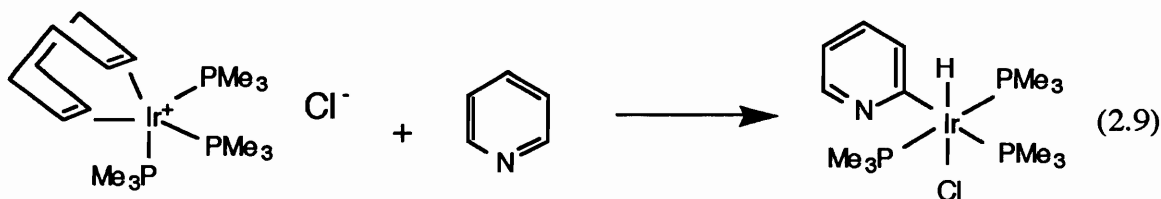


Figure 2.23 Palladium histidine complex

The synthesis of the $[\text{Ir}(\ell\text{-hist})(\text{H})(\text{PMe}_3)_3]\text{Cl}$ complex was clean. The $^1\text{H-NMR}$ spectrum resembled the expected 5-membered metallacycle product obtained for all other amino acid products. The literature examples of histidine and platinum metal complexes consistently show binding of the amino acid to the metal through the amine nitrogen and the imidazole nitrogen to give a 6-membered metallacycle.^{11a,b,c} This complex needs to be studied further to elucidate its structure.

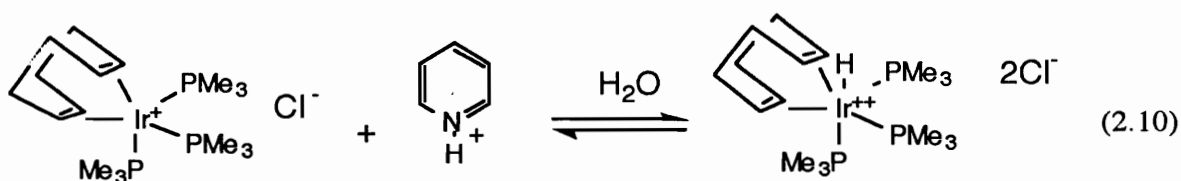
A final study to discuss in this chapter on the synthesis of these amino acid complexes is one that gave insight into the mechanism of formation of these complexes. It was known by the work done by H. Selnau in the Merola group that pyridine could undergo a C-H addition with the iridium metal center.¹² (equation 2.9)



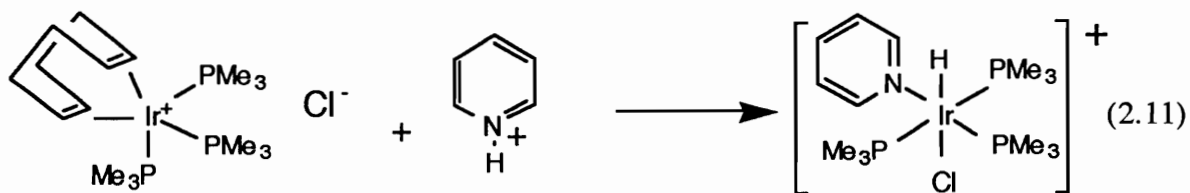
The study that gave insight into the mechanism of formation of the complexes was derived from the C-H addition of pyridine. The question

was what would happen if pyridinium chloride was reacted with the iridium system. Is a N-H activation be possible in this situation?

Pyridinium chloride was made by bubbling HCl through pyridine. The off-white precipitate was filtered from the solution using cannula techniques. The solids were dried under reduced pressure and used with no further purification. On initial treatment of $[\text{Ir}(\text{COD})(\text{PMe}_3)_3]\text{Cl}$ with pyridinium chloride the formation of the protonated $[\text{Ir}(\text{COD})(\text{PMe}_3)_3]\text{Cl}$ was observed in the NMR spectrum. (equation 2.10)



The protonation of the $[\text{Ir}(\text{COD})(\text{PMe}_3)_3]\text{Cl}$ was a surprising result in the fact that an already cationic species was being protonated to a dicationic species. Since pyridinium has a pKa of approximately 5.2, this means that the $[\text{Ir}(\text{COD})(\text{PMe}_3)_3]\text{Cl}$ has a pKa in the same vicinity. This gives an idea of the basicity of the $[\text{Ir}(\text{COD})(\text{PMe}_3)_3]\text{Cl}$ species. This also suggests that the first step in the formation of the amino acid complexes is the protonation of the iridium center. Heating the reaction to 100°C gives rise to NMR signals that correlate to the N-H oxidative addition product. (equation 2.11)



This reaction suggests that the mechanism of formation of the amino acid complexes may proceed first via the protonation of the iridium center, followed by the nucleophilic attack of the metal by the amino acid. The observation of the hydride resonance in the exploratory NMR reactions supports this postulation of protonation from the quaternary amine group and then nucleophilic attack at the metal center.

It is again worth pointing out that amino acid complexes are not novel. As the literature review pointed out there are numerous examples of amino acid complexes in the literature.¹³ These complexes are of interest because they are iridium amino acid complexes of which very few exist in the literature.¹⁴ The complexes that have been synthesized in this work are also novel because they are the first reported amino acid-hydride complexes of platinum metals. Complexes of this type are non-existent in the literature.

2.2.1 References

¹Beck, W.; Wanjack, I.; Polborn, H.; Kramer, R.; *Chem. Ber.*, **123**, 1990 (776).

²Ladipo, F.T; Merola, J.S; *Inorg. Chem.*, **29**, 1990 (4172) .

Matsumoto, K.; Ooi, S.; Kurova, H.; *J. Chem. Soc. Chem. Comm.* 1973(170).

¹²Selnau, H. Ph.D. Thesis, Virginia Polytechnic Institute and State U. 1991.

¹³Hay, R.W.; Nolan, K.B.; *Amino acids, Peptides and Proteins*, Chemical Society, London, 1991 (296).

¹⁴Beck, W.; Wanjack, I.; Polborn, H.; Kramer, R.; *Chem. Ber.*, **123**, 1990 (776).

2.2.2 Experimental

All reactions were carried out under an atmosphere of prepurified nitrogen. Air sensitive materials were stored in a drybox under N₂ atmosphere. All solvents were dried by the appropriate procedure and distilled under a nitrogen atmosphere prior to use. Conventional glass vessels were used and standard Schlenk line techniques were employed. IrCl₃ • 3 H₂O was purchased from Johnson Matthey. All amino acids were purchased from Aldrich and/ or Sigma Chemical Co. All other chemicals were reagent grade and were used without further purification.

The ¹H-NMR spectra were obtained on either a Bruker WP270SY or a WP200SY instrument. The ³¹P NMR data were obtained on a Bruker WP200SY (at 81 MHz) instrument and referenced to an internal standard of 85% H₃PO₄. ¹³C NMR spectra were obtained on a Bruker WP200SY (at

67 MHz) instrument. Elemental analyses were performed by Atlanta Microlab Inc. X-ray crystal structures were obtained using a Siemens R3m/v diffractometer and MoK α ($\lambda = 0.71071 \text{ \AA}$) radiation at 298 K.

Synthesis of [Ir(COD)(PMe₃)₃]Cl (Frazier, J.; Merola, J.S., *Polyhedron*, **11**, 1992 (2197).

A 250 mL flask equipped with a stir bar and septum was charged with 2 g (3 mmol) of [Ir(COD)Cl]₂ under N₂ in the drybox. The flask was then connected to a double manifold (vacuum/nitrogen) Schlenk line and 80 mL of distilled toluene was added to the flask via syringe. The clear red solution was stirred for 10 minutes to allow all solids to dissolve. The flask was then charged with 2 mL (6.1 equiv.) of PMe₃ via syringe. A cream - white precipitate formed immediately on addition of PMe₃. The heterogenous mixture was stirred for 12 hours. The solids were filtered under N₂ and washed with toluene and pentane. The solids were then dried under reduced pressure to yield 3.2 g (5.6 mmol, 95.5% yield based on amount of [Ir(COD)Cl]₂) of [Ir(COD)(PMe₃)₃]Cl identified on the basis of the following data:

¹H NMR (CDCl₃): δ 1.49 (m, 27H, PMe₃ ligands),
 2.25 (m, 8H, COD), 3.15 (br s, 4H,
 COD) ppm.

Exploratory reaction attempt between [Ir(COD)(PMe₃)₃]Cl and glycine in d₆ benzene (CPRI173)

Glycine (6 mg, 0.08 mmol) was placed in a screw-cap NMR tube equipped with a septum. The tube was placed in the drybox where it was charged with 20 mg (0.035 mmol) of [Ir(COD)(PMe₃)₃]Cl. Benzene - d₆ (0.5 mL) was then added via syringe outside of the drybox. The tube was shaken and monitored at room temperature by ¹H NMR spectroscopy. No reaction was observed. The reaction tube was heated to 50°C and monitored. The spectrum showed a complex mixture of products.

Initial reaction attempt between [Ir(COD)(PMe₃)₃]Cl and glycine in D₂O (CPRI175)

Glycine (6 mg, 0.08 mmol) was placed in a screw-cap NMR tube equipped with a septum. The tube was placed in the drybox where it was charged with 20 mg (0.035 mmol) of [Ir(COD)(PMe₃)₃]Cl. Benzene - d₆ (0.5 mL) was then added via syringe outside of the drybox. The tube was shaken and monitored at room temperature by ¹H NMR spectroscopy. No reaction was observed. The NMR tube was heated to 50°C and monitored for days; again with no reaction evident. On heating the reaction mixture to 100°C, a ¹H NMR spectrum was obtained after 18 hours. The [Ir(gly)(H)(PMe₃)₃]Cl product was indicated on the basis of the following data:

^1H NMR (D_2O): δ 1.51 (t, 18H, trans PMe_3), 1.65 (d, 9H, cis PMe_3), 3.43 (s, 2H, $-\text{CH}_2-$), -19.09 (q, 1H, Ir-H) ppm

Synthesis of $[\text{Ir}(\text{gly})(\text{H})(\text{PMe}_3)_3]\text{Cl}$ (CPRI185)

A 100 mL flask equipped with a stir bar and septum was charged with 90 mg (1.12 mmol) of glycine. The flask was then charged 300 mg (0.532 mmol) of $[\text{Ir}(\text{COD})(\text{PMe}_3)_3]\text{Cl}$ under N_2 in the drybox. The flask was then connected to a double manifold (vacuum/nitrogen) Schlenk line and 25 mL of distilled water was added to the flask via syringe. The solution was stirred magnetically and heated to reflux. After 18 hours at reflux, the reaction mixture was cooled and the solvent was removed in vacuo. The white solid residue was treated with distilled methylene chloride (3 x 10 mL) to extract the product from the excess amino acid. The solution was filtered from the solid using cannula techniques. The methylene chloride was removed in vacuo and the solids were dried under reduced pressure to yield 270 mg (0.51 mmol, 95.7% yield based on the amount of $[\text{Ir}(\text{COD})(\text{PMe}_3)_3]\text{Cl}$) of $[\text{Ir}(\text{gly})(\text{H})(\text{PMe}_3)_3]\text{Cl}$. $[\text{Ir}(\text{gly})(\text{H})(\text{PMe}_3)_3]\text{Cl}$ identified on the basis of the following data:

C,H analysis: Calculated for $\text{C}_{11}\text{H}_{32}\text{P}_3\text{NO}_2\text{IrCl}$: C, 24.9% H, 6.0%

Found: C, 24.7% H, 6.18%

^1H NMR (CDCl_3) δ 1.62 (vt, 18H, $J_{\text{P-H}} = 3.5$ Hz, trans PMe_3),
1.78(d, 9H, $J_{\text{P-H}} = 10.5$ Hz cis PMe_3) 3.39 (t, 2H,
- CH_2 -), 6.11 (br t, 2H, - NH_2), -19.15 (q, 1H, $J_{\text{P-H}}$
= 18.7 Hz, Ir-H) ppm

^{31}P NMR (CDCl_3) δ -47.52 (t, $J_{\text{P-P}} = 20\text{Hz}$, cis PMe_3), -33.78 (d,
 $J_{\text{P-P}} = 18\text{Hz}$, trans PMe_3) ppm

^{13}C NMR (CDCl_3) δ 18.71 (vt, $J_{\text{C-P}} = 10$ Hz, trans PMe_3), 20.63 (d,
 $J_{\text{c-p}} = 39$ Hz, cis PMe_3), 43.09 (s, - CH_2 -)
185.43 (s, - COO) ppm

Exploratory reaction between $[\text{Ir}(\text{COD})(\text{PMe}_3)_3]\text{Cl}$ and *l*-valine (CPRI177)

l-Valine (8.8 mg 0.075 mmol) was placed in a screw-cap NMR tube equipped with a septum. The tube was placed in the drybox where it was charged with 20 mg (0.035 mmol) of $[\text{Ir}(\text{COD})(\text{PMe}_3)_3]\text{Cl}$. D_2O (0.5 mL) was added via syringe outside the drybox. The tube was shaken and heated to 100°C . A NMR spectrum was obtained after 18 hours and the $[\text{Ir}(\textit{l}\text{-val})(\text{H})(\text{PMe}_3)_3]\text{Cl}$ product was identified on the basis of the following data:

^1H NMR (D_2O): δ 1.09 (d d, 6H, $-\text{CH}_3$ of isopropyl), 1.52 (t, 18H, trans PMe_3), 1.71 (d, 9H, cis PMe_3), 2.49 (m, 1H, $-\text{CH}-$ of isopropyl), 3.23 (d, 1H, $-\text{CH}-$ α proton of aa), -19.65 (q, 1H, Ir-H) ppm

Synthesis of $[\text{Ir}(\ell\text{-val})(\text{H})(\text{PMe}_3)_3]\text{Cl}$ (CPRI179)

A 100 mL flask equipped with a stir bar and septum was charged with 112 mg (0.972 mmol) of ℓ -valine. The flask was then charged 250 mg (0.443 mmol) of $[\text{Ir}(\text{COD})(\text{PMe}_3)_3]\text{Cl}$ under N_2 in the drybox. The flask was then connected to a double manifold (vacuum/nitrogen) Schlenk line and 20 mL of distilled water was added to the flask via syringe. The solution was stirred magnetically and heated to reflux. After 18 hours at reflux the solvent was removed in vacuo. The white solid residue was treated with distilled methylene chloride (3 x 10 mL) to extract the product from the excess amino acid. The solution was filtered from the solid using cannula techniques. The methylene chloride was removed in vacuo and the solids were dried under reduced pressure to yield 180 mg (0.315 mmol, 71.3% based on the amount of $[\text{Ir}(\text{COD})(\text{PMe}_3)_3]\text{Cl}$) of $[\text{Ir}(\ell$ -

val)(H)(PMe₃)₃]Cl. [Ir(*l*-val)(H)(PMe₃)₃]Cl identified on the basis of the following data:

C,H analysis: Calculated for C₁₅H₃₇NO₂P₃IrCl C, 29.0% H, 6.6%

Found: C, 28.74% H, 6.6%

¹H NMR (CDCl₃): δ 1.10 (dd, 6H, -CH₃- of isopropyl), 1.57 (vt, 18H, J_{P-H} = 5.6 Hz trans PMe₃) 1.65 (d, 9H, J_{P-H} = 5.8 Hz, PMe₃) 1.92 (d, 9H, J_{P-H} = 10.4 Hz cis PMe₃) 2.55 (m, 1H, -CH- of isopropyl) 2.98 (m, 1H, -CH- of α carbon), 3.22 (t, 1H, -NH) 6.91 (br t, 1H, -NH₂) 6.89 (br m, 1H, -NH). -19.10 (q, 1H, J_{P-H} = 17 Hz, Ir-H) ppm

³¹P NMR (CDCl₃): δ -49.35 (t, J_{P-P} = 20 Hz, cis PMe₃), -34.02 (d, J_{P-P} = 20 Hz, trans PMe₃) ppm

¹³C NMR (CDCl₃): δ 18.16 (t, J_{C-P} = 17 Hz, trans PMe₃), 21.17 (d, J_{C-P} = 37 Hz, cis PMe₃), 29.43 (s, -CH₃), 54.28 (s, -CH), 109.31 (s, -CH of isopropyl), 181.51 (s, -COO) ppm

Synthesis of [Ir(*l*-val)(H)(PMe₃)₃][PF₆]

An excess of K[PF₆] was dissolved in distilled water, this solution was added dropwise to solution of [Ir(*l*-val)(H)(PMe₃)₃]Cl in distilled water. A yellow - white precipitate formed immediately. The precipitate was filtered using cannula techniques. The solid was recrystallized from methylene chloride/ether. An X-ray structure of the crystals was obtained. (See appendix) (¹H NMR shows it to be identical to the Cl salt)

Exploratory reaction between [Ir(COD)(PMe₃)₃]Cl and *l*-proline (CPRI187)

l-Proline (9.0 mg, 0.078 mmol) was placed in a screw-cap NMR tube equipped with a septum. The tube was placed in the drybox where it was charged with 20 mg (0.035 mmol) of [Ir(COD)(PMe₃)₃]Cl. D₂O (0.5 mL) was added via syringe outside the drybox. The tube was shaken and heated to 100°C, a NMR spectrum was obtained after 18 hours. and the [Ir(*l*-pro)(H)(PMe₃)₃]Cl product was identified on the basis of the following data:

¹H NMR (D₂O): δ 1.55 (d, 9H, PMe₃), 1.75 (d, 9H, PMe₃) 1.91 (d, 9H, PMe₃) 2.21 (m, 2H, -CH₂-) 3.23(m, 2H, -CH₂-) 3.82 (m, 1H, α carbon) 4.0 (q, 2H, -CH₂-) ppm

Synthesis of [Ir(*l*-pro)(H)(PMe₃)₃]Cl (CPRI197)

A 100 mL flask equipped with a stir bar and septum was charged with 117.5 mg (1.02 mmol) of *l*-proline. The flask was then charged with 250 mg (0.443 mmol) of [Ir(COD)(PMe₃)₃]Cl under N₂ in the drybox. The flask was then connected to a double manifold (vacuum/nitrogen) Schlenk line and 20 mL of distilled water was added to the flask via syringe. The solution was stirred magnetically and heated to reflux. After 18 hours at reflux the reaction mixture was allowed to cool and solvent was removed in vacuo. The white solid residue was treated with distilled methylene chloride (3 x 10 mL) to extract the product from the excess amino acid. The solution was filtered from the solid using cannula techniques. The methylene chloride was removed in vacuo and the solids were dried under reduced pressure to yield 150 mg (0.263 mmol, 60.7% yield based on the amount of Ir(COD)(PMe₃)₃]Cl) of [Ir(*l*-pro)(H)(PMe₃)₃]Cl identified on the basis of the following data:

C,H analysis: Calculated for C₁₄H₃₆NO₂P₃IrCl: C, 29.4% H, 6.3%

Found: C, 29.17%; H, 6.2%

¹H NMR (CDCl₃): δ 1.45 (d, 9H, J_{P-H} = 6.3 Hz, PMe₃) 1.58 (d, 9H,
J_{P-H} = 6.6 Hz, PMe₃) 1.76 (d, 9H, J_{P-H} = 10.2 Hz
PMe₃) 1.98 (m, 2H, -CH₂), 2.18 (m, 2H, -CH₂)
2.52 (m, 1H, -CH αcarbon) 3.55 (q, 2H, -CH₂)

3.71 (br m, 1H, -NH), 7.49 (m, 1H, -NH), -20.32
(q, $J_{P-H} = 20$ Hz, Ir-H) ppm

^{31}P NMR (CDCl_3): δ -48.59 (t, $J_{p-p} = 20$ Hz, cis PMe_3) -35.38 (d,
 $J_{p-p} = 22$ Hz, trans PMe_3) ppm

^{13}C NMR (CDCl_3): δ 18.06(t, $J_{C-P} = 17$ Hz, trans PMe_3), 21.17 (d,
 $J_{C-P} = 41$ Hz, trans PMe_3), 26.81 (s, $-\text{CH}_2$),
30.45(s, $-\text{CH}_2$) 53.20 (s, α carbon), 57.72 (s,
 $-\text{CH}_2$) 18.89(, s, $-\text{COO}$) ppm

Synthesis of $[\text{Ir}(\ell\text{-pro})(\text{H})(\text{PMe}_3)_3]\text{PF}_6$ (CPRI249)

An excess of $\text{K}[\text{PF}_6]$ was dissolved in distilled water, this solution was added dropwise to solution of $[\text{Ir}(\ell\text{-pro})(\text{H})(\text{PMe}_3)_3]\text{Cl}$ in distilled water. A white-yellow precipitate formed immediately. The precipitate was filtered using cannula techniques. The solid was recrystallized from methylene chloride/ether. An X-ray structure of the crystals was obtained. (See appendix) (^1H NMR identical to Cl salt)

Exploratory reaction between $[\text{Ir}(\text{COD})(\text{PMe}_3)_3]\text{Cl}$ and ℓ -threonine (CPRI189)

ℓ -Threonine (8.9 mg, 0.0747 mmol) was placed in a screw- cap NMR tube equipped with a septum. The tube was placed in the drybox where

it was charged with 20 mg (0.035 mmol) of $[\text{Ir}(\text{COD})(\text{PMe}_3)_3]\text{Cl}$. D_2O (0.5 mL) was added via syringe outside the drybox. The tube was shaken and heated to 100°C , a ^1H NMR spectrum was obtained after 18 hours, and the $[\text{Ir}(\ell\text{-threo})(\text{H})(\text{PMe}_3)_3]\text{Cl}$ product was identified on the basis of the following data:

^1H NMR (D_2O): δ 1.21 (d, 9H, PMe_3), 1.49 (d, 9H, PMe_3), 1.67 (d, 9H, PMe_3), 3.13 (d, 1H, -CH α carbon), 3.49 (d, 3H, - CH_3), 4.13 (m, 2H, - CH_2), -20.15 (q, 1H, Ir-H) ppm

Exploratory reaction between $[\text{Ir}(\text{COD})(\text{PMe}_3)_3]\text{Cl}$ and ℓ -tryptophan (CPRI193)

ℓ -Tryptophan (15.2 mg, 0.074 mmol) was placed in a screw - cap NMR tube equipped with a septum. The tube was placed in the drybox where it was charged with 20 mg (0.035 mmol) of $[\text{Ir}(\text{COD})(\text{PMe}_3)_3]\text{Cl}$. 0.5 mL of D_2O was added via syringe. The tube was shaken and on heating the reaction mixture to 100°C , a NMR spectrum was obtained after 18 hours. The $[\text{Ir}(\ell\text{-tryp})(\text{H})(\text{PMe}_3)_3]\text{Cl}$ product was identified on the basis of the following data:

^1H NMR (D_2O): δ 0.61 (d, 9H, PMe_3) 1.42 (d, 9H, PMe_3), 1.51 (d, 9H, PMe_3), 3.30 (d, 2H, - CH_2) 3.91 (d, 1H, α carbon) 7.12 (br m 2H, aromatic H), 7.39(br m, 2H, aromatic H), 8.1 (br s, 1H, imidazole H) ppm

Synthesis of [Ir(*l*-trypt)(H)(PMe₃)₃]Cl (CPRIII035)

A 100 mL flask equipped with a stir bar and septum was charged with 152 mg (0.745 mmol) of *l*-tryptophan. The flask was then charged 250 mg (0.354 mmol) of Ir(COD)(PMe₃)₃Cl under N₂ in the drybox. The flask was then connected to a double manifold (vacuum/nitrogen) Schlenk line and 20 mL of distilled water was added to the flask via syringe. The solution was stirred magnetically and heated to reflux. After 18 hours at reflux the reaction was allowed to cool and solvent was removed in vacuo. The white solid residue was treated with distilled methylene chloride (3 x 10 mL) to extract the product from the excess amino acid. The solution was filtered from the solid using cannula techniques. The methylene chloride was removed in vacuo and the solids were dried under reduced pressure to yield 150 mg (0.227 mmol, 64.2% yield based on the amount of Ir(COD)(PMe₃)₃Cl) of [Ir(*l*-trypt)(H)(PMe₃)₃]Cl identified on the basis of the following data:

C,H analysis: Calculated for: C₂₀H₃₉N₂O₂P₃IrCl C, 34.4% H, 5.9%

Found: C, 34.1% H, 5.82%

¹H NMR (CDCl₃) δ 0.69 (d, 9H, J_{P-H} = 6.8 Hz PMe₃), 1.59 (d,
9H, J_{P-H} = 10.4 Hz, PMe₃), 1.64 (d,
9H, J_{P-H} = 6.05 Hz, PMe₃) 3.17 (m, 2H, -CH₂),
3.42 (d, 1H, α carbon) 7.16 (m, 2H, aromatic H),

7.37 (m, 2H, aromatic H), 8.08 (d, 1H, imidazole H) -19.42 (q, 1H, $J_{P-H} = -19$ Hz, Ir-H) ppm

^{31}P NMR (CDCl_3) δ -48.36 (t, $J_{p-p} = 20$ Hz, cis PMe_3), -34.34(t, $J_{p-p} = 21$ Hz, trans PMe_3) ppm

^{13}C NMR (CDCl_3) Complex precipitated before a clean spectrum could be obtained

Exploratory reaction between $[\text{Ir}(\text{COD})(\text{PMe}_3)_3]\text{Cl}$ and *l*-alanine (CPRI199)

l-Alanine (7.0 mg, 0.0785 mmol) of was placed in a screw - cap NMR tube equipped with a septum. The tube was placed in the drybox where it was charged with 20 mg (0.035 mmol) of $[\text{Ir}(\text{COD})(\text{PMe}_3)_3]\text{Cl}$. D_2O (0.5 mL) was added via syringe outside the drybox. The tube was shaken and heated to 100°C , a NMR spectrum was obtained after 18 hours and the $[\text{Ir}(\textit{l}\text{-ala})(\text{H})(\text{PMe}_3)_3]\text{Cl}$ product was identified on the basis of the following data:

^1H NMR (D_2O): δ 1.28 (d, 3H, $-\text{CH}_3$), 1.37 (d, 9H, PMe_3), 1.55 (d, 9H, PMe_3), 1.68 (d, 9H, PMe_3), 3.32(m, 1H, $-\text{CH}$) -20.9 (q, 1H, Ir-H) ppm

Synthesis of [Ir(*l*-ala)(H)(PMe₃)₃]Cl (CPRII037)

A 100 mL flask equipped with a stir bar and septum was charged with 70 mg (0.785 mmol) of *l*-alanine. The flask was then charged with 200 mg (0.35 mmol) of [Ir(COD)(PMe₃)₃]Cl under N₂ in the drybox. The flask was then connected to a double manifold (vacuum/nitrogen) Schlenk line and 25 mL of distilled water was added to the flask via syringe. The solution was stirred magnetically and heated to reflux. After 18 hours at reflux the reaction was allowed to cool and the solvent was removed in vacuo. The white solid residue was treated with distilled methylene chloride (3 x 10 mL) to extract the product from the excess amino acid. The solution was filtered from the solid using cannula techniques. The methylene chloride was removed in vacuo and the solids were allowed to dry under reduced pressure to yield 150 mg (0.275 mmol, 78.6% yield based on the amount of Ir(COD)(PMe₃)₃]Cl of [Ir(*l*-ala)(H)(PMe₃)₃]Cl identified on the basis of the following data:

C,H analysis: Calculated for C₁₂H₃₄NO₂P₃IrCl: C, 26.4% H, 6.2%

Found: C, 26.44% H, 6.44%

¹H NMR (CDCl₃): δ 1.65 (d, 9H, J_{P-H} = 10 Hz, PMe₃) 1.73 (d, 9H, J_{P-H} = 10HZ, PMe₃), 1.92 (d, 9H, J_{P-H} = 6Hz, PMe₃) 3.09 (br d, 1H, -CH), 3.26 (br s, 1H, -NH), 6.69 (br s, 1H, -NH) -19.36 (q, 1H, J_{P-H} = 17 Hz, Ir-H) ppm

^{31}P NMR (CDCl_3): δ -48.31 (t, $J_{\text{P-P}} = 20$ Hz, cis PMe_3) -34.52 (t, $J_{\text{P-P}} = 21$ Hz, trans PMe_3) ppm

^{13}C NMR (CDCl_3): δ 17.25 (t, $J_{\text{C-P}} = 20$ Hz, trans PMe_3), 21.5 (d, $J_{\text{C-P}} = 40$ Hz, cis PMe_3), 21.1 (s, $-\text{CH}_3$), 52.3 (s, $-\text{CH}-$), 181.5 (s, $-\text{COO}$) ppm

Exploratory reaction between $[\text{Ir}(\text{COD})(\text{PMe}_3)_3]\text{Cl}$ and *l*-histidine
(CPRII089)

l-Histidine (12 mg, 0.077 mmol) of was placed in a screw - cap NMR tube equipped with a septum. The tube was placed in the drybox where it was charged with 20 mg (0.035 mmol) of $[\text{Ir}(\text{COD})(\text{PMe}_3)_3]\text{Cl}$. D_2O (0.5 mL) was added via syringe outside the drybox. The tube was shaken and heated to 100°C . A ^1H NMR spectrum was obtained after 18 hours, and the $[\text{Ir}(\textit{l}\text{-hist})(\text{H})(\text{PMe}_3)_3]\text{Cl}$ product was identified on the basis of the following data:

^1H NMR (D_2O): δ 1.29 (d, 9H, PMe_3), 1.31 (d, 9H, PMe_3) 1.67(d, 9H, PMe_3), 2.35(t, 1H, $-\text{CH}-$), 3.05 (t, 2H, $-\text{CH}_2$), 6.89 (s, 1H, imid H), 6.98 (s, 1H, imid H) ppm

Exploratory reaction between [Ir(COD)(PMe₃)₃]Cl and *l*-phenylalanine (CPRI201)

l-Phenylalanine (12.3 mg, 0.0745 mmol) of was placed in a screw - cap NMR tube equipped with a septum. The tube was placed in the drybox where it was charged with 20 mg (0.035 mmol) of [Ir(COD)(PMe₃)₃]Cl. D₂O (0.5 ml) was added via syringe outside the drybox. The tube was shaken and heated to 100°C. A ¹H NMR spectrum was obtained after 18 hours and the [Ir(*l*-phen)(H)(PMe₃)₃]Cl product was identified on the basis of the following data:

¹H NMR (D₂O): δ 1.03 (d, 9H, PMe₃), 1.51 (d, 9H, PMe₃), 1.63 (d, 9H, PMe₃), 3.09(m, 2H, -CH₂), 3.15 (t, 1H, -CH-
7.32 (m, 5H, aromatic H's) ppm

Synthesis of [Ir(*l*-phen)(H)(PMe₃)₃]Cl (CPR215)

A 100 mL flask equipped with a stir bar and septum was charged with 185 mg (1.12 mmol) of *l*-phenylalanine. The flask was then charged 300 mg (0.532 mmol) of [Ir(COD)(PMe₃)₃]Cl under N₂ in the drybox. The flask was then connected to a double manifold (vacuum/nitrogen) Schlenk line and 20 mL of distilled water was added to the flask via syringe. The solution was stirred magnetically and heated to reflux. After 18 hours at reflux the reaction was allowed to cool and the solvent

was removed in vacuo. The white solid residue was treated with distilled methylene chloride (3 x 10 mL) to extract the product from the excess amino acid. The solution was filtered using cannula techniques. The methylene chloride was removed in vacuo and the solids were allowed to dry under reduced pressure to yield 222 mg (0.357 mmol, 67.1% based on the amount of Ir(COD)(PMe₃)₃Cl) of [Ir(*l*-phen)(H)(PMe₃)₃]Cl identified on the basis of the following data:

C,H analysis: Calculated for: C₁₈H₃₈NO₂P₃IrCl C, 34.8% H, 6.1%

Found: C, 34.26% H, 6.33%

¹H NMR (CDCl₃) δ 0.96 (d, 9H, J_{P-H} = 6.4 Hz, PMe₃) 1.64 (d, 9H, J_{P-H} = 6.2 Hz, PMe₃), 1.76 (d, J_{P-H} = 10.2 Hz, PMe₃), 2.51 (m, 2H, -CH₂) , 3.25(t, 1H, -CH-) 7.19 (m, 1H, aromatic H), 7.23(m, 2H, aromatic H), 7.48(d, 2H, aromatic H) -19.48 (q, 1H, J_{P-H} = 12 Hz, Ir-H) ppm

³¹P NMR (CDCl₃) δ -48.6(t, J_{p-p} = 21 Hz, cis PMe₃) -34.51 (d, J_{p-p} = 19 Hz, trans PMe₃) ppm

¹³C NMR (CDCl₃) δ 15.11 (d, J_{C-P} = 17 Hz, PMe₃) 18.80 (t, J_{C-P} = 17 Hz, PMe₃), 21.66 (d, J_{C-P} = 42Hz, PMe₃), 55.66 (s, -CH₂), 58.94 (s, -CH-), 132.9 (s,aromatic C), 134.66 (s, aromatic C), 137.37(s, aromatic C), 142.05 (s, aromatic C) 189.38 (s, -COO) ppm

Exploratory reaction between [Ir(COD)(PMe₃)₃]Cl and pipercolic acid
(CPR277)

Pipercolic acid (9.6 mg, 0.074 mmol) of was placed in a screw - cap NMR tube equipped with a septum. The tube was placed in the drybox where it was charged with 20 mg (0.035 mmol) of [Ir(COD)(PMe₃)₃]Cl. D₂O(0.5 mL) was added via syringe outside the drybox. The tube was shaken and heated to 100°C. A ¹H NMR spectrum was obtained after 18 hours and the [Ir(pip)(H)(PMe₃)₃]Cl product was identified on the basis of the following data:

¹H NMR (D₂O): δ 1.42 (d, 9H, PMe₃), 1.53 (d, 9H, PMe₃), 1.71 (d, 9H, PMe₃), 2.01 (d, 1H, -CH-), 2.12 (d, 2H, -CH₂-), 2.93 (q, 2H, -CH₂), 3.32 (br s 2H, -CH₂), 3.51 (br d, 2H, -CH₂) ppm

Exploratory reaction between [Ir(COD)(PMe₃)₃]Cl and picolinic acid
(CPR285)

Picolinic acid (9.2 mg (0.075 mmol) was placed in a screw - cap NMR tube equipped with a septum. The tube was placed in the drybox

where it was charged with 20 mg (0.035 mmol) of $[\text{Ir}(\text{COD})(\text{PMe}_3)_3]\text{Cl}$. D_2O (0.5 ml) was added via syringe outside the drybox. The tube was shaken and heated to 100°C . A ^1H NMR spectrum was obtained after 18 hours and the $[\text{Ir}(\text{pic})(\text{H})(\text{PMe}_3)_3]\text{Cl}$ product was identified on the basis of the following data:

^1H NMR (D_2O): δ 1.12 (d, 9H, PMe_3), 1.27 (d, 9H, PMe_3), 1.78 (d, 9H, PMe_3), 7.9 (br s, 1H, aromatic H), 8.25 (br s, 1H, aromatic H), 8.4 (m, 1H, aromatic H), 8.63 (br s, 1 H, aromatic H) ppm

Exploratory reaction between $[\text{Ir}(\text{COD})(\text{PMe}_3)_3]\text{Cl}$ and *l*-tyrosine (CPR237)

l-Tyrosine (13.5 mg, 0.0745 mmol) of was placed in a screw - cap NMR tube equipped with a septum. The tube was placed in the drybox where it was charged with 20 mg (0.035 mmol) of $[\text{Ir}(\text{COD})(\text{PMe}_3)_3]\text{Cl}$. D_2O (0.5 mL) was added via syringe outside the drybox. The tube was shaken and heated to 100°C . A ^1H NMR spectrum was obtained after 18 hours and the $[\text{Ir}(\textit{l}\text{-tyr})(\text{H})(\text{PMe}_3)_3]\text{Cl}$ product was identified on the basis of the following data:

^1H NMR (D_2O): δ 1.06(d, 9H, PMe_3), 1.51 (d, 9H, PMe_3) 1.62 (d, 9H, PMe_3), 2.93 (t, 2H, $-\text{CH}_2$), 3.52 (d, 1H, $-\text{CH}$), 6.79 (t, 2H, aromatic H), 7.12 (t, 2H, aromatic H), -20.12 (q, 1H, Ir-H) ppm

Synthesis of $[\text{Ir}(\ell\text{-tyr})(\text{H})(\text{PMe}_3)_3]\text{Cl}$ (CPRIII161)

A 100 mL flask equipped with a stir bar and septum was charged with 169 mg (0.932 mmol) of ℓ -tyrosine. The flask was then charged with 250 mg (0.44 mmol) of $[\text{Ir}(\text{COD})(\text{PMe}_3)_3]\text{Cl}$ under N_2 in the drybox. The flask was then connected to a double manifold (vacuum/nitrogen) Schlenk line and 20 mL of distilled water was added to the flask via syringe. The solution was stirred magnetically and heated to reflux. After 18 hours at reflux the reaction was allowed to cool and the solvent was removed in vacuo. The white solid residue was treated with distilled methylene chloride (3 x 10 mL) to extract the product from the excess amino acid. The solution was filtered using cannula techniques. The methylene chloride was removed in vacuo and the solids were dried under reduced pressure to yield 120 mg (0.188 mmol, 42.8% yield based on the amount of $[\text{Ir}(\text{COD})(\text{PMe}_3)_3]\text{Cl}$) of $[\text{Ir}(\ell\text{-tyr})(\text{H})(\text{PMe}_3)_3]\text{Cl}$ identified on the basis of the following data

^1H NMR (CDCl_3) δ 1.34 (d, 9H, $J_{\text{P-H}} = 6.2$ Hz, PMe_3), 1.9 (d, 9H, $J_{\text{P-H}} = 6$ Hz PMe_3), 2.02 (d, 9H, $J_{\text{P-H}} = 10$ Hz PMe_3), 3.45 (br m, 1H, $-\text{CH}-$), 3.62 (m, 2H,

-CH₂-), 7.31 (d, 2H, aromatic H), 7.58 (d, 2H, aromatic H), -19.5 (q, 1H, Ir-H) ppm

³¹P NMR (CDCl₃) δ -48.99 (t, J_{p-p} = 20 Hz, cis PMe₃), -33.71(t, J_{p-p} = 21 Hz, 2P, trans PMe₃) ppm

¹³C NMR (CDCl₃) Complex precipitated before suitable spectrum could be obtained.

Exploratory reaction between [Ir(COD)(PMe₃)₃]Cl and *l*-serine (CPR279)

l-Serine 7.8 mg (0.074 mmol) was placed in a screw - cap NMR tube equipped with a septum. The tube was placed in the drybox where it was charged with 20 mg (0.035 mmol) of [Ir(COD)(PMe₃)₃]Cl. D₂O (0.5 mL) was added via syringe outside the drybox. The tube was shaken and heated to 100°C. A ¹H NMR spectrum was obtained after 18 hours and the [Ir(*l*-ser)(H)(PMe₃)₃]Cl product was identified on the basis of the following data:

¹H NMR (D₂O): δ 1.45 (d, 9H, PMe₃). 1.54 (d, 9H, PMe₃), 1.72 (d, 9H, PMe₃), 3.7 (d, 1H, -CH-), 3.9 (t, 2H, -CH₂-), -19.9 (q, 1H, Ir-H) ppm

Synthesis of [Ir(*l*-ser)(H)(PMe₃)₃]Cl (CPRIII163)

A 100 mL flask equipped with a stir bar and septum was charged with 98 mg (0.932 mmol) of *l*-serine. The flask was then charged with 250 mg (0.44 mmol) of [Ir(COD)(PMe₃)₃]Cl under N₂ in the drybox. The flask was then connected to a double manifold (vacuum/nitrogen) Schlenk line and 20 mL of distilled water was added to the flask via syringe. The solution was stirred magnetically and heated to reflux. After 18 hours at reflux the reaction was allowed to cool and the solvent was removed in vacuo. The white solid residue was treated with distilled methylene chloride (3 x 10 mL) to extract the product from the excess amino acid. The solution was filtered using cannula techniques. The methylene chloride was removed in vacuo and the solids were dried under reduced pressure to yield 88 mg (0.188 mmol, 42.8% yield based on the amount of Ir(COD)(PMe₃)₃]Cl) of [Ir(*l*-ser)(H)(PMe₃)₃]Cl identified on the basis of the following data:

¹H NMR (D₂O): δ 1.45 (d, 9H, PMe₃). 1.54 (d, 9H, PMe₃), 1.72 (d, 9H, PMe₃), 3.7 (d, 1H, -CH-), 3.9 (t, 2H, -CH₂-), -19.9 (q, 1H, Ir-H) ppm

³¹P NMR (CDCl₃): δ -33.72 (t, J_{P-P} = 22 Hz, 2P, trans PMe₃) -47.30 (t, J_{P-P} = 16 Hz, 1P, cis PMe₃) ppm

(s, -CH₃), 27.2 (s, -CH-), 55.6 (s, -CH-), 181.5 (s, -COO) ppm

Exploratory reaction between [Ir(COD)(PMe₃)₃]Cl and β-alanine (CPR229)

β-Alanine (6.7 mg, 0.0745 mmol) was placed in a screw - cap NMR tube equipped with a septum. The tube was placed in the drybox where it was charged with 20 mg (0.035 mmol) of [Ir(COD)(PMe₃)₃]Cl. D₂O (0.5 mL) was added via syringe outside the drybox. The tube was shaken and heated to 100°C. A ¹H NMR spectrum was obtained after 18 hours. The ¹H NMR showed a complex series of resonances and no definite product was observed,

Exploratory reaction between [Ir(COD)(PMe₃)₃]Cl and *l*-cysteine (CPR287)

l-Cysteine (9.0 mg, 0.075 mmol) was placed in a screw - cap NMR tube equipped with a septum. The tube was placed in the drybox where it was charged with 20 mg (0.035 mmol) of [Ir(COD)(PMe₃)₃]Cl. D₂O (0.5 mL) was added via syringe outside the drybox. The tube was shaken and heated to 100°C. A ¹H NMR spectrum was obtained after 18 hours. The ¹H NMR spectrum showed a complex series of resonances and no definite product was observed,

Exploratory reaction between [Ir(COD)(PMe₃)₃]Cl and *l*-aspartic acid
(CPRII187)

l-Aspartic acid (10.0 mg, 0.0745 mmol) was placed in a screw - cap NMR tube equipped with a septum. The tube was placed in the drybox where it was charged with 20 mg (0.035 mmol) of [Ir(COD)(PMe₃)₃]Cl. D₂O (0.5 mL) was added via syringe. The tube was shaken and on heating the reaction mixture to 100°C, a NMR spectrum was obtained after 18 hours. The ¹H NMR spectrum showed a complex series of resonances and no definite product was observed,

Exploratory reaction between [Ir(COD)(PMe₃)₃]Cl and *l*-asparagine
(CPRII189)

l-Asparagine (12.0 mg, 0.0745 mmol) was placed in a screw - cap NMR tube equipped with a septum. The tube was placed in the drybox where it was charged with 20 mg (0.035 mmol) of [Ir(COD)(PMe₃)₃]Cl. D₂O (0.5 mL) was added via syringe outside the drybox. The tube was shaken and heated to 100°C. A ¹H NMR spectrum was obtained after 18 hours and the [Ir(*l*-asp)(H)(PMe₃)₃]Cl product was identified on the basis of the following data:

¹H NMR (D₂O): δ 1.51 (d, 9H, PMe₃), 1.58 (d, 9H, PMe₃), 1.69 (d, 9H, PMe₃), 2.81 (d, 2H, -CH₂-), 3.19 (d, 1H, -CH-), -20.07 (q, 1H, Ir-H) ppm

Exploratory reaction between [Ir(COD)(PMe₃)₃]Cl and pyridinium chloride (CPR209)

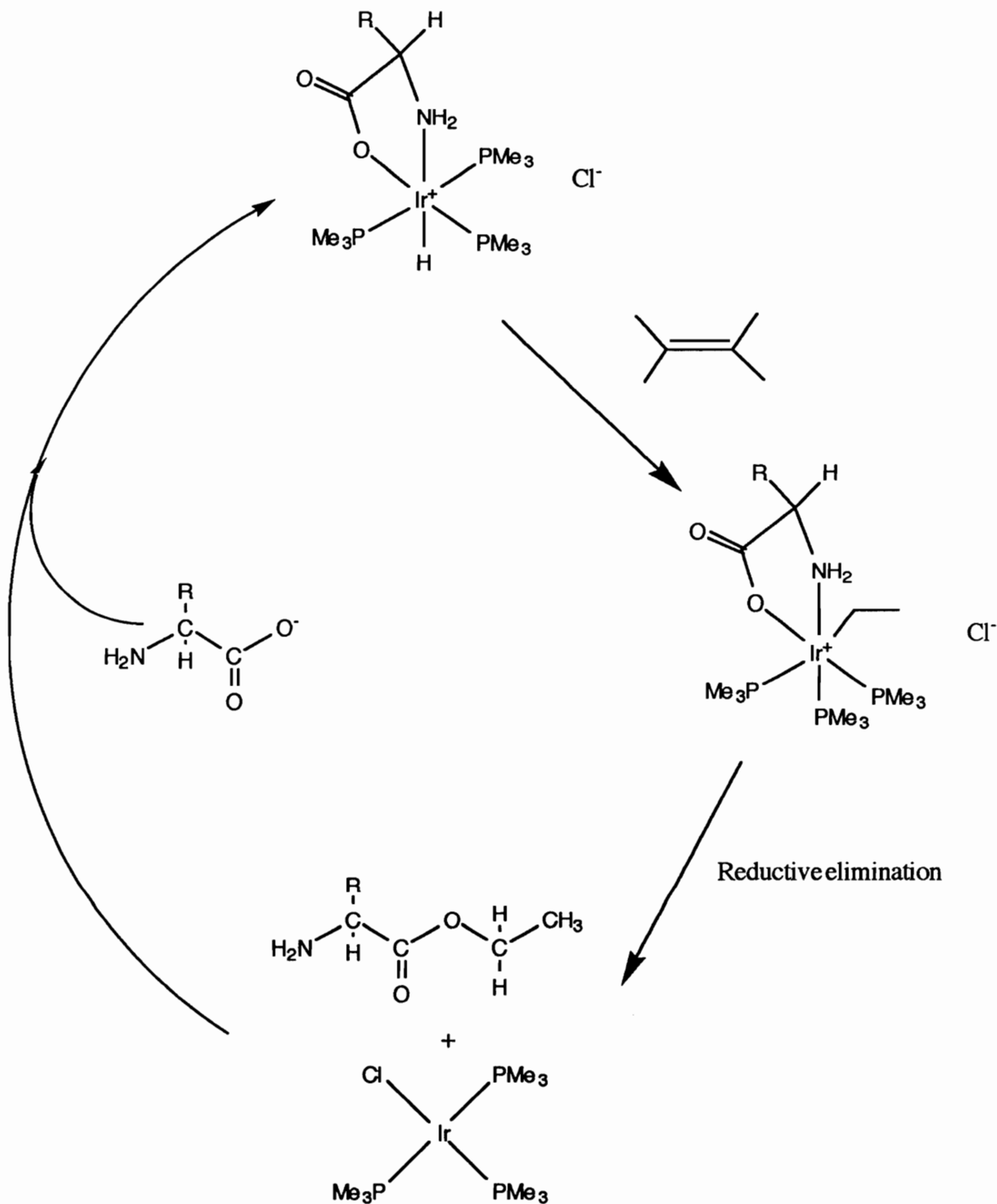
Pyridinium chloride (8.6 mg, 0.075 mmol) was placed in a screw - cap NMR tube equipped with a septum. The tube was placed in the drybox where it was charged with 20 mg (0.035 mmol) of [Ir(COD)(PMe₃)₃]Cl. D₂O (0.5 mL) was added via syringe outside the drybox. The tube was shaken and heated to 100°C. A ¹H NMR spectrum was obtained after 18 hours and the [Ir(pyr)(H)(PMe₃)₃]Cl product was identified on the basis of the following data:

¹H NMR (D₂O): δ 1.23 (br d, 18H, trans PMe₃), 1.65 (d, 9H, PMe₃), 7.5 (t, 1H, aromatic H), 8.0 (m, 2H, aromatic H), 8.5 (t, 2H, aromatic H)

Chapter 3 Reactivity Studies of Oxidative Addition Products

3.1 Introduction

The objective of the research in the Merola group is not only the synthesis of novel E-H iridium complexes formed from oxidative additions, but the study of the reactivity of these complexes. The numerous amino acid complexes that were synthesized were studied for their potential reactivity with unsaturates. The desired reactivity for these complexes is the insertion of the unsaturate into the Ir-H bond and then the reductive elimination of the new organic fragment. Scheme 3.1, for example, shows one possible catalytic cycle for the production of amino acid esters.



Scheme 3.1 Proposed pathway for formation of esters

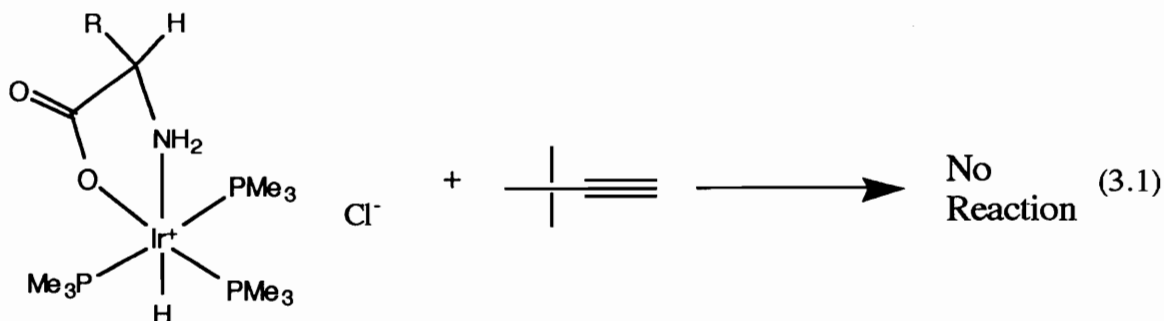
Scheme 3.1 proposes a system that will produce a new organic fragment and regenerate itself on re-addition of the amino acid.

This type of behavior is not unreasonable to expect from these types of complexes. Dr. Fola Ladipo's work demonstrated that unsaturates could insert into the Ir-H bond of the $[\text{Ir}(\text{O}_2\text{CC}_6\text{H}_5)(\text{PMe}_3)_3\text{Cl}]$ complex. The specific case was the insertion of phenyl acetylene and the products of the enol ester.¹

It was thought that the amino acids complexes may have similar activity to Ladipo's complexes. The following chapter will discuss the reactions and methods used to try to uncover that reactivity.

3.2 Results and Discussion

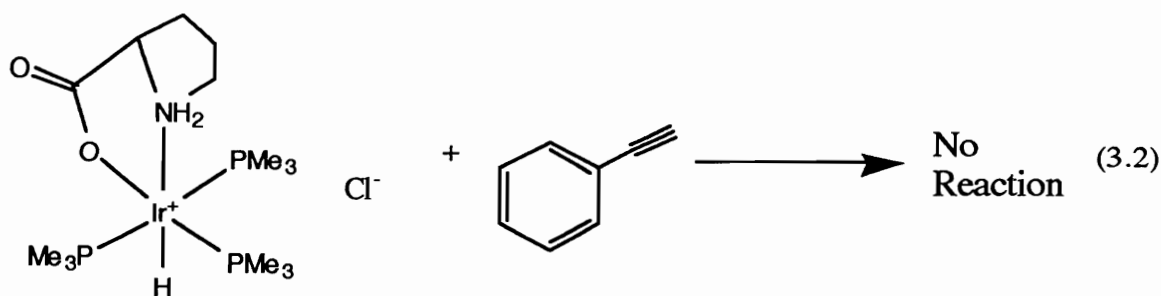
The fact that the amino acid complexes have excellent water solubility raised hopes that they would be homogenous catalysts for esterification in aqueous solution. The interest in aqueous catalytic systems is growing considerably. The reasons for this interest in aqueous catalysis is the phasing out of many organic solvents by the EPA and the low cost of water as a solvent. The first of these reactions attempted in water was that between $[\text{Ir}(\text{gly})(\text{H})(\text{PMe}_3)_3\text{Cl}]$ and *t*-butylacetylene. (equation 3.1) Here it was envisioned that the alkyne would first react via insertion into the Ir-H bond, perhaps followed by a reductive elimination of a vinyl ester.



The reaction was monitored at room temperature for days with no observable reaction. On heating the solution to 55°C and monitoring via ^1H NMR spectroscopy, again no reaction was observed.

The first step for reactivity with unsaturates in these systems is binding of the unsaturate to the metal. A coordination site must open for that binding to occur, then migration of the hydride to that unsaturate may occur. One possible problem with these amino acid iridium hydride systems is that they are coordinatively saturated and therefore have no open sites for the binding of the substrate. Moreover, under the reaction conditions employed, the ligands are not labile and do not leave to open up a coordination site. One method of aiding in opening a coordination site is the weakening of a ligand - metal bond. The proline complex was used in the second study due to its ring system which incorporates the amine group. It was postulated that due to steric consideration the ring system may weaken the Ir-N bond and facilitate insertion of the acetylene.

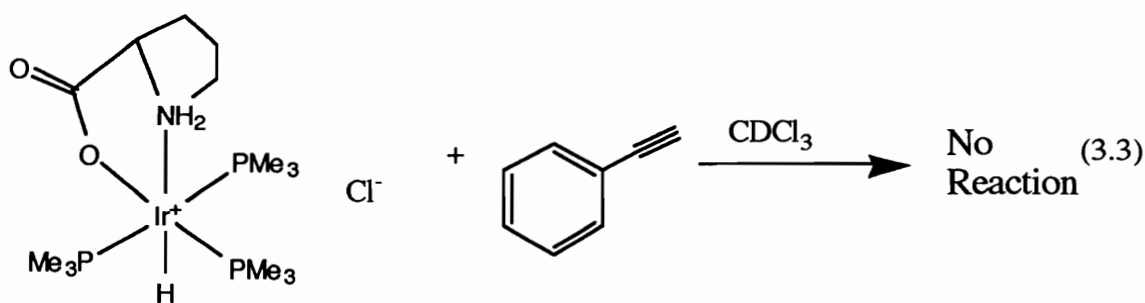
$[\text{Ir}(\text{pro})(\text{H})(\text{PMe}_3)_3]\text{Cl}$ was allowed to react with phenylacetylene in a solution of D_2O . (equation 3.2) After monitoring the solution for days at room temperature by ^1H NMR spectroscopy, no reaction was observed.



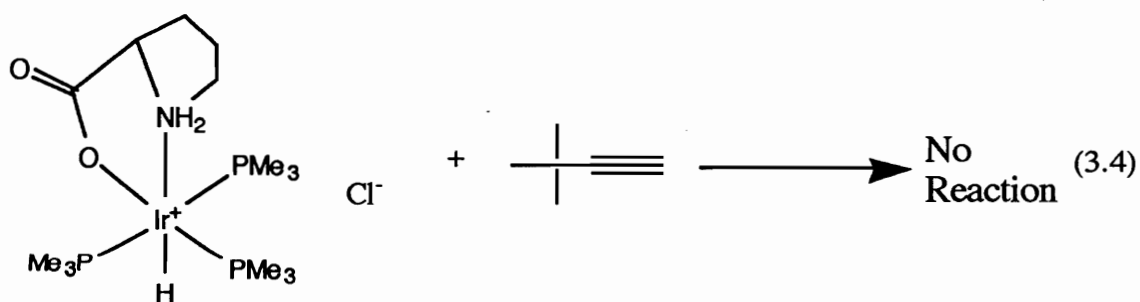
The reaction was then heated to 50°C for several days and monitored by ^1H NMR spectroscopy. Again, no reaction was observed. The temperature was then raised to 100°C and a small amount of brown precipitate was observed in the NMR tube. The precipitate was filtered from solution and the NMR spectrum of the solid was obtained which indicated the solid was a complex mixture. The spectrum of the solution showed only resonances corresponding to starting material.

The proline complex was also allowed to react with *t*-butyl acetylene in a D_2O solution. The reaction was monitored at room temperature by ^1H NMR spectroscopy. After days at room temperature, there was no visible reaction. The NMR study also showed no reaction when the solution was heated to 50°C and 100°C.

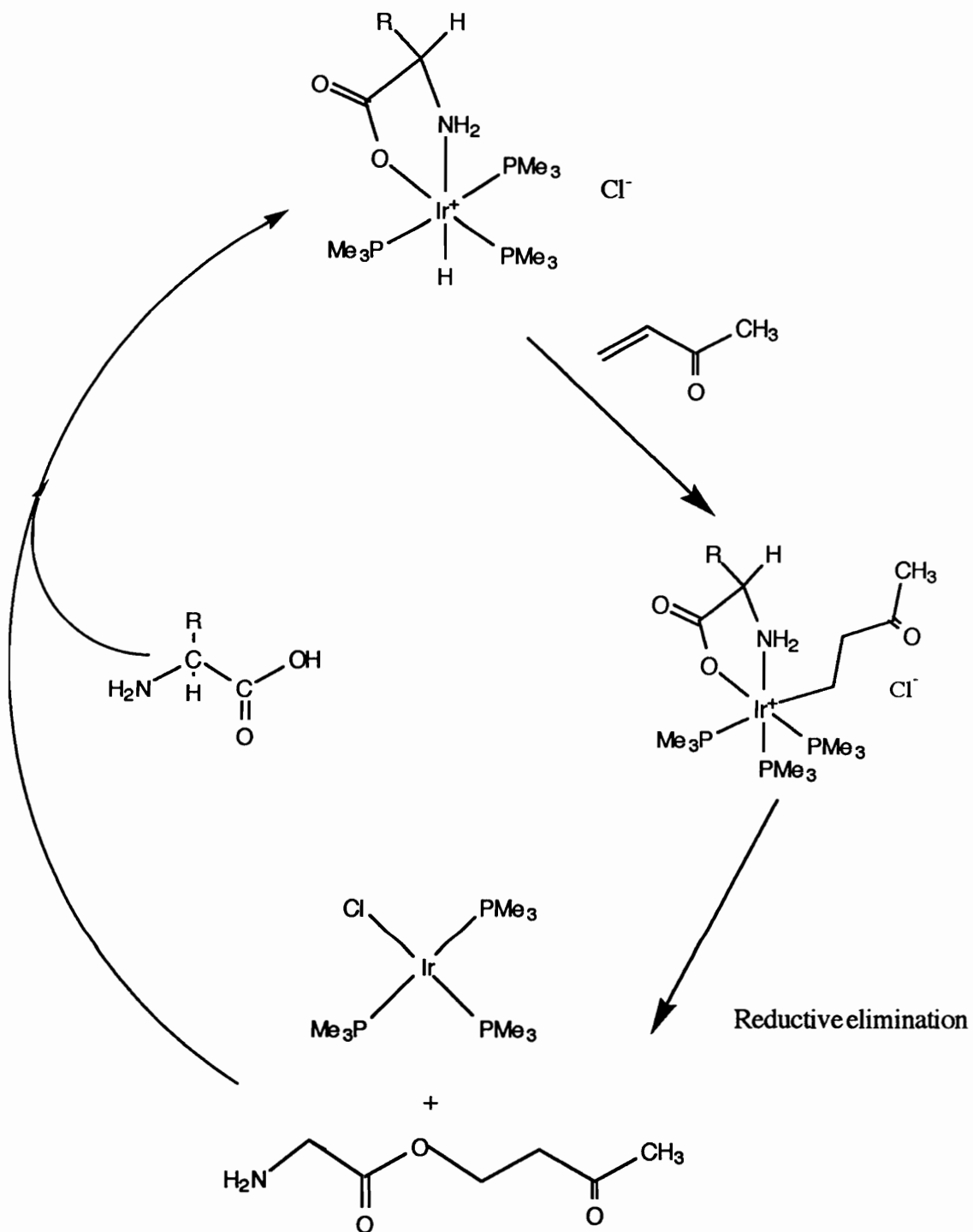
One of the problems with these systems is the fact that the acetylenes used are not water soluble. The proline complex was allowed to react with an excess of phenylacetylene in CDCl_3 to insure both reactants were in solution. (equation 3.3) The reaction was monitored for days by ^1H NMR spectroscopy and no reaction was observed. The solution was heated to 60°C, and still no reaction was observable.



$[\text{Ir}(\text{pro})(\text{H})(\text{PMe}_3)_3]\text{Cl}$ was also allowed to react with *t*-butyl acetylene in CDCl_3 . (equation 3.4) The solution was monitored by NMR spectroscopy for days. Again, no reaction was observed. The mixture was heated to 60°C and after 18 hours new resonances appeared in the spectrum, but the retention of the hydride resonance suggested that insertion of the acetylene was not occurring.

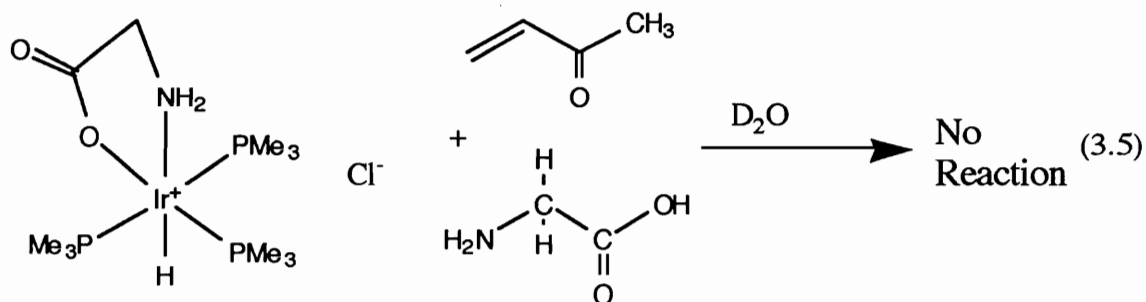


A possible scheme for reactivity is the treatment of the amino acid complex with free amino acid and unsaturate. The postulate here was the the possibility of catalytic reactivity of the amino acid complex. The reductive elimination step would give an ester as a product [Scheme3.2]



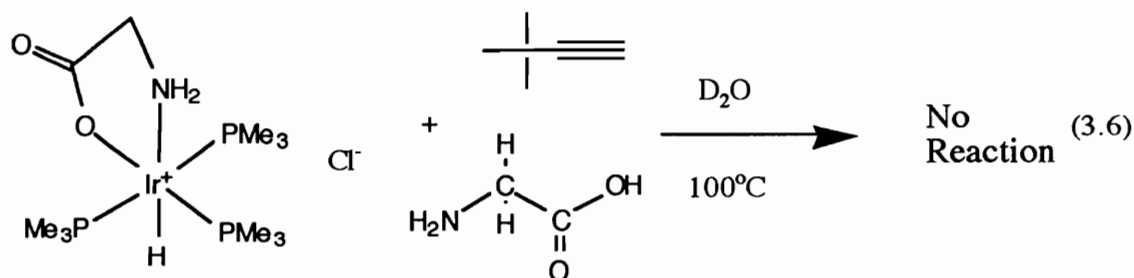
Scheme 3.2 Formation of ester product from reductive elimination.

$\text{Ir}(\text{gly})(\text{H})(\text{PMe}_3)_3\text{Cl}$ was allowed to react with excess glycine and vinyl acetate in D_2O at room temperature. The reaction was monitored by ^1H NMR spectroscopy for days and no reaction was observed. (equation 3.5)



$[\text{Ir}(\text{pro})(\text{H})(\text{PMe}_3)_3]\text{Cl}$ was also allowed to react with vinyl acetate and free proline to see if any reactivity could be induced. This reaction was also monitored by NMR spectroscopy at room temperature, but no reaction was observed after days of monitoring the solution.

Reactions similar to that previously described were done replacing the vinyl acetate with alkyne. The amino acid complex used in this study was the glycine product. The glycine product, free glycine and t-butylacetylene were dissolved in D_2O and heated to 100°C . The solution was monitored by NMR spectroscopy, but no reaction was observed. (equation 3.6)



An attempt at inducing reactivity of these complexes in aqueous solution involved the use of water-soluble unsaturates. These unsaturates included acrylamide, dimethylacetylenedicarboxylate, and 2-butenal. (Figure 3.1)

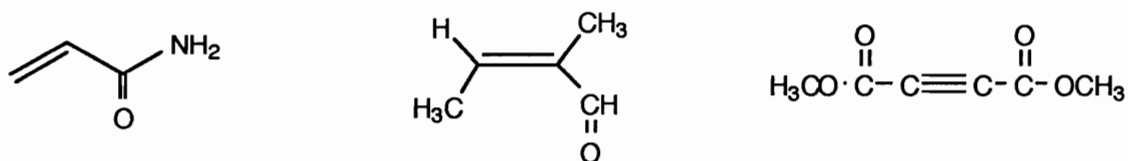


Figure 3.1 Water soluble unsaturates

The increased water solubility of these compounds was the primary factor in choosing them for the study. These compounds were allowed to react with $[Ir(\text{val})(H)(PMe_3)_3]Cl$ and $[Ir(\text{pro})(H)(PMe_3)_3]Cl$ in this study. These reactions were all done as 1H NMR studies and a variety of conditions were employed. The temperature was adjusted from room temperature, to $50^\circ C$, and then to $100^\circ C$ based on the observation of no reaction at the previous temperature. The concentrations of unsaturates were also varied in these studies. Finally, the addition of free amino acid to the solution with unsaturate and amino acid complex was attempted. In all cases, the retention of the hydride peak was the most convincing

evidence that no reactions were occurring. It was rather disappointing that no reactivity could be seen between these iridium amino acid complexes and organic unsaturates. The varying solvent systems, concentrations of reactants, temperature, all had no effect on the reactivity of the amino acid complexes. The importance in opening up a coordination site for the unsaturate remained the primary focus. The use of a coordinatively unsaturated complex seemed to be the most likely answer. There were a number of alternative changes that could be explored in order to induce reactivity and these alternatives will be discussed in the remainder of the chapter.

3.2.1 Experimental

Reaction attempt between [Ir(gly)(PMe₃)₃]Cl and t-butylacetylene in D₂O (CPR243)

[Ir(gly)(PMe₃)₃]Cl (20 mg, 0.0377 mmol) was placed in a screw-cap NMR tube equipped with a septum under an N₂ atmosphere in a drybox.. The tube was removed from the drybox where it was charged with 0.5 mL of D₂O via syringe. T-butylacetylene (6.0 μL ,0.079 mmol) was added to the tube via syringe. The tube was shaken and monitored at room temperature by ¹H NMR spectroscopy. No reaction was observed. The reaction was heated to 55°C and monitored for days. Again, no reaction was seen. The only resonances present were those assignable to starting material

Reaction attempt between [Ir(pro)(PMe₃)₃]Cl and phenylacetylene in D₂O
(CPR261)

[Ir(pro)(PMe₃)₃]Cl (20 mg, 0.035) was placed in a screw - cap NMR tube equipped with a septum under an N₂ atmosphere in a drybox.. The tube was removed from the drybox where it was charged 0.5 mL of D₂O via syringe. Phenylacetylene (4.6 μL, 0.0735 mmol) was added to the tube via syringe. The tube was shaken and monitored at room temperature by ¹H NMR spectroscopy. No reaction was seen. The reaction was heated to 55°C and monitored for days. Again, no reaction was seen. The only resonances present were the corresponding starting material signals. The reaction mixture was heated to 100°C and a brown solid fell out of solution. The brown solid gave a complex mixture of resonances in the NMR spectrum in CDCl₃. The D₂O solution spectrum showed starting material resonances.

Reaction attempt between [Ir(pro)(PMe₃)₃]Cl and t-butylacetylene in D₂O
(CPR263)

[Ir(gly)(PMe₃)₃]Cl (20 mg, 0.035 mmol) was placed in a screw - cap NMR tube equipped with a septum under an N₂ atmosphere in a drybox.. The tube was removed from the drybox where it was charged 0.5 mL of D₂O via syringe. T-butylacetylene (5.0 μL, 0.0735 mmol) was added to the tube via syringe. The tube was shaken and monitored at room temperature by NMR. No reaction was seen. The NMR tube was heated to 55°C and monitored for days. Again, no reaction was seen. The NMR tube was then heated to 100°C, no reaction was observed. The only resonances present were those assignable to starting material.

Reaction attempt between [Ir(pro)(PMe₃)₃]Cl and t-phenylacetylene in CDCl₃ (CPR265)

[Ir(pro)(PMe₃)₃]Cl (20 mg, 0.035 mmol) was placed in a screw - cap NMR tube equipped with a septum under an N₂ atmosphere in a drybox.. The tube was removed from the drybox where it was charged 0.5 ml of CDCl₃ via syringe. Phenylacetylene (4.6 μL, 0.0735 mmol) was added to the tube via syringe. The tube was shaken and monitored at room temperature by NMR. No reaction was seen. The NMR tube was heated to 60°C and monitored for days. Again, no reaction was seen. The only resonances present were those assignable to starting material.

Reaction attempt between [Ir(pro)(PMe₃)₃]Cl and t-butylacetylene in CDCl₃ (CPR267)

[Ir(gly)(PMe₃)₃]Cl (20 mg, 0.0377 mmol) was placed in a screw - cap NMR tube equipped with a septum under an N₂ atmosphere in a drybox.. The tube was removed from the drybox where it was charged 0.5 mL of CDCl₃ via syringe. T-butylacetylene (5.0 μL , 0.0735 mmol) was added to the tube via syringe. The tube was shaken and monitored at room temperature by ¹H NMR. No reaction was seen. The NMR tube was heated to 60°C and monitored for days. Again, no reaction was seen. The only resonances present were those assignable to starting material.

Reaction attempt between [Ir(gly)(PMe₃)₃]Cl, glycine and vinyl acetate in D₂O (CPR299)

Glycine (6 mg, 0.081 mmol) of was placed in a screw - cap NMR tube equipped with a septum. The tube was placed in the drybox where it was charged with 20 mg (0.035 mmol) of [Ir(gly)(PMe₃)₃]Cl. D₂O (0.5 mL) was added via syringe to the NMR tube outside the drybox. The solution was then charged with 5 μL (0.0735 mmol) of vinyl acetate. The tube was shaken and monitored by ¹H NMR at room temperature. No reaction was observed.

Reaction attempt between [Ir(pro)(PMe₃)₃]Cl, *l*-proline and vinyl acetate in D₂O (CPRII075)

Proline (10 mg, 0.086 mmol) was placed in a screw - cap NMR tube equipped with a septum. The tube was placed in the dry box where it was charged with 20 mg (0.035 mmol) of [Ir(pro)(PMe₃)₃]Cl. D₂O (0.5 mL) was added via syringe to the NMR tube outside the drybox. The solution was then charged with 5 μL (0.0735 mmol) of vinyl acetate. The tube was shaken and monitored by ¹H NMR spectroscopy at room temperature. No reaction was observed.

Reaction attempt between [Ir(gly)(PMe₃)₃]Cl, glycine and t-butylacetylene in D₂O (CPRII093)

Glycine (14 mg, 0.189 mmol) of was placed in a screw - cap NMR tube equipped with a septum. The tube was placed in the drybox where it was charged with 20 mg (0.0337) of [Ir(gly)(PMe₃)₃]Cl. D₂O (0.5 mL)

was added via syringe to the NMR tube outside the drybox. The solution was then charged with 23 μL (0.338 mmol) of t-butylacetylene. The tube was shaken and monitored by ^1H NMR spectroscopy at room temperature. No reaction was observed. The tube was then heated to 50°C. Again, no reaction was observed after heating for days.

Reaction attempt between $[\text{Ir}(\text{gly})(\text{PMe}_3)_3]\text{Cl}$ and DMAD in D_2O (CPR223)

$[\text{Ir}(\text{gly})(\text{PMe}_3)_3]\text{Cl}$ (20 mg, 0.0337 mmol) of was placed in a screw - cap NMR tube equipped with a septum under an N_2 atmosphere in a drybox.. The tube was removed from the drybox where it was charged 0.5 mL of D_2O via syringe. T-butylacetylene (4.4 μL , 0.071 mmol) was added to the tube via syringe. The tube was shaken and monitored at room temperature by ^1H NMR spectroscopy. No reaction was observed. The NMR tube was heated to 100°C and monitored for days, Again, no reaction was observed.

Reaction attempt between $[\text{Ir}(\text{val})(\text{PMe}_3)_3]\text{Cl}$ and acrylamide in D_2O (CPRII129)

Acrylamide (5.2 mg, 0.073 mmol) was placed in a screw - cap NMR tube equipped with a septum. The tube was placed in the drybox where it was charged with 20 mg (0.035 mmol) of $[\text{Ir}(\text{val})(\text{PMe}_3)_3]\text{Cl}$. The tube was removed from the drybox where it was charged 0.5 ml of D_2O via syringe. The tube was shaken and monitored at room temperature by ^1H

NMR spectroscopy. No reaction was observed. The NMR tube was heated to 100°C and monitored for days, Again, no reaction was observed.

Reaction attempt between [Ir(val)(PMe₃)₃]Cl and 2-butenal in D₂O (CPRII147)

[Ir(val)(PMe₃)₃]Cl (20 mg, 0.035 mmol) of was placed in a screw - cap NMR tube equipped with a septum under an N₂ atmosphere in a drybox.. The tube was removed from the drybox where it was charged 0.5 mL of D₂O via syringe. T-butylacetylene (7.0 μL, 0.077 mmol) was added to the tube via syringe. The tube was shaken and monitored at room temperature by ¹H NMR spectroscopy. No reaction was observed. The NMR tube was heated to 100°C and monitored for days, Again, no reaction was observed.

3.2.2 Alternative strategies to amino acid complex reactivity

The formation of a coordinatively unsaturated complex would be ideal for reactivity with unsaturates. This alternative would alleviate the need for a site to open for the unsaturate prior to insertion into the metal hydride bond. This alternative seemed a likely route for activity with unsaturated compounds. The first of these alternative strategies was exploring the use of [Ir(COD)(DMPE)]Cl. This compound is a new material which was thought to have been synthesized previously by Frazier in the Merola lab.² The attempted synthesis of this compound followed a route similar to that of synthesizing the [Ir(COD)(PMe₃)₃]Cl complex.

The addition of the phosphine to a solution of $[\text{Ir}(\text{COD})\text{Cl}]_2$ in toluene at room temperature was postulated to give desired product. This pathway did not, in fact, give the desired complex. The complex was synthesized using a methylene chloride solution of the dimer at 0°C with slow addition of the phosphine ligand. The dimethyl phosphinoethane ligand [DMPE] chelates to the metal and only occupies two sites. The result is a square planar molecule which is unsaturated coordinatively. This complex has the possibility of binding an unsaturate because of its open sites even after coordinating an amino acid. (Figure 3.2)

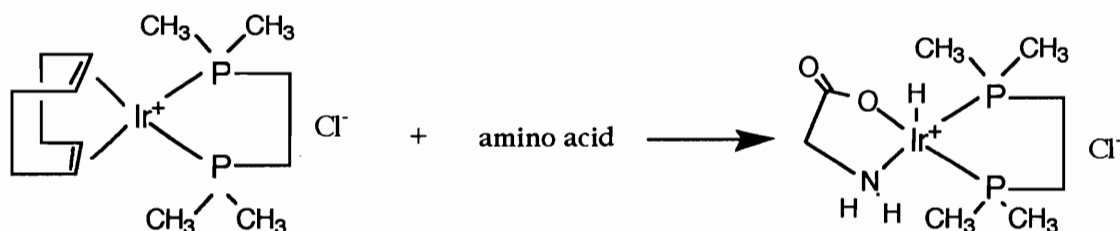
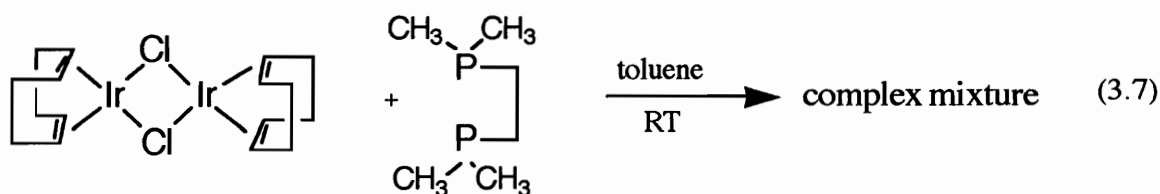


Figure 3.2 Proposed formation of amino acid complex

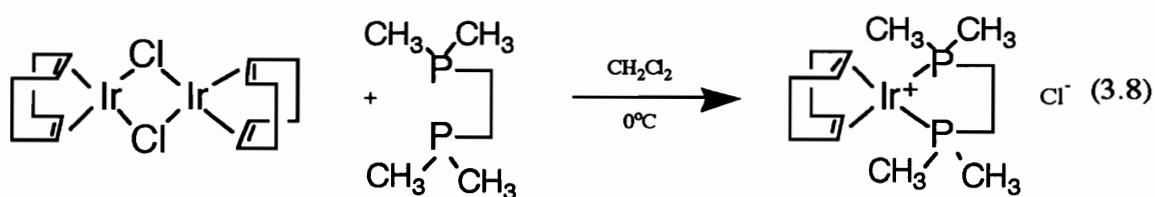
The open coordination site is ideal for an unsaturated complex to bind to and "push" the insertion step of the process.

The first step in the synthesis of $[\text{Ir}(\text{aa})(\text{DMPE})]$ was the synthesis of the square planar $[\text{Ir}(\text{COD})(\text{DMPE})]\text{Cl}$ complex. The first attempt at making this complex used conditions similar to those used in the synthesis of the $[\text{Ir}(\text{COD})(\text{PMe}_3)_3]\text{Cl}$ complex.² A toluene solution of DMPE is added slowly to a solution of $[\text{Ir}(\text{COD})\text{Cl}]_2$. In the case of DMPE however, on slow addition to the $[\text{Ir}(\text{COD})\text{Cl}]_2$ solution an orange tar forms immediately. The solution and the orange tar both give rise to

complex NMR spectra and neither shows resonances corresponding to the desired square planar complex. (equation 3.7)



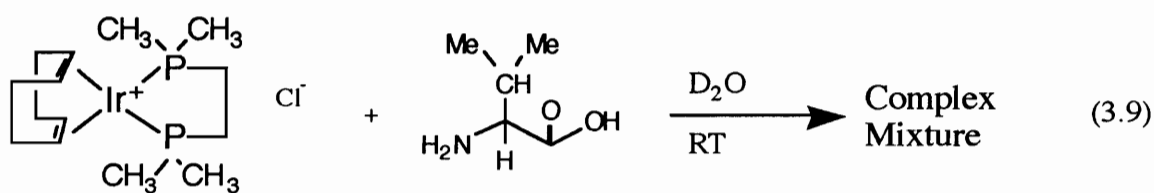
The synthesis was attempted again in methylene chloride at 0°C, (equation 3.8) in the attempt to keep everything in solution and to allow enough time for the desired product to form. The red solution of $[\text{Ir}(\text{COD})\text{Cl}]_2$ turns bright yellow on final addition of the DMPE at 0°C. The solvent is removed under reduced pressure to yield a yellow solid. The ^1H -NMR spectrum of the solid gives resonances consistent with $[\text{Ir}(\text{COD})(\text{DMPE})]\text{Cl}$:



A doublet corresponding to 12 protons is observed in the phosphine region of the spectrum. The doublet arises from the coupling of the 4 equivalent methyl groups to the phosphorous atoms. A second doublet integrated to 4 protons also is observed, this resonance is due to the protons of the ethylene bridge. The doublet again is due to coupling of

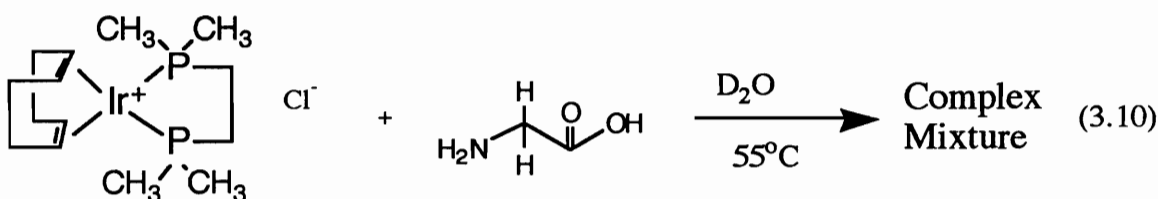
the phosphorous atoms. The only other resonances correspond to attached cyclooctadiene. These COD resonances are almost identical to the COD resonances observed for Ir(COD)(PMe₃)₃Cl.

The synthesis of the coordinatively unsaturated complex was only the first step. The reaction of the complex with amino acids to form the oxidative addition products is the important step. The first attempt at the synthesis of the square planar amino acid complex was done with *l*-valine. (equation 3.9)



The reaction was heated to 100°C and the solution monitored by ¹H NMR spectroscopy. The spectrum became complex and no hydride resonance was observed in the ¹H NMR spectrum.

The next reaction was attempted using glycine instead of *l*-valine (equation 3.10). The solution was heated to 55°C instead of 100° to see if only one product would form at the lower temperature. The reaction was monitored by ¹H NMR spectroscopy and again the NMR spectrum obtained of the reaction mixture was complex. There was no hydride resonance observed in the spectrum.



The reaction of $[\text{Ir}(\text{COD})(\text{DMPE})]\text{Cl}$ with *l*-valine was attempted again, but with varying solvents this time. The reaction was tried with CDCl_3 and d_6 -benzene. The d_6 -benzene study was stopped almost immediately due to the insolubility of both the iridium complex and the amino acid at room temperature. The CDCl_3 study at reflux showed promising results in that a complex spectrum was observed in the methyl phosphine region of the spectrum and a hydride resonance was observed. The hydride resonance was a triplet indicative of a hydrogen cis to two phosphines.

This reaction was scaled up to a preparative size with 100mg of $[\text{Ir}(\text{COD})(\text{DMPE})]\text{Cl}$ allowed to react with 50 mg of *l*-valine in methylene chloride. The reaction was stirred for two days at room temperature. Product was analyzed using NMR spectroscopy. The ^1H NMR spectrum of the product was complex and no hydride resonance was observed.

The preparative reaction was attempted again in water and again a product was obtained whose ^1H NMR spectrum was complex and contained no resonances attributable to Ir-H.

One interesting result did come out of all these studies with $[\text{Ir}(\text{COD})(\text{DMPE})]\text{Cl}$. A preparative scale reaction with *l*-valine in CHCl_3 was allowed to stir at 50°C overnight. On workup of the reaction, a ^1H NMR spectrum of the product was obtained that had resonances corresponding to a valine molecule bound to the iridium center (based on the splitting and chemical shift of the isopropyl methyl protons) and a hydride. The solid was recrystallized from methylene chloride/ether to give good quality crystals. An X-ray structure of the complex was solved

and it turned out to be the $[\text{Ir}(\mu^1, \mu^3 \text{C}_8\text{H}_{12})(\text{DMPE})]\text{Cl}$ complex. The π -bound cyclooctadiene had rearranged to form a σ bond and an allyl bond with the metal center. (Figure 3.3)

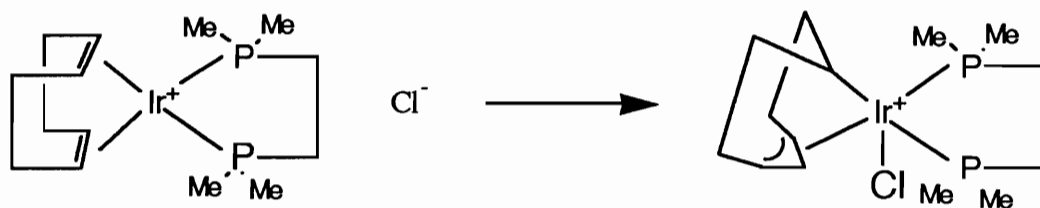


Figure 3.3 Rearrangement of $[\text{Ir}(\text{COD})(\text{DMPE})]\text{Cl}$

The complex crystallizes in the monoclinic $P2_1/m$ with $a = 7.100(2)\text{\AA}$, $b = 15.295(5)\text{\AA}$, $c = 8.784(4)\text{\AA}$, $V = 880.0(5)\text{\AA}^3$ and $d_{\text{calc}} = 1.834 \text{ Mg/m}^3$ for $Z = 2$. The ORTEP is shown in figure 3.4 The complex is extremely interesting in that the π -bound COD has rearranged to form the σ bond and an allyl bond. The Ir-C bond of $2.076(15)\text{\AA}$ is considerably shorter than that of the allyl carbon - iridium bond lengths of $2.209(13)\text{\AA}$, $2.128(15)\text{\AA}$ and $2.209(13)\text{\AA}$ as expected for a σ bond compared to the π bonding of the allyl group.

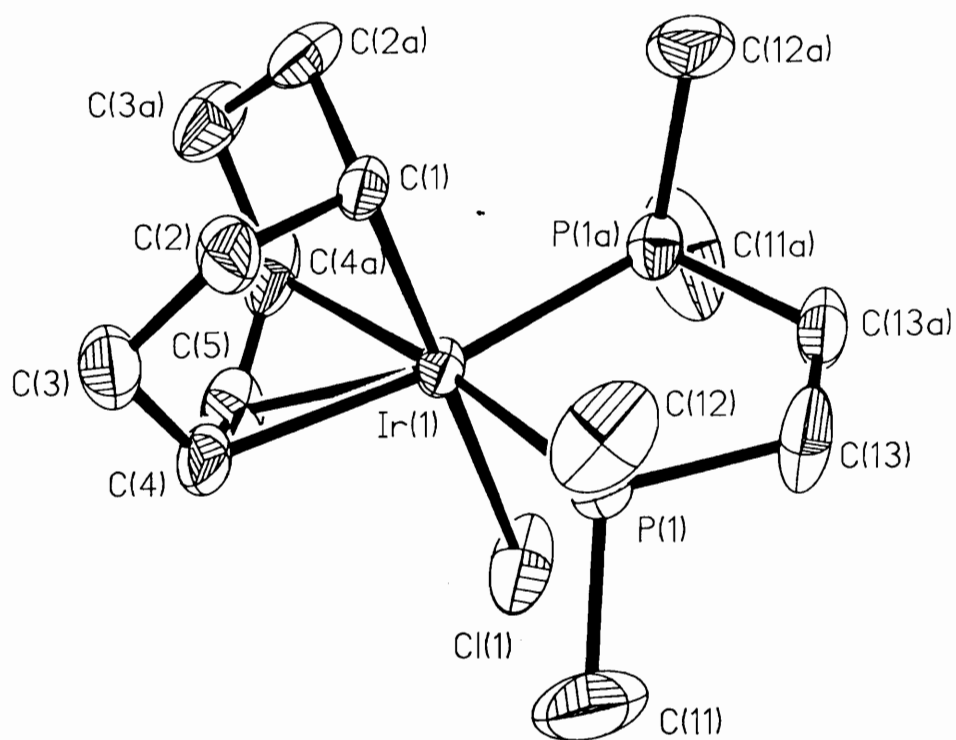


Figure 3.4 ORTEP plot of rearranged COD product

This was a rather unusual rearrangement and as it turns out a study done by Werner et al showed a similar rearrangement on an analogous system.³ Their work showed that $[\text{Ir}(\text{COD})(\text{DPPM})]\text{Cl}$ complex could undergo a rearrangement to form the following complex.(Figure 3.4) Unfortunately there was no crystal structure done with which to compare. While the isolation and characterization of this complex was interesting, it underscores one pitfall of X-ray crystallography: The single crystal on which the experiment is formed may not be representative of the bulk of the product.

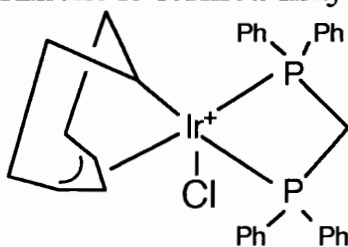


Figure 3.5 Literature example of rearranged product

The work that was done with $[\text{Ir}(\text{COD})(\text{DMPE})]\text{Cl}$ did not give the desired reactivity. Quite the opposite actually, the amino acid complexes of this type could not be made based on the studies done. Thus another alternative would have to be used in order to gain the desired reactivity.

3.2.3 Experimental

Attempted synthesis of $[\text{Ir}(\text{COD})(\text{DMPE})]\text{Cl}$ (CPRI251)

A 250 mL flask equipped with a stir bar and septum was charged with 2.3 g (0.003 mol) of $[\text{Ir}(\text{COD})\text{Cl}]_2$ under N_2 in the drybox. The flask was then connected to a double manifold (vacuum/nitrogen) Schlenk

line and 75 mL of distilled toluene was added to the flask via syringe. The clear red solution was stirred for 10 minutes to allow all solids to dissolve. The flask was then charged with 1 g (.0066 mol, 2.1 equiv.) of DMPE via syringe. A dark orange precipitate formed immediately on addition of DMPE. The heterogeneous mixture was stirred for 12 hours. The orange solid was filtered from solution and the NMR spectrum indicated a complex mixture.

Synthesis of [Ir(COD)(DMPE)Cl] (CPRII019)

A 100 mL flask equipped with a stir bar and septum was charged with 200 mg (0.298 mmol) of [Ir(COD)Cl]₂ under N₂ in the drybox. The flask was then connected to a double manifold (vacuum/nitrogen) Schlenk line and 20 mL of distilled methylene chloride was added to the flask via syringe. The clear red solution was stirred for 10 minutes to allow all solids to dissolve and cooled to 0°C in an ice bath. The flask was then charged with 0.10 mL (0.599 mmol, 2.1 equiv.) of DMPE via syringe added slowly over a period of 30 minutes. The solution went bright yellow on final addition of DMPE. The product was obtained by removing the methylene chloride in vacuo. The solids were dried under reduced pressure to yield 105 mg (0.216 mmol, 36% yield) of Ir(COD)(DMPE) identified on the basis of the following data:

C, H analysis	Calculated for: C ₁₄ H ₃₀ P ₂ IrCl	C, 34.3%	H, 6.13%
	Found:	C, 33.9%	H, 5.84%

^1H NMR (CDCl_3): δ : 1.43 (d, 12H, PMe_3) 1.75 (d, 4H, $-\text{CH}_2-$), 1.95 (m, 8H, COD), 3.7 (br s, 4H, COD)

Initial reaction between $[\text{Ir}(\text{COD})(\text{DMPE})]\text{Cl}$ and *l*-valine in D_2O (CPRII021)

l-Valine (5.5 mg, 0.047 mmol) was placed in a screw - cap NMR tube equipped with a septum. The tube was placed in the drybox where it was charged with 20 mg (0.041 mmol) of $[\text{Ir}(\text{COD})(\text{DMPE})]\text{Cl}$. D_2O (0.5 mL) was added via syringe outside the drybox. The tube was shaken and heated to 100°C , a ^1H NMR spectrum was obtained after 18 hours. The spectrum only had broad resonances indicative of product being insoluble.

Initial reaction between $[\text{Ir}(\text{COD})(\text{DMPE})]\text{Cl}$ and *l*-valine in CDCl_3 (CPRII039)

l-Valine (10.0 mg, 0.085 mmol) was placed in a screw - cap NMR tube equipped with a septum. The tube was placed in the drybox where it was charged with 20 mg (0.041 mmol) of $[\text{Ir}(\text{COD})(\text{DMPE})]\text{Cl}$. CDCl_3 (0.5 mL) was added via syringe outside the drybox. The tube was shaken and heated to 60°C . A ^1H NMR spectrum was obtained after 18 hours.

^1H NMR (D_2O): The resonances were broad in the phosphine region and in the isopropyl methyl region, but a hydride at -16.23 Hz (triplet, cis to two P) was observed indicating an addition had occurred.

Reaction between $[\text{Ir}(\text{COD})(\text{DMPE})]\text{Cl}$ and *l*-valine in CH_2Cl_2 (CPRII039)

l-Valine (50 mg, 0.43 mmol) was placed in a 50 mL side-arm flask equipped with a septum and magnetic stir bar. The tube was placed in the drybox where it was charged with 100 mg (0.388) of $[\text{Ir}(\text{COD})(\text{DMPE})]\text{Cl}$. The flask was then charged with 20 mL of distilled methylene chloride. The reaction was allowed to stir at room temperature for 2 days. The solvent was removed in vacuo. The solid was recrystallized from methylene chloride/ether to yield $[\text{Ir}\mu^1, \mu^3 \text{C}_8\text{H}_{12})(\text{DMPE})]\text{Cl}$. The crystal structure was solved from the solid product. (See appendix)

Reaction between $[\text{Ir}(\text{COD})(\text{DMPE})]\text{Cl}$ and *l*-valine in water (CPRII051)

l-Valine (80 mg, 0.682 mmol) was placed in a 50 mL side-arm flask equipped with a septum and magnetic stir bar. The tube was placed in the drybox where it was charged with 150 mg (0.306 mmol) of $[\text{Ir}(\text{COD})(\text{DMPE})]\text{Cl}$. The flask was then charged with 25 mL of distilled water. The reaction was allowed to stir at room temperature for 2 days. The solvent was removed in vacuo. The solids were dried under reduced pressure. The NMR spectrum of the solids was obtained to determine that starting material had been recovered on work up.

Initial reaction between [Ir(COD)(DMPE)]Cl and diphenylphosphate in D₂O CPRII059

Diphenylphosphate (22.0 mg, 0.0879 mmol) was placed in a screw - cap NMR tube equipped with a septum. The tube was placed in the drybox where it was charged with 20 mg (0.040 mmol) of [Ir(COD)(DMPE)]Cl. D₂O (0.5 mL) was added via syringe outside the drybox. The tube was shaken and heated to 100°C. A ¹H NMR spectrum was obtained after 18 hours. The NMR spectrum revealed only resonances assignable to starting materials.

Initial reaction between [Ir(COD)(DMPE)]Cl and glycolic acid in D₂O (CPRII061)

Glycolic acid (7.0 mg, 0.092 mmol) was placed in a screw - cap NMR tube equipped with a septum. The tube was placed in the drybox where it was charged with 20 mg (0.040 mmol) of [Ir(COD)(DMPE)]Cl. D₂O (0.5 mL) was added via syringe outside the drybox. The tube was shaken and heated to 100°C. After 18 hours at temperature, a ¹H NMR spectrum was obtained. The NMR spectrum revealed only resonances assignable to starting materials.

Initial reaction between [Ir(COD)(DMPE)]Cl and in D₂O CPRII063

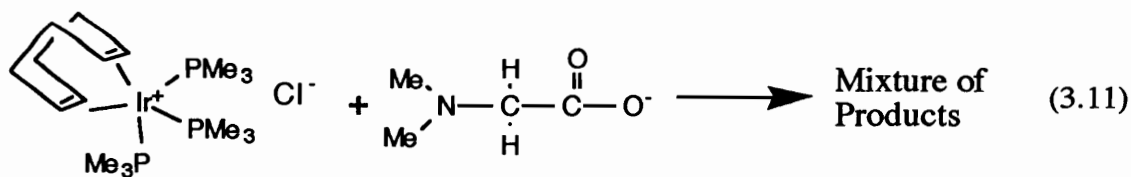
A NMR tube equipped with a septum was placed in the drybox where it was charged with 20 mg (0.040) of [Ir(COD)(DMPE)]Cl. D₂O (0.5 mL) was added via syringe outside the drybox. The tube was then charged with 6 μL (0.0537) of pyruvic acid via syringe. The tube was shaken and

heated to 100°C. After 18 hours at temperature, a ^1H NMR spectrum was obtained. The NMR spectrum revealed only resonances assignable to starting materials.

3.2.4 N-substituted Amino Acids

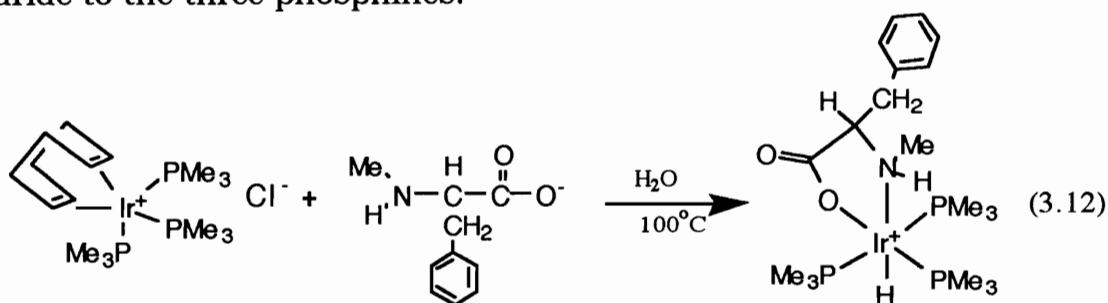
The third strategy followed in an attempt to increase the reactivity of these iridium amino acid hydride complexes used N-substituted amino acids. It was thought that substitution on the amine group would increase the steric congestion around the metal center and weaken the Ir-N bond. This in turn would allow for a facilitated insertion of an unsaturate into the Ir-H bond.

The first step again was the synthesis of the amino acid complexes. The reaction of N,N dimethylglycine with $[\text{Ir}(\text{COD})(\text{PMe}_3)_3]\text{Cl}$ was done under conditions similar to those used for the unsubstituted amino acids. (equation 3.11) The product was analyzed by ^1H NMR spectroscopy to reveal a complex mixture.

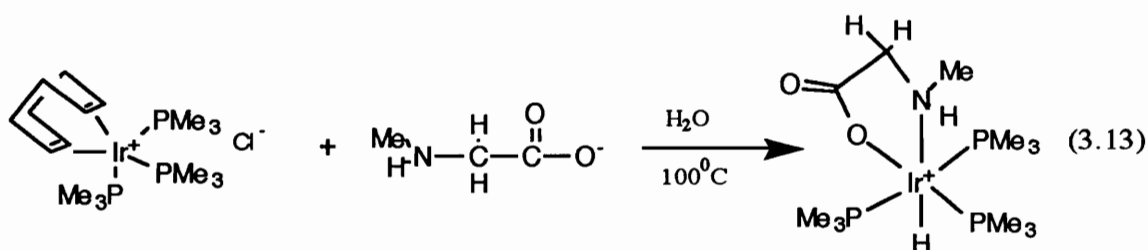


While the N,N dimethylglycine results were discouraging, the reaction of N-methyl *l*-phenylalanine gave the desired products from its reaction with $[\text{Ir}(\text{COD})(\text{PMe}_3)_3]\text{Cl}$. The reaction conditions that were used were milder than those used for the unsubstituted amino acids. The work-up was the same as used for the common amino acid

complexes. The complex formed was the N-methyl amino acid chelate complex.(equation 3.12) The hydride resonance was indicative of a meridional arrangement of the phosphines in the octahedron. This hydride resonance is a quartet arising from the cis coupling of the hydride to the three phosphines.



The other N-substituted amino acid complex made was that of N-methyl glycine.(equation 3.13) This complex showed a very clean initial spectrum in the ^1H NMR study. The complex was synthesized using the same conditions as the unsubstituted amino acid complexes. The reaction gave the expected product and the ^1H NMR spectrum confirmed the formation of the chelate complex.



The N-methylglycine and the N-methylphenylalanine products were allowed to react with a number of unsaturates. It was hoped that there

would be enhanced reactivity of these N-substituted amino acid complexes due to the weakening of the Ir-N bond. These complexes when treated with acrylamide showed no resonances corresponding to a change in acrylamide, nor were there variations in the resonances of the amino acid complexes. These results support the stability of 5-membered ring systems involving a metal center. Even on extreme heating for long periods of time, no reactivity could be induced between the unsaturated and the amino acid complexes.

3.2.5 Experimental

Exploratory reaction attempt between [Ir(COD)(PMe₃)₃]Cl and N,N dimethylglycine in D₂O CPRII109

N,N dimethylglycine (7.7 mg, 0.0746 mmol) was placed in a screw - cap NMR tube equipped with a septum. The tube was placed in the drybox where it was charged with 20 mg (0.035 mmol) of [Ir(COD)(PMe₃)₃]Cl. D₂O (0.5 mL) was added via syringe outside the drybox. The tube was shaken and monitored at room temperature by ¹H NMR. No reaction was observed. The NMR tube was heated to 50°C and monitored for days. Again, no reaction was seen. On heating the reaction mixture to 100°C, a complex mixture of products was observed in the NMR spectrum.

Exploratory reaction attempt between [Ir(COD)(PMe₃)₃]Cl and N-methylphenylalanine in D₂O (CPRII233)

N-methylphenylalanine (10 mg, 0.075 mmol) was placed in a screw - cap NMR tube equipped with a septum. The tube was placed in the drybox where it was charged with 20 mg (0.035 mmol) of [Ir(COD)(PMe₃)₃]Cl. D₂O (0.5 mL) was added via syringe outside the drybox. The tube was shaken and heated to 100°C. The [Ir(N-Mephe)(H)(PMe₃)Cl] product was identified on the following basis:

¹H-NMR(D₂O): δ 1.54 (d, 9H, PMe₃), 1.61 (d, 9H, PMe₃), 1.69 (d, 9H, PMe₃), 3.0 (s, 3H, -CH₃), 3.2 (d, 2H, -CH₂-), 3.8 (t, 1H, -CH-), 7.2 - 7.4 (br m, 5H, aromaticH)
ppm

Synthesis of [Ir(N-Methylphenylalanine)(H)(PMe₃)₃]Cl (CPRII253)

A 100 mL flask equipped with a stir bar and septum was charged with 335 mg (1.874 mmol) of N-methylphenylalanine. The flask was then charged 500 mg (0.886 mmol) of [Ir(COD)(PMe₃)₃]Cl under N₂ in the drybox. The flask was then connected to a double manifold (vacuum/nitrogen) Schlenk line and 20 mL of distilled water was added to the flask via syringe. The solution was stirred magnetically and heated to reflux. After 18 hours at reflux the reaction was allowed to cool and the solvent was removed in vacuo. The white solid residue was treated with distilled methylene chloride (3 x 10 mL) to extract the

product from the excess amino acid. The solution was filtered from the solid using cannula techniques. The methylene chloride was removed in vacuo and the solids were dried under reduced pressure to yield 260 mg . (0.409 mmol, 46.2% based on the amount of Ir(COD)(PMe₃)₃Cl) of [Ir(N-mephe)(H)(PMe₃)₃]Cl identified on the basis of the following data:

C,H analysis: Calculated for C₁₉H₄₀NO₂P₃IrCl C,35.8% H,6.3%

Found: C, 35.6% H, 6.36%

¹H NMR(CDCl₃) δ 1.52 (d, 9H, J_{P-H} = 10 Hz cis PMe₃), 1.59 (d, 9H, J_{P-H} = 10 Hz, PMe₃) 1.78 (d, 9H, J_{P-H} = 10Hz, PMe₃), 2.91(d, 3H, -CH₃), 3.43 (m, 1H, -CH-), 3.5 (m, 2H, -CH₂-), 7.14 (d, 1H, aromatic H), 7.22 (t, 2H, aromatic H), 7.49(d, 2H, aromatic H), -21.1 (q, 1H, Ir-H) ppm

³¹P NMR(CDCl₃) δ -50.0 (t, J_{p-p} = 20 Hz, 1P, PMe₃), -35.2 (d, J_{p-p} = 20 Hz, 1P, PMe₃), -33.0 (d, J_{p-p} = 20 Hz, 1P, PMe₃) ppm

¹³C NMR(CDCl₃) δ 16.52 (d, J_{c-p} = 30 Hz, PMe₃), 18.59 (t, J_{c-p} = 37 Hz, PMe₃), 21.43 (d, J_{c-p} = 41 Hz, PMe₃), 38.31 (s, -CH₂), 58.64 (s, -CH-), 71.87 (s, N-

CH₃), 128.12 (s, aromatic C), 130.33 (s, aromatic C), 134.65 (s, aromatic C), 139.87.0 (s, aromatic C), 182.1 (s, -COO) ppm

Exploratory reaction between [Ir(COD)(PMe₃)₃]Cl and N-methylglycine in D₂O (CPRII273)

N-methylglycine (6.6 mg, 0.075 mmol) was placed in a screw - cap NMR tube equipped with a septum. The tube was placed in the drybox where it was charged with 20 mg (0.035 mmol) of [Ir(COD)(PMe₃)₃]Cl. D₂O (0.5 mL) was added via syringe outside the drybox. The tube was shaken and heated to 100°C. The [Ir(N-Megly)(H)(PMe₃)₃]Cl product was identified on the following basis:

¹H-NMR(D₂O) δ 1.49(d, 9H, PMe₃), 1.53 (9H, PMe₃), 1.68 (d, 9H, PMe₃), 2.67 (d, 3H, -CH₃-), 3.48 (m, 2H, -CH₂-) ppm

Synthesis of [Ir(N-methylglycine)(H)(PMe₃)₃]Cl (CPRII285)

A 100 ml flask equipped with a stir bar and septum was charged with 82.5 mg (0.936 mmol) of N-methylglycine. The flask was then charged 250 mg (0.443 mmol) of [Ir(COD)(PMe₃)₃]Cl under N₂ in the drybox. The flask was then connected to a double manifold (vacuum/nitrogen) Schlenk line and 30 mls of distilled water was added to the flask via syringe. The solution was stirred magnetically and heated to reflux. After 18 hours at reflux the reaction was allowed to cool and the solvent was removed in vacuo. The white solid residue was

treated with distilled methylene chloride (3 x 10 mL) to extract the product from the excess amino acid. The solution was filtered from the solid using cannula techniques. The methylene chloride was removed in vacuo and the solids were dried under reduced pressure to yield 110 mg, 0.184 mmol mmol 41.5% based on the amount of Ir(COD)(PMe₃)₃Cl) of [Ir(N-Me-gly)(H)(PMe₃)₃Cl identified on the basis of the following data:

¹H NMR(CDCl₃) δ 1.56 (d, 9H, J_{P-H} = 7 Hz PMe₃), 1.63 (d, 9H, J_{P-H} = 10 Hz PMe₃), 1.79 (d, 9H, J_{P-H} = 11 Hz PMe₃), 2.80 (d, 3H, -CH₃), 3.76 (m, 2H, -CH₂), 7.41 (br s, 1H, -NH) ppm

³¹P NMR(CDCl₃) δ -48.7 (m, J_{P-P} = 16 Hz, cis PMe₃), -35.1 (dd, 2P, J_{P-P} = 20 Hz, trans PMe₃) ppm

¹³C NMR(CDCl₃) δ 18.34 (t, J_{C-P} = 17 Hz, trans PMe₃), 21.25 (d, J_{C-P} = 40 Hz, cis PMe₃), 53.62 (s, -CH-) 56.62 (s, N-CH₃), 183.15 (s, -COO) ppm

Reaction attempt between [Ir(N-Megly)(PMe₃)₃Cl and acrylamide in D₂O (CPRII293)

Acrylamide (5.3 mg, 0.075 mmol) was placed in a screw - cap NMR tube equipped with a septum. The tube was placed in the drybox where

it was charged with 20 mg (0.035 mmol) of $[\text{Ir}(\text{N-megly})(\text{PMe}_3)_3]\text{Cl}$. The tube was removed from the drybox where it was charged 0.5 mL of D_2O via syringe. The tube was shaken and monitored at room temperature by ^1H NMR spectroscopy. No reaction was observed. The NMR tube was heated to 100°C and monitored for days. Again, no reaction was observed.

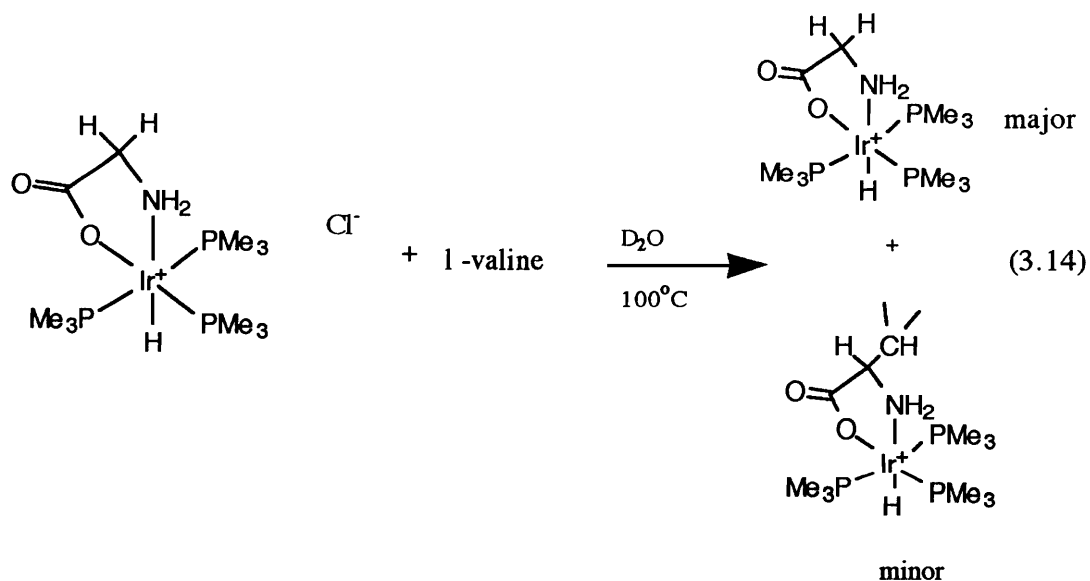
Reaction attempt between $[\text{Ir}(\text{N-Me-phe})(\text{PMe}_3)_3]\text{Cl}$ and acrylamide in D_2O (CPRII269)

Acrylamide 50.0 mg, 0.703 mmol) of was placed in a screw - cap NMR tube equipped with a septum. The tube was placed in the drybox where it was charged with 25 mg (0.443) of $[\text{Ir}(\text{N-Me-phe})(\text{PMe}_3)_3]\text{Cl}$. The tube was removed from the drybox where it was charged 0.5 mL of D_2O via syringe. The tube was shaken and monitored at room temperature by ^1H NMR spectroscopy. No reaction was observed. The NMR tube was heated to 100°C and monitored for days, No reaction was observable by NMR spectroscopy.

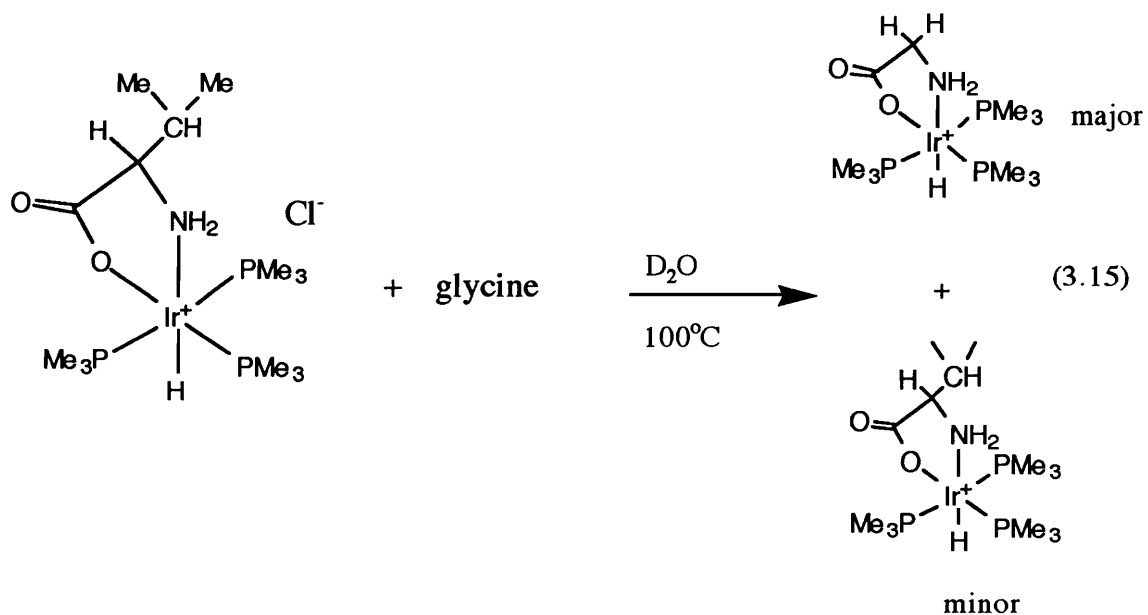
3.2.6 Exchange Reactions

The reactivity studies of the amino acid complexes and N-substituted amino acid complexes were not very encouraging as far as activity towards unsaturates. There were two studies however, that indicated reactivity is possible with these complexes.

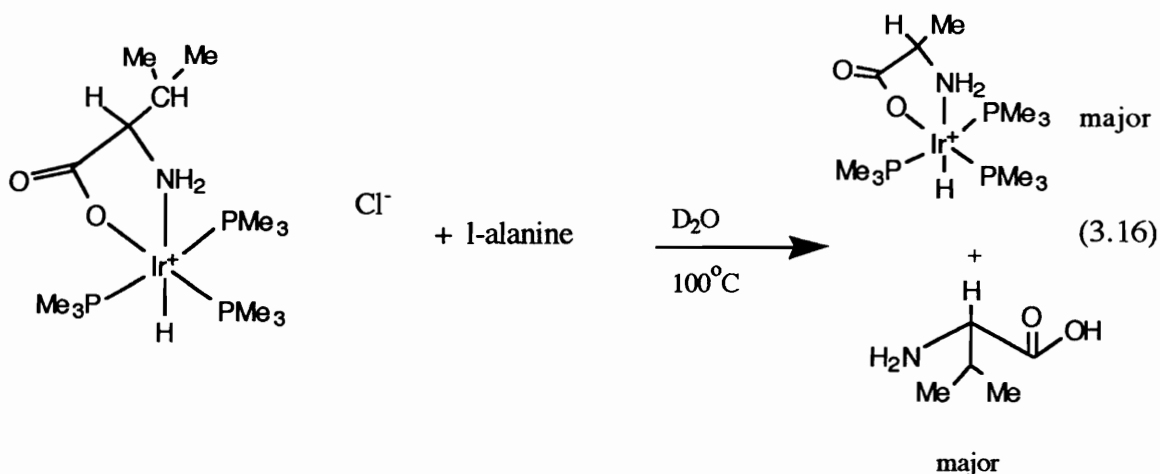
The first of these studies was a series of exchange reaction experiments. The question being whether or not an amino acid complex of one acid would exchange its ligand for another amino acid in solution. The first of these reactions was done with the glycine product and free *l*-valine (equation 3.14). On observing the reaction by ^1H NMR spectroscopy for days at room temperature, no reaction was seen. On heating to 100°C overnight a small amount of *l*-valine iridium complex is formed and a resonance corresponding to the methylene protons of free glycine is observed.



The next exchange reaction was done with the valine complex and free glycine (equation 3.15), at 100°C in D_2O , the valine complex was almost completely converted to the $[\text{Ir}(\text{gly})(\text{PMe}_3)_3]\text{Cl}$ complex. The resonances for free valine and attached glycine were clearly evident in the ^1H NMR spectrum.



The final study of this type was done with the valine complex and free *l*-alanine (equation 3.16). When these two reactants are heated to 100°C in D₂O overnight, the formation of alanine complex and liberation of free valine is evident from the resonances observed in the ¹H NMR spectrum. Based on the hydride resonances the ratio of alanine complex to valine complex in the study is 5:1.



This exchange reaction study can be explained simply by looking at the sidechain of the amino acid. The larger the side chain the easier to replace that amino acid. The smaller side chain amino acid will replace the complexed amino acid with the larger side chain in high yield. This clearly shows the amino acids are somewhat labile which raises the question of why no reactivity was observed. Clearly more investigations are warranted.

3.2.7 Experimental

Reaction attempt between [Ir(gly)(PMe₃)₃]Cl and *l*-valine in D₂O (CPRII023)

l-Valine (10 mg, 0.086 mmol) was placed in a screw-cap NMR tube equipped with a septum. The tube was placed in the drybox where it was charged with 20 mg (0.0377 mmol) of [Ir(gly)(PMe₃)₃]Cl. D₂O (0.5 mL) was added via syringe to the NMR tube outside the drybox. The tube

was shaken and monitored by ^1H NMR spectroscopy at room temperature. No reaction was observed. The tube was then heated to 100° , the NMR spectrum display resonances indicative of a small amount of exchange between the two amino acids.

^1H -NMR (D_2O):
 δ 0.81 (d d, start of formation of valine complex)
1.57 (t, 18H, trans PMe_3 of glycine complex)
1.66 (d, 9H, cis PMe_3 of glycine complex) 2.16
(m, -CH of isopropyl (free valine), 3.44 (s, - CH_2 -
of glycine product), 3.49 (d, -CH- α carbon H)
ppm

Reaction between $[\text{Ir}(\ell\text{-val})(\text{PMe}_3)_3]\text{Cl}$ and glycine in D_2O (CPRII177)

Glycine (3 mg, 0.0405 mmol) was placed in a screw-cap NMR tube equipped with a septum. The tube was placed in the drybox where it was charged with 20 mg (0.0405 mmol) of $[\text{Ir}(\text{val})(\text{PMe}_3)_3]\text{Cl}$. D_2O (0.5) mL was added via syringe to the NMR tube outside the drybox. The tube was shaken and monitored by ^1H NMR at room temperature. No reaction was observed. The tube was then heated to 100° , the NMR spectrum showed resonances indicative of exchange between the two amino acids.

$^1\text{H-NMR}$ (D_2O): δ 1.56 (t, 18H, PMe_3 of glycine complex) 1.64(d, 9H, PMe_3 of glycine complex) 3.44(s, $-\text{CH}_2-$ of glycine product) ppm

Reaction between $[\text{Ir}(\ell\text{-val})(\text{PMe}_3)_3]\text{Cl}$ and ℓ -alanine in D_2O (CPRII193)

ℓ -Alanine (3 mg, 0.034 mmol) was placed in a screw-cap NMR tube equipped with a septum. The tube was placed in the drybox where it was charged with 20 mg (0.040 mmol) of $[\text{Ir}(\text{val})(\text{PMe}_3)_3]\text{Cl}$. D_2O (0.5 mL) was added via syringe to the NMR tube outside the drybox. The tube was shaken and monitored by ^1H NMR spectroscopy at room temperature. No reaction was observed. The tube was then heated to 100° , the NMR spectrum showed resonances indicative of exchange between the two amino acids.

$^1\text{H-NMR}$ (D_2O): δ 0.87 (free valine isopropyl methyls), 1.44 (d, 9H, PMe_3 of alanine complex) 1.51 (d, 9H, PMe_3 of alanine complex) 1.65 (d, 9H, PMe_3 of alanine complex), 3.35 (q, $-\text{CH}-\alpha$ carbon H of alanine complex) ppm

3.2.8 Insertion reaction with 2-amino-4-pentenoic acid

The study that best supports possible reactivity of the amino acid complexes involved reaction with 2-amino-4-pentenoic acid. This amino acid has an olefin tethered on its side chain. [Figure 3.5]

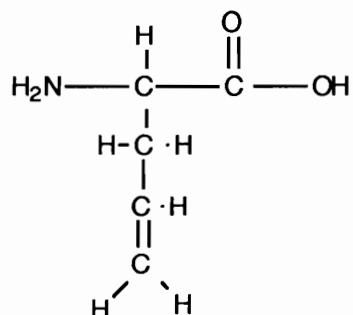
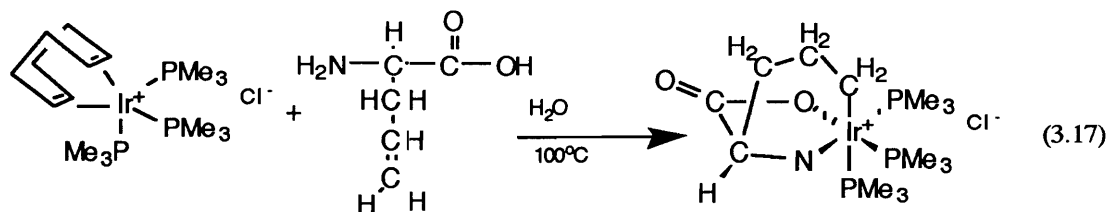


Figure 3.6 Amino acid with tethered olefin

On chelation the amino acid should allow the olefin to get within proximity to the Ir-H bond to insert. The ^1H NMR study of 2-amino-4-pentenoic acid was done in a manner analogous to the initial NMR studies described in Chapter 2 (equation 3.17). The important piece of analytical data in this study was the fact that the proton NMR was clean, showed resonances corresponding to a facial arrangement of phosphines in the octahedron (based on the splitting and chemical shifts of the trimethyl phosphine protons.) and there was no hydride resonance present in the spectrum. The only other resonances were the methylene protons of the amino acid side chain, This is the result expected for the amino acid complex with the side chain olefin inserted into the Ir-H bond.



The preparative scale reaction of this experiment was done in order to obtain enough product to gather more analytical data. The ^{31}P NMR and ^{13}C NMR spectra both support the fact that the amino acid has chelated to the metal and the olefin has inserted into the hydride bond. The most important part of the spectrum is the resonance at 6ppm in the ^{13}C NMR. This doublet of triplets is shifted upfield due to the high electron density around this particular carbon bound directly to the metal. The carbon is cis to two phosphines giving rise to the triplet splitting and is trans to another phosphine giving rise to the larger coupling constant for the doublet. All of this data completely supports the insertion of the olefin into the hydride bond. [Figure 3.7]

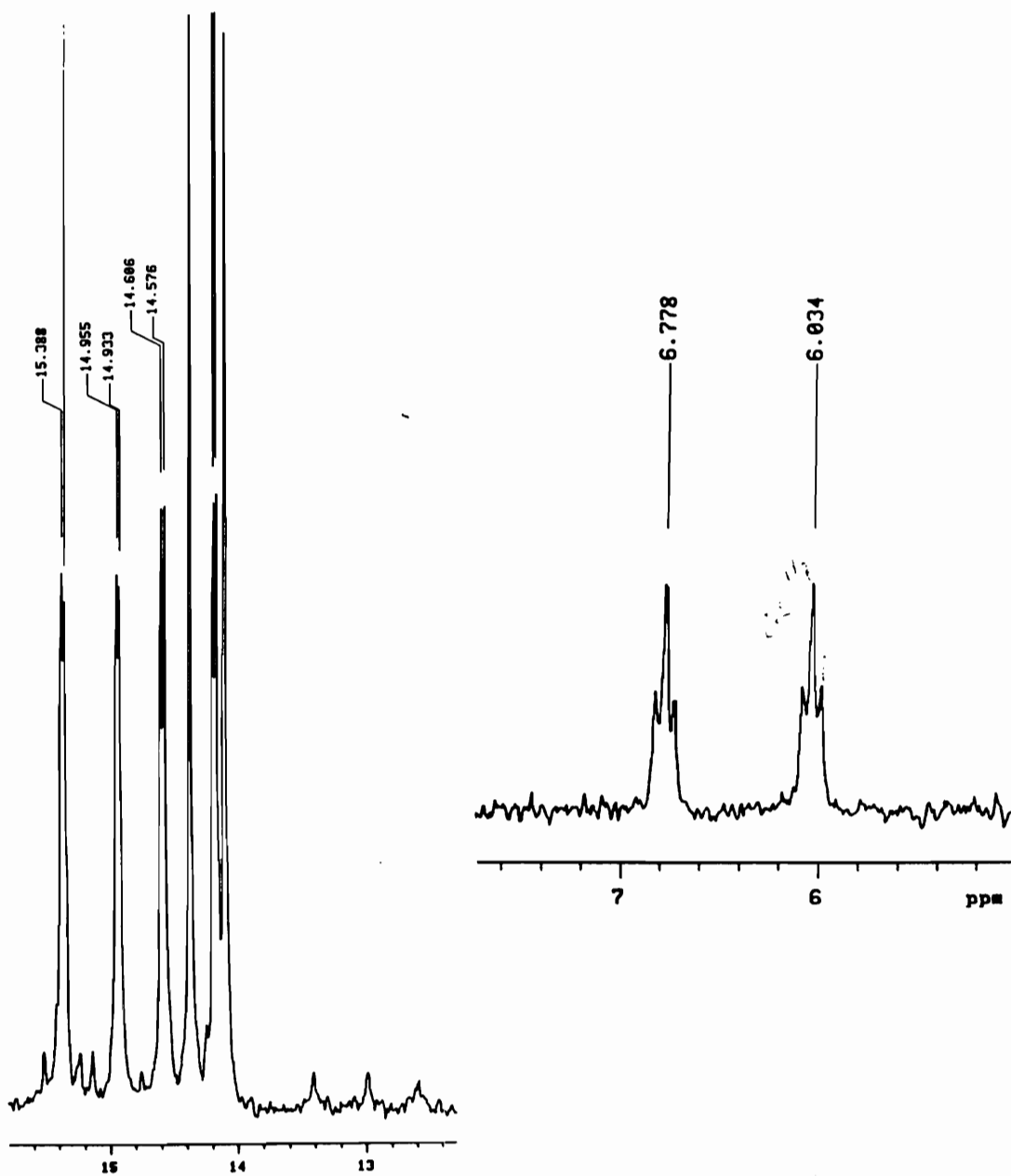


Figure 3.7 ^{13}C NMR of 2-amino-4-pentenoic acid product in CDCl_3 (400 MHz)

To gain definitive proof of the structure, a single crystal was grown to carry out an X-ray diffraction study. Crystals were grown by layering ether over a methylene chloride solution of the 2 amino 4 pentenoic acid product. The complex crystallizes in the monoclinic $P2_1/C$ space group with $a = 9.317(2)\text{\AA}$, $b = 17.028(5)\text{\AA}$, $c = 16.855(8)\text{\AA}$, $V = 2607(2)\text{\AA}^3$ and $d_{\text{calcd}} = 1.757 \text{ Mg/m}^3$ for $Z = 4$. (Figure 3.8) The Ir-N bond length of $2.156(9)\text{\AA}$ is shorter than the Ir-N bonds of the valine and proline complexes. ($2.190(11)\text{\AA}$ and $2.211(7)\text{\AA}$). The nitrogen is trans to hydride in the valine and proline complexes and the Ir-N bond is lengthened due to the strong trans effect of hydride. The nitrogen of the 2-amino4-pentenoic acid complex is trans to PMe_3 which has weaker trans effect. The Ir-O bond of $2.110(6)\text{\AA}$ is in line with the Ir-O bond lengths found for the valine and proline complexes. The complex itself is of interest in the fact that that it has a 5, 6, 7 ring system based on the tridentate ligand and the metal center. It would be of considerable interest if the ring system could be reductively eliminated to form heterocyclic fragments. Studies were done to see if this reductive elimination of the tridentate ligand from the metal center was possible.

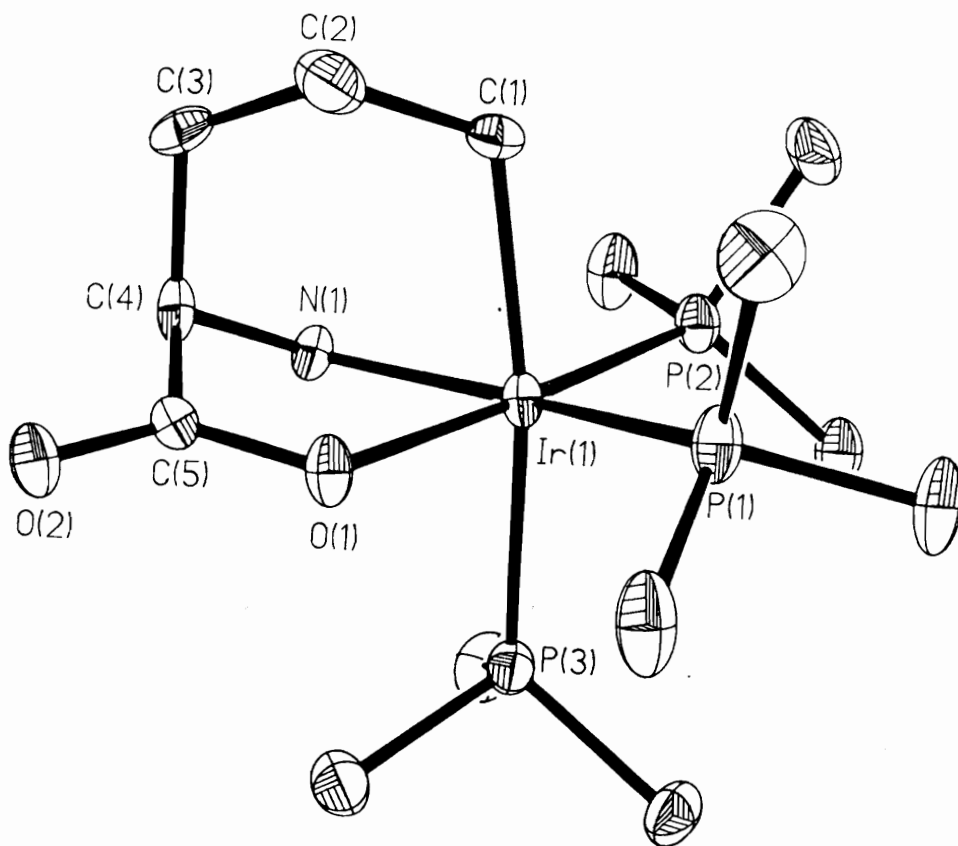
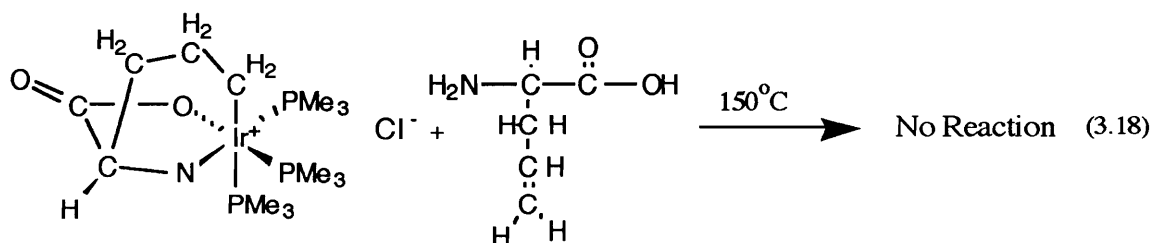


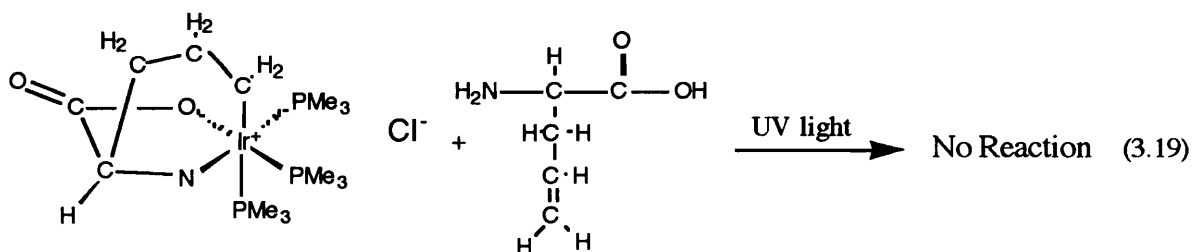
Figure 3.8 ORTEP plot of the 2-Amino-4-penteneoic acid product

The first of these studies was done by attempting thermal activation of the complex (equation 3.18). The complex was placed in solution, treated with free 2-amino-4-pentenoic acid, heated and monitored by NMR spectroscopy. The solution was heated to 100°C and then to 150°C and in both cases the NMR spectra showed that the starting materials remained unchanged.

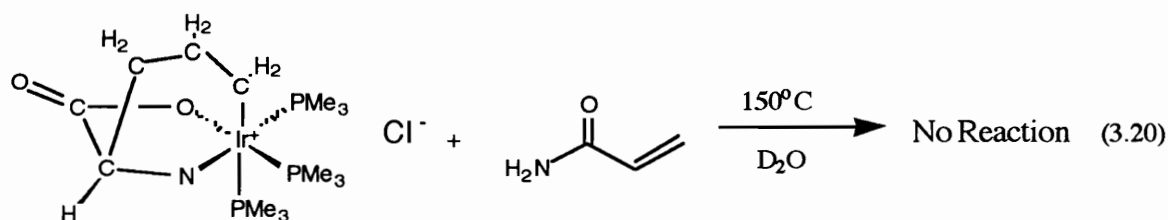


The use of heat has no effect on the complex at all. The solution was heated to 150°C for days with no change in the NMR spectrum.

The same reaction was attempted, but instead of heating the solution, the complex was exposed to UV light in a quartz EPR tube. (equation 3.19) The solution was irradiated over night and monitored at intervals for evidence of photochemical induced elimination. This study showed no reactivity of the complex either.



The last study attempted was the reaction of the complex with unsaturates to see if there was any reactivity. The complex was reacted with acrylamide in an NMR study (equation 3.20). The reaction was started at 100°C and was heated to 150°C when no reaction was observed by ¹H NMR spectroscopy. The study showed that the tridentate complex was as unreactive as the bidentate amino acid complexes.



The studies on reactivity of these complexes with unsaturates has shown that the complexes are very stable. The prolonged heating and treatment with unsaturates has not produced any reactivity of these complexes. The study that does have an insertion occurring is with the olefin tethered to the amino acid and further studies on that complex do not show any reactivity. The tridentate complex is just as stable, if not more so than the bidentate complexes.

3.2.9 Experimental

Exploratory reaction attempt between [Ir(COD)(PMe₃)₃]Cl and 2-amino-4-pentenoic acid in D₂O (CPRII113)

2-Amino-4-pentenoic acid (9 mg, 0.0735 mmol) was placed in a screw - cap NMR tube equipped with a septum. The tube was placed in the drybox where it was charged with 20 mg (0.035 mmol) of [Ir(COD)(PMe₃)₃]Cl. D₂O (0.5 mL) was added via syringe outside the drybox. The tube was shaken and monitored at room temperature by ¹H NMR spectroscopy. No reaction was observed. The reaction mixture was heated to 100°C. A ¹H NMR spectrum was obtained after 18 hours. The [Ir(2-amino-4-pent)(PMe₃)₃]Cl product was identified on the basis of the following data:

¹H NMR (D₂O): δ 1.4 (d, 9H, PMe₃), 1.5 (d, 9H, PMe₃), 1.57(d, 9H, PMe₃), 1.88 (br, 2H, -CH₂-), 2.5 (br m, 2H, -CH₂), 3.7 (t, 1H, -CH-), 3.9 (m, 2H, -CH₂-) ppm

Synthesis of [Ir(2-amino-4-pentenoate)(H)(PMe₃)₃]Cl (CPRII115)

A 100 mL flask equipped with a stir bar and septum was charged with 90 mg (0.075 mmol) of 2-amino-4-pentenoic acid. The flask was then charged 200 mg (0.354 mmol) of [Ir(COD)(PMe₃)₃]Cl under N₂ in the drybox. The flask was then connected to a double manifold (vacuum/nitrogen) Schlenk line and 25 mL of distilled water was added to the flask via syringe. The solution was stirred magnetically and

heated to reflux. After 18 hours at reflux the reaction was allowed to cool and the solvent was removed in vacuo. The white solid residue was treated with distilled methylene chloride (3 x 10 mls) to extract the product from the excess amino acid. The solution was filtered from the solid using cannula techniques. The methylene chloride was removed in vacuo and the solids were dried under reduced pressure to yield 150 mg (0.262 mmol, 74.2% based on the amount of Ir(COD)(PMe₃)₃]Cl) of [Ir(2-amino-4-pent)(PMe₃)₃]Cl identified on the basis of the following data:

C,H analysis: Calculated for: C₁₄H₃₆NO₂P₃Cl C, 29.3 %, H, 6.3%

Found: C, 28.97%, H, 6.47%

¹H NMR (CDCl₃): δ 1.40 (d, 9H, J_{P-H} = 8 Hz, PMe₃), 1.48 (d, 9H, J_{P-H} = 10 Hz, PMe₃), 1.51 (d, 9H, J_{P-H} = 10 Hz, PMe₃), 1.82 (m, 2H, -CH₂-), 3.53 (m, 1H, -CH-) 3.92 (t, 2H, -CH₂-), 4.2 (m, 2H, -CH₂-) ppm

³¹P NMR (CDCl₃): δ -48.5 (d, 1P, J_{P-P} = 21 Hz, PMe₃), -35.2 (d, 1P, J_{P-P} = 20 Hz, PMe₃), -33.1 (d, 1P, J_{P-H} = 20 Hz, PMe₃)
ppm

^{13}C NMR(CDCl_3) δ 6.36 (dt, $J_{\text{C-P}} = 37.2$ Hz, 75 Hz, 1C, Ir-C),
4.16(d, $J_{\text{C-p}} = 28$ Hz, PMe_3), 14.38 (d, $J_{\text{C-p}} =$
40 Hz, PMe_3), 14.99 (d, $J_{\text{C-p}} = 21$ Hz, PMe_3),
20.09 (s, $-\text{CH}_2-$), 57.53 (s, $-\text{CH}_2-$), 121.73 (s,
 $-\text{CH}_2$), 186.13 (s, $-\text{COO}-$) ppm

Reaction attempt between $[\text{Ir}(2\text{-amino-4-pentenoate})(\text{PMe}_3)_3]\text{Cl}$ and 2-amino-4-pentenoic acid in D_2O (CPRII169)

2-Amino-4-pentenoic acid (25 mg, 0.217 mmol) was placed in a screw - cap NMR tube equipped with a septum. The tube was placed in the drybox where it was charged with 20 mg (0.035) of $[\text{Ir}(2\text{-amino-4-pentenoate})(\text{PMe}_3)_3]\text{Cl}$. D_2O (0.5 mL) was added via syringe to the NMR tube outside the drybox. The tube was shaken and monitored by ^1H NMR spectroscopy at room temperature. No reaction was observed. The tube was then heated to 100°C . No reaction was observed after heating for days. After heating the tube to 150°C , no reaction was observed by NMR spectroscopy.

Reaction attempt between $[\text{Ir}(2\text{-amino-4-pentenoate})(\text{PMe}_3)_3]\text{Cl}$ and 2-amino-4-pentenoic acid in D_2O (CPRII171)

2-Amino-4-pentenoic acid 25 mg, 0.217) of was placed in a quartz EPR tube equipped with a septum. The tube was placed in the drybox where it was charged with 20 mg (0.035 mmol) of $[\text{Ir}(2\text{-amino-4-pentenoate})(\text{PMe}_3)_3]\text{Cl}$. D_2O (0.5 mL) was added via syringe to the NMR tube outside the drybox. The tube was shaken and monitored by ^1H

NMR spectroscopy at room temperature. No reaction was observed. The tube was then exposed to UV light, no reaction was observed after exposure for days.

Reaction attempt between [Ir(2-amino-4-pentenoate)(PMe₃)₃]Cl and acrylamide in D₂O (CPRII241)

Acrylamide (5.23 mg, 0.075 mmol) was placed in a screw - cap NMR tube equipped with a septum. The tube was placed in the drybox where it was charged with 20 mg (0.035 mmol) of [Ir(2-amino-4-pentenoate)(PMe₃)₃]Cl. D₂O (0.5 ml) was added via syringe to the NMR tube outside the drybox. The tube was shaken and monitored by ¹H NMR spectroscopy at room temperature. No reaction was observed. The tube was then heated to 100°C, Again, no reaction was observed after heating for days. After heating the tube to 150°C, no reaction was observed by NMR spectroscopy.

3.3 Biological Assay Studies of Amino Acid Complexes

A number of the amino acid hydride complexes that were synthesized were sent to the NCI for anti-cancer and anti-AIDS assay testing. The interest in inorganic complexes for use in biological

applications has been strong since the success of cisplatin in treating tumors. The complexes sent were to be test in both anti cancer and in anti AIDS assays. The results will presented in this section.

The complexes that were tested were the amino acid complexes of threonine, proline, histidine, phenylalanine, tryptophan, tyrosine, picolinic acid, pipercolic acid, serine, isoleucine. In the cancer assays the complexes were found to have no activity that merited further testing or study. A surprising result in the anti- HIV assay has suggested that these complexes may have some biological applications.

The procedure⁴ that is used in the NCI test for activity against HIV is designed to detect activity against the virus at any stage of the reproductive cycle. The assay is designed to monitor the killing of T4 lymphocytes by HIV. Small amounts of the virus are added to the cells and a complete reproductive cycle is necessary to obtain cell killing. Agents that interact with the cells or virus gene-products to interfere with the activity of the virus will prevent the cells from cytolysis. All tests are compared with at least one positive control done under identical conditions.

The results for the phenylalanine complex suggested that it has moderate activity against HIV. The results are represented graphically Figure (3.3.1) and show the response curve of the complex. The dotted line of the data curve shows the response of the cell culture not treated with HIV, to the complex. The solid line represents the response curve of the infected cell culture to the complex. In the case of phenylalanine the protection percentage approaches 77% protected. The results are very

promising. An interesting observation is made when comparing the results of phenylalanine complex with the results from the assay with tyrosine complex. The structures of the two complexes only varies by the addition of a hydroxyl group to the phenyl ring of tyrosine.

But if one looks at the graphical representation of the data obtained for tyrosine in the assay, it is obvious that all activity is lost. (Figure 3.3.2)

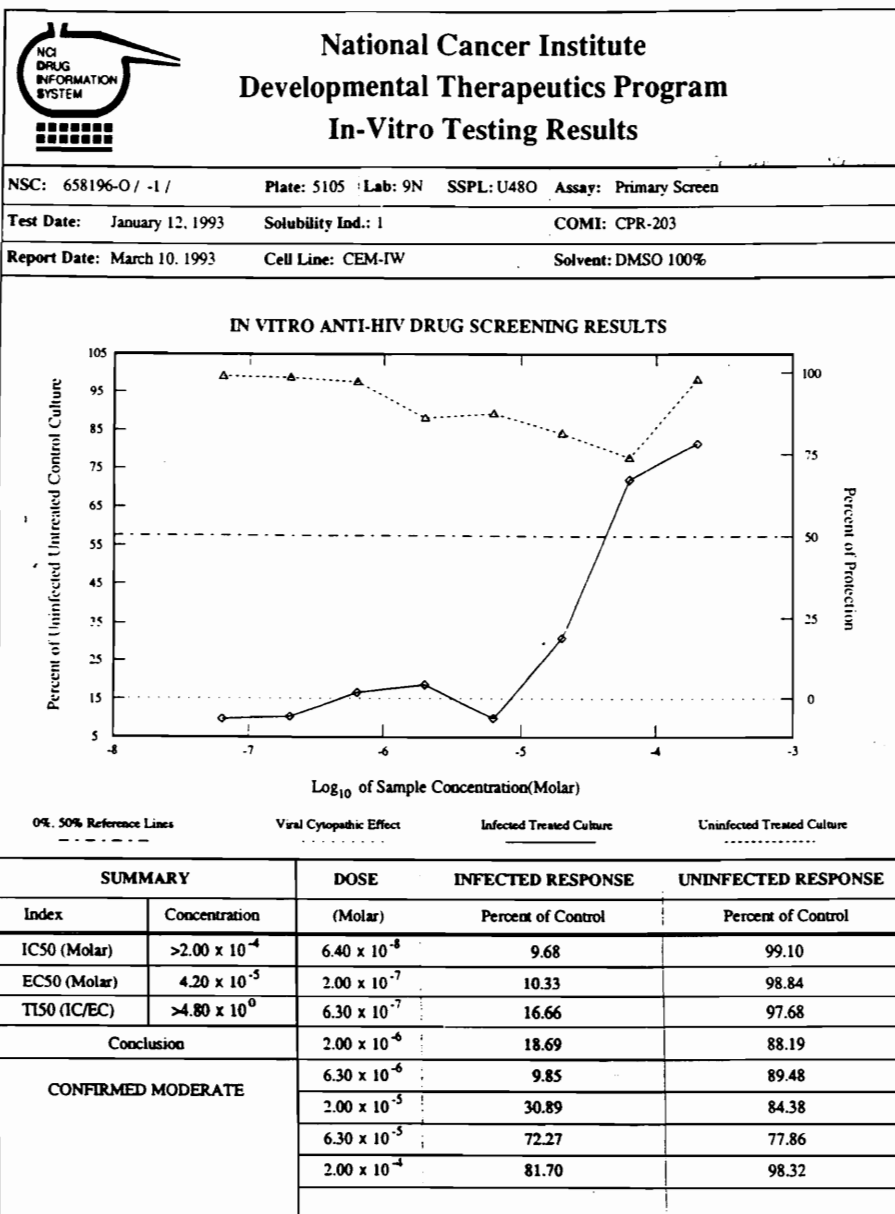
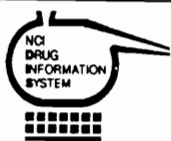
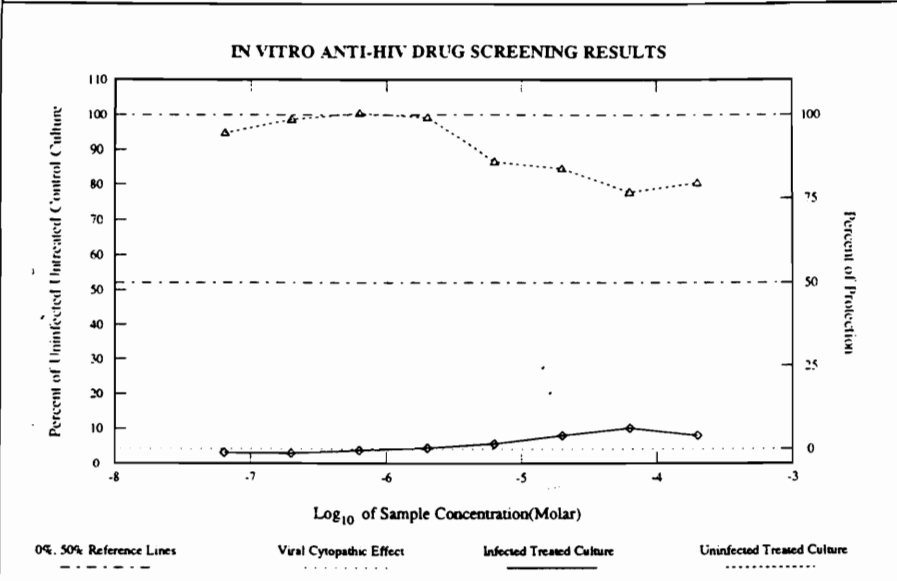


Figure 3.3.1 Graph of HIV assay with phenylalanine complex



**National Cancer Institute
Developmental Therapeutics Program
In-Vitro Testing Results**

NSC: 658197-P / -1 / Plate: 6147 Lab: 9N SSPL: U480 Assay: Primary Screen
 Test Date: February 17, 1993 Solubility Ind.: 1 COMI: CPR-237
 Report Date: March 10, 1993 Cell Line: CEM-1W Solvent: DMSO 100%



SUMMARY		DOSE	INFECTED RESPONSE	UNINFECTED RESPONSE
Index	Concentration	(Molar)	Percent of Control	Percent of Control
IC50 (Molar)	>2.00 x 10 ⁻⁴	6.40 x 10 ⁻⁸	3.14	94.76
EC50 (Molar)		2.00 x 10 ⁻⁷	2.98	98.62
TI50 (IC/EC)		6.30 x 10 ⁻⁷	3.82	100.47
Conclusion		2.00 x 10 ⁻⁶	4.54	99.10
CONFIRMED INACTIVE		6.30 x 10 ⁻⁶	5.71	86.71
		2.00 x 10 ⁻⁵	8.04	84.70
		6.30 x 10 ⁻⁵	10.18	77.70
		2.00 x 10 ⁻⁴	8.00	80.36

Figure 3.3.2 Graph of HIV assay with tyrosine complex

The results from this study are encouraging. The next step is to synthesize analogs of the phenylalanine complex and have them tested for activity. The graphical data is extremely interesting that a simple change, such as the addition of a hydroxyl group, can totally change the complexes activity. The study of these complexes as possible therapeutic agents is a worthwhile endeavor. The variety of amino acids available makes the number of analogs that can be synthesized a project that demands study.

3.4 References

- ¹ Ladipo, F., Ph.D. Thesis, Virginia Polytechnic and State University, 1991.
- ² Frazier, J. MS Thesis, Virginia Polytechnic and State University, 1990.
- ³ Werner et al., *Organomet.* , **11**, 1992 (1126).
- ⁴Weislow, O.W., Kiser, R., Fine, D., Bader, J., Shoemaker, R.H., *J. Natl. Cancer Inst.* , **81**, 1989 (577).

Chapter 4 Oxidative Addition of other Biologically Interesting Compounds

4.1 Introduction

The final study which will be discussed is the reactions between $[\text{Ir}(\text{COD})(\text{PMe}_3)_3]\text{Cl}$ and biologically interesting molecules. A number of amino acid complexes had been submitted to the NCI for testing as anti-cancer and anti-AIDS agents. The majority of these complexes did not have any activity, but there was some activity determined for one of the compounds. The activity of this one compound led us to work on other compounds of biological interest. The bioinorganic chemistry of iridium is virtually unknown. The formation of complexes of biological compounds with iridium should have potential value when one considers the interest in cisplatin over the years. The enhancement of biological activity or inhibition of activity of these compounds by addition to a metal center is a worthwhile study. These complexes are the first bioinorganically related complexes of iridium to be reported. The biological molecules were studied for their potential as oxidative addition products with the metal center.

4.2 Results and Discussion

In terms of simple, biologically important molecules, urea is one of the simplest. While oxidative addition of N-H groups of amides to $[\text{Ir}(\text{COD})(\text{PMe}_3)_3]\text{Cl}$ has not yet been demonstrated, it seemed that

studying the reaction between Ir and urea was a worthwhile endeavor.
(Figure 4.1)

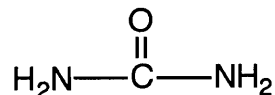
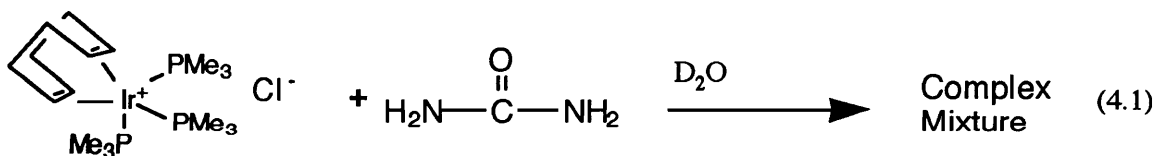


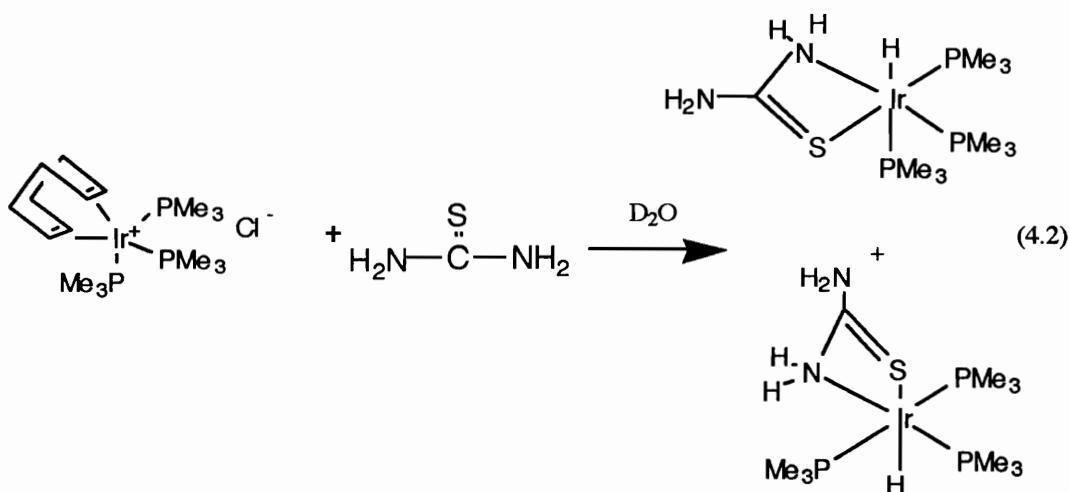
Figure 4.1 Urea has the potential to bind through two sites.

The reaction between urea and $[\text{Ir}(\text{COD})(\text{PMe}_3)_3]\text{Cl}$ was initially set up as an NMR study (equation 4.1). At room temperature, no reaction was observed. Upon increasing the temperature to 50°C , a complex mixture of products was observed in the NMR spectrum. The solution was then heated to 100°C to see if the formation of one product could be induced. The ^1H NMR spectrum showed that a complex mixture of products remained after prolonged heating at high temperature,



Iridium (and most other 3rd row transition elements) has been shown to have a high affinity for sulfur. The sulfur analog of urea, was used in a study similar to that of the urea reaction. The thiourea compound underwent a reaction much cleaner than urea. The solution was monitored by ^1H -NMR at room temperature, heated to 50°C , and then heated to 100°C (equation 4.2). After heating at 100°C for 18 hours, a mixture of two isomers was observed in the ^1H NMR spectrum. This mixture was readily identifiable from the hydride region of the

spectrum. A doublet of triplets corresponding to a hydride being trans to a phosphine and cis to two phosphines (facial isomer) was observed at -10.05 ppm. The hydride of the meridional isomer was also observed as a quartet shifted to -19.43 ppm. The quartet arises from the hydride being oriented cis to all three trimethyl phosphines of the complex. The ratio of isomers was 1:1 based on integration of the hydride peaks.



The reaction was scaled up and the mixture was treated in a manner analogous to that used for the amino acid products. The ¹H-NMR of the clean product again showed a mixture of facial and meridional isomers. The ratio of isomers was 1:1 based on integration of the hydride peaks. The product(s) were dissolved in water and treated with a solution of K⁺PF₆⁻. A solid precipitated, was filtered from solution using cannula techniques and dried under reduced pressure. The product was recrystallized from methylene chloride/ether and a crystal structure was solved based on one of the crystals obtained.(Figure 4.2)

The complex crystallizes in the monoclinic space group Cc with $a = 12.834(4)\text{\AA}$, $b = 15.287(4)\text{\AA}$, $c = 13.433(4)\text{\AA}$, $V = 2331.4(12)\text{\AA}^3$, and $d_{\text{calcd}} = 1.828\text{ Mg/m}^3$ for $Z = 4$. The solid state structure supported one of the proposed structures for the compound. The octahedral complex is facial in its arrangement of PMe_3 around the metal center. The crystal that was selected from the batch was a facial isomer. The Ir-S bond of $2.470(9)\text{\AA}$ is considerably longer than that of the benzothiophene ring opening product described by Selnau¹ with an Ir-S bond length of $2.374(2)\text{\AA}$. This is most readily explained by the sulfur sharing in the π system of the benzothiophene system, giving it more double bond character, thus shortening the bond. The Ir-N bond length of $2.100(37)\text{\AA}$ is shorter than that of the amino acid complexes, Ir-N of proline complex $2.211(7)\text{\AA}$. This is explained by the hydride trans effect observed in the amino acid complex lengthening the bond, but the N in the thiourea complex is now trans to PMe_3 instead of the hydride. The hydride was not found in this experiment but occupies the open site trans to PMe_3 .

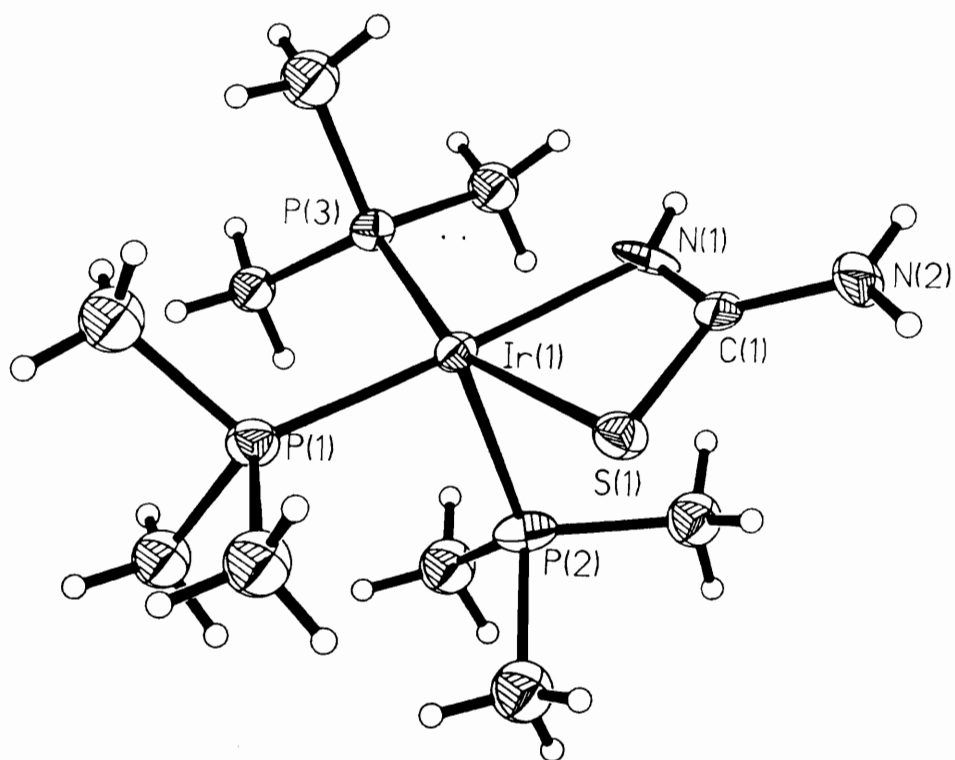


Figure 4.2 ORTEP plot of [Ir(thiourea)(H)(PMe₃)₃]⁺PF₆⁻

Similar NMR reactions were run on a number of sulfur containing compounds. These compounds include thiohydantoin, thioacetamide and thiouracil.(Figure 4.3)

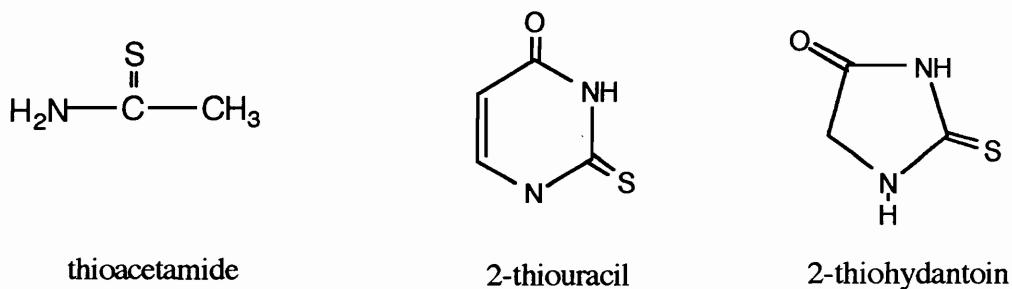


Figure 4.3 Sulfur containing compounds used in study

All of these compounds showed reactivity similar to that of thiourea. In all cases a mixture of facial and meridional isomers was observed in the ^1H -NMR spectra as evidence to those isomers. The thioacetamide complex was also prepared on a preparative scale. The reaction was done using methods analogous to that of thiourea and $[\text{Ir}(\text{COD})(\text{PMe}_3)_3]\text{Cl}$. The PF_6^- salt was prepared by treating an aqueous solution of thioacetamide complex with a solution of K^+PF_6^- . The crystals of the thioacetamide complex were grown from a solution of methylene chloride and ether. The X-ray structure was solved for the complex. (Figure 4,4)

The complex crystallizes in the orthorhombic Pnma space group with $a = 13.299(3)\text{\AA}$, $b = 12.002(4)\text{\AA}$, $c = 14.958(4)\text{\AA}$, $V = 2387.5(11)\text{\AA}^3$ and $d_{\text{calc}} = 1.785 \text{ Mg/m}^3$ for $Z = 4$. The solid state structure determined that the crystal studied was the meridional isomer. The complex has a longer Ir-S bond ($2.487(6)\text{\AA}$) than the $2.470(9)\text{\AA}$ bond length found for the

thiourea complex. This lengthening is explained by the strong hydride trans effect on the sulfur in this complex. The Ir-N bond of the thioacetamide complex (2.126(17) is slightly longer than that of the thiourea complex by 0.02Å. The S-Ir-N bonds angles on both complexes are consistent with each other. The S-Ir-N bond angle of the thiourea complex is 66.5(7)°, as compared to that of thioacetamide complex, 64.8(5)°. The hydride was not found in this experiment, but as mentioned is located on the open site trans to the sulfur.

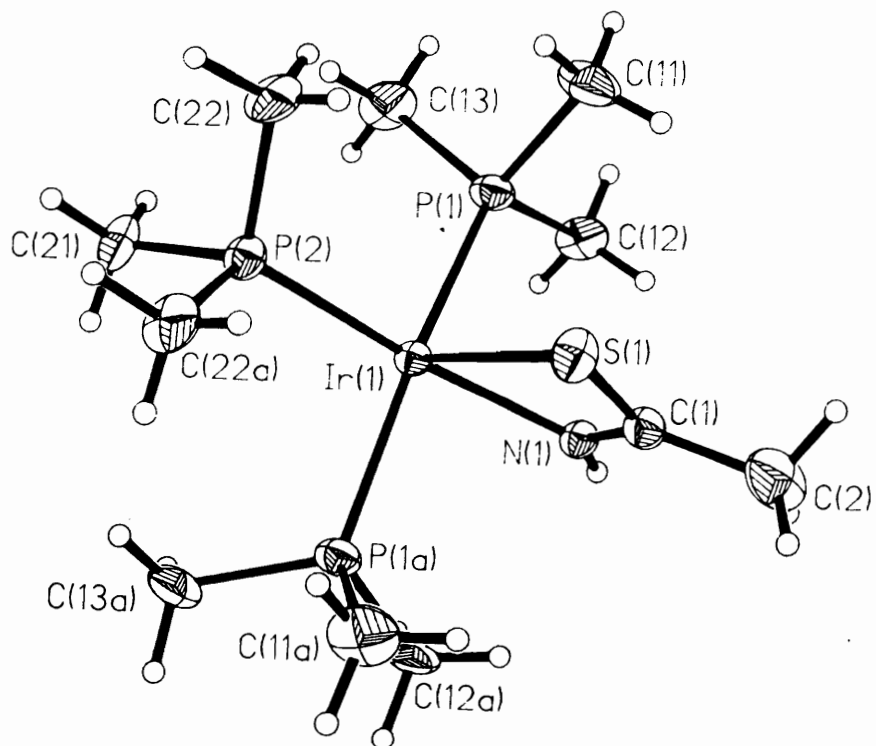


Figure 4.4 ORTEP plot of [Ir(thioacetamide)(H)(PMe₃)₃]PF₆

The sulfur containing compounds all showed a mixture of facial and meridional isomers in the ^1H NMR spectra. The oxygen analogs of these compounds were also studied but the NMR studies all showed that a complex mixture of products was forming. The crystal structures show the formation of a four membered iridacycle which should be more reactive than the stable 5 membered ring systems formed with amino acids². The study of these complexes with unsaturates is the next set of future studies.

4.2.1 Experimental

Exploratory reaction attempt between $[\text{Ir}(\text{COD})(\text{PMe}_3)_3]\text{Cl}$ and urea in D_2O (CPRIII017)

Urea (5 mg, 0.0735 mmol) was placed in a screw - cap NMR tube equipped with a septum. The tube was placed in the drybox where it was charged with 20 mg (0.035 mmol) of $[\text{Ir}(\text{COD})(\text{PMe}_3)_3]\text{Cl}$. D_2O (0.5 ml) was added via syringe outside the drybox. The tube was shaken and monitored at room temperature by ^1H NMR spectroscopy. No reaction was observed. The NMR tube was heated to 50°C and monitored for days. Again, no reaction was observed. The reaction mixture was heated to 100°C . A ^1H NMR spectrum was obtained after 18 hours. The NMR spectrum showed that a complex mixture of products was formed. Similar results were obtained with acetamide.

Exploratory reaction attempt between [Ir(COD)(PMe₃)₃]Cl and thiourea in D₂O (CPRII289)

Thiourea (6 mg, 0.0735) was placed in a screw - cap NMR tube equipped with a septum. The tube was placed in the drybox where it was charged with 20 mg (0.035 mmol) of [Ir(COD)(PMe₃)₃]Cl. D₂O (0.5 mL) was added via syringe outside the drybox. The tube was shaken and monitored at room temperature by ¹H NMR spectroscopy. No reaction was observed. The NMR tube was heated to 50°C and monitored for days. Again, no reaction was observed. The reaction mixture was heated to 100°C. A NMR spectrum was obtained after 18 hours and the [Ir(thiourea)(H)(PMe₃)₃]Cl product was identified on the basis of the following data:

¹H NMR (D₂O): (mixture of isomers)

δ 1.41 (d, J_{P-H} = 10.8 Hz, PMe₃), 1.52 (vt, J_{P-H} = 3.5 Hz), 1.57 (d, J_{P-H} = 3 Hz, PMe₃), 1.62 (t, J_{P-H} = 4Hz). 1.68 (d, J_{P-H} = 6 Hz) No resonances observed for NH₂ due to exchange)

Synthesis of [Ir(thiourea)(H)(PMe₃)₃]PF₆

An excess of K[PF₆] was dissolved in distilled water, this solution was added dropwise to solution of [Ir(thiourea)(H)(PMe₃)₃]Cl in distilled water. A white - yellow precipitate dropped out of solution immediately. The precipitate was filtered from solution using cannula techniques. The solid was recrystallized from methylene chloride/ether. An X-ray structure of the crystals was obtained. See appendix

Synthesis of [Ir(thioacetamide)(H)(PMe₃)₃]Cl (CPRIII025)

A 100 ml flask equipped with a stir bar and septum was charged with 42 mg (1.11 mmol) of thioacetamide. The flask was then charged with 150 mg (0.532 mmol) of [Ir(COD)(PMe₃)₃]Cl under N₂ in the drybox. The flask was then connected to a double manifold (vacuum/nitrogen) Schlenk line and 30 mls of distilled water was added to the flask via syringe. The solution was stirred magnetically and heated to reflux. After 18 hours at reflux the reaction was allowed to cool and the solvent was removed in vacuo. The white solid residue was treated with distilled methylene chloride (3 x 10 mL) to extract the product from the excess amino acid. The solution was filtered from the solid using cannula techniques. The methylene chloride was removed in vacuo and the solids were allowed to dry under reduced pressure to yield 80 mg (0.150,

28.3% yield based on the amount of Ir(COD)(PMe₃)₃Cl) of [Ir(thioacetamide)(H)(PMe₃)₃Cl identified on the basis of the following data:

¹H NMR δ The isomers overlapped one another in the phosphine region making it difficult to isolate resonances. 2.61 (s, methyl of bound thiacetamide) -10.09 (dt, 1H, Ir-H). -19.12 (q, 1H, Ir-H)

Synthesis of [Ir(thioacetamide)(H)(PMe₃)₃]PF₆

An excess of K[PF₆] was dissolved in distilled water, this solution was added dropwise to solution of [Ir(thioacetamide)(H)(PMe₃)₃Cl in distilled water. A white - yellow precipitate dropped out of solution immediately. The precipitate was filtered from solution using cannula techniques. The solid was recrystallized from methylene chloride/ether. An X-ray structure of the crystals was obtained. See appendix

Exploratory reaction attempt between [Ir(COD)(PMe₃)₃]Cl and thiohydantoin in D₂O (CPRIII073)

Thiohydantoin (9 mg, 0.0735) was placed in a screw - cap NMR tube equipped with a septum. The tube was placed in the drybox where it was charged with 20 mg (0.035 mmol) of [Ir(COD)(PMe₃)₃Cl. D₂O (0.5)

mL was added via syringe outside the drybox. The tube was shaken and monitored at room temperature by ^1H NMR spectroscopy. No reaction was observed. The NMR tube was heated to 50°C and monitored for days. Again, no reaction was observed. The reaction mixture was heated to 80°C . A NMR spectrum was obtained after 18 hours. The $[\text{Ir}(\text{thiohydantoin})(\text{H})(\text{PMe}_3)_3]\text{Cl}$ product was identified on the basis of the following data:

^1H NMR (D_2O): δ 1.55 (t, 18 H, trans PMe_3), 1.68 (d, 9H, cis PMe_3) 1.15 (d, PMe_3 of facial isomer) 1.45 (d, PMe_3 of facial isomer), 1.59 (d, PMe_3 of facial isomer) -21.39 (q, 1H, Ir-H for meridional isomer) hydride for fac isomer was indistinguishable from baseline noise. ppm

Exploratory reaction attempt between $[\text{Ir}(\text{COD})(\text{PMe}_3)_3]\text{Cl}$ and thiouracil in D_2O (CPRIII077)

Thiouracil (9.5 mg ,2.1 equiv.) was placed in a screw - cap NMR tube equipped with a septum. The tube was placed in the drybox where it was charged with 20 mg (0.035 mmol) of $[\text{Ir}(\text{COD})(\text{PMe}_3)_3]\text{Cl}$. D_2O (0.5 mL) was added via syringe outside the drybox. The tube was shaken and monitored at room temperature by ^1H NMR spectroscopy. No reaction was observed. The NMR tube was heated to 50°C and monitored

for days. Again, no reaction was observed. The reaction mixture was heated to 80°C. A ^1H NMR spectrum was obtained after 18 hours.

This spectrum was very complex with overlapping peaks in the phosphine region and separate products could not be distinguished. No hydride resonances were observed.

4.3 References

¹Selnau, H., Ph.D. thesis, Virginia Polytechnic Institute and State University, 1992.

²Wilkinson, G. ed., "Comprehensive Coordination Chemistry", Pergamon Press, Oxford, 1987.

Chapter 5 Conclusion and Future Goals

5.1 Conclusion

The studies carried out in this thesis were aimed at exploring the synthesis and reactivity of amino acid hydride complexes of iridium. The biological activity and the possible catalytic uses of these types of systems was studied. The literature is void of platinum metal hydride complexes with amino acids as ligands. The complexes in this thesis are the first of this type to be studied.

The oxidative addition of amino acids to an iridium metal center has been demonstrated with a wide variety of amino acids. Almost all of the naturally occurring amino acids have been studied. The acids that give clean products have been characterized in the very least by ^1H NMR studies. The resulting complexes from the addition of amino acids to the metal center have been treated with a variety of unsaturates in varying conditions. The fact that very little reactivity has been observed is an indication that these 5 membered ring systems are extremely stable.

The study done on 2-amino-4-pentenoic acid did show that an olefin tethered to the amino acid could insert into the Ir-H bond. This study indicates that unsaturate insertion is possible and reactivity of these insertion products is still a possibility.

The exchange study done with the amino acid complexes and free amino acid also indicates that removal of the complexes amino acid is possible. The exchange of one amino acid for another seems to be dependent on the sterics of the side chain of the amino acid. This

information could be important when studies on reductive elimination of insertion products are considered.

The square planar $[\text{Ir}(\text{COD})(\text{DMPE})]\text{Cl}$ complex was also studied. The complex was treated with various amino acids at varying conditions to see if coordinately unsaturated complexes could be prepared. The studies indicate that the preparation of these amino acid complexes is not as facile as that of $[\text{Ir}(\text{COD})(\text{PMe}_3)_3]\text{Cl}$ with amino acids. An interesting rearrangement did arise from this study with the $[\text{Ir}(\text{COD})(\text{DMPE})]\text{Cl}$ complex. The complex rearranges to the $[\text{Ir}(\mu^1, \mu^3, \text{C}_8\text{H}_{12})(\text{DMPE})]\text{Cl}$ complex on treatment with acid. The crystal structure of this rearranged product was solved. N-methyl substituted amino acid complexes were also synthesized. These complexes were studied for their possible reactivity with unsaturates. The complexes were hoped to have weakened Ir-N bonds due to the steric hindrance of substitution on the nitrogen. This weakened bond would facilitate the insertion step of the unsaturate. Studies involving a variety of unsaturates and conditions showed that the substituted compounds were not reactive.

Finally a number of other biologically interesting molecules were studied with $[\text{Ir}(\text{COD})(\text{PMe}_3)_3]\text{Cl}$. These compounds contained sulfur atoms that could donate to the metal center. The complexes that were made were found to bind through the sulfur donor and the nitrogen donor centers. The four membered ring systems that were formed are hoped to be more reactive than the 5 membered ring systems of the amino acid complexes.

This thesis has presented the synthesis of a number of novel amino acid hydride complexes. The reactivity of these complexes has been studied with a variety of unsaturated compounds. The biological activity of these complexes has also been studied. A number of biologically interesting molecules have been oxidatively added to the iridium metal center and the reactivity studies of these complexes is the subject of future work.

5.2 Future Goals

The immediate future work involves studies with the complexes that contain 4 membered iridacycles. These ring systems should be less stable than the 5 membered ring systems of the amino acids. The decreased stability will hopefully mean increased reactivity. The rhodium analogs of the amino acid complexes is another study that is readily apparent. The rhodium complexes should be more reactive than their iridium counterparts and synthesis of the rhodium amino acid hydride complexes is all ready being studied.

The biological aspects of these complexes should also be studied in more detail. The preliminary studies by the NIH indicate that the phenylalanine complex has some biological activity. The next step is to improve this activity by making various analogs of the phenylalanine complex and studying their biology. These types of complexes should have some application in biological studies.

The amino acid complexes need to be studied in greater detail in asymmetric hydrogenation catalytic studies. Preliminary studies were

done with prochiral substrates and the results were encouraging. The chiral centers of these complexes may be able to induce asymmetric hydrogenation.

There are other substituted amino acids that need to be studied. N-phenyl substituents would give steric bulk and electron withdrawing properties that would weaken the Ir-N bond. The weakening of that bond may facilitate the addition of an unsaturate to the metal and allow for reactivity of the complexes.

More studies need to be done with the square planar coordinatively unsaturated compound, $[\text{Ir}(\text{COD})(\text{DMPE})]\text{Cl}$. The possibility of hydrogenating the complex and then adding the amino acid may allow for formation of the square planar amino acid hydride complex. If the amino acid can be oxidatively added, this may give rise to a very reactive system.

The possibilities go on, such as adding compounds that all ready have biological activity . The binding of such compounds to a metal center may enhance the reactivity (or inhibit), but the information gained from these types of studies may aid in designing new systems with better reactivity. A number of studies remain to be done, not the least of is the pursuane of a system that will show reactivity of the novel amino acid hydride complexes presented in this study.

Appendix: X-ray Crystallographic Data

STRUCTURE DETERMINATION SUMMARY OF [Ir(pro)(H)(PMe₃)₃]PF₆**Crystal Data**

Empirical Formula C₁₄H₃₆F₆IrNO₂P₄
 Color; Habit Clear rectangular prism
 Crystal Size (mm) 0.4 x 0.4 x 0.5
 Crystal System Monoclinic
 Space Group P2₁
 Unit Cell Dimensions

a = 10.824(2) Å
 b = 20.021(4) Å
 c = 11.826(2) Å
 β = 91.150(10)°
 Volume 2562.1(7) Å³

Volume

Z

4

Formula weight

680.5

Density(calc.)

1.764 Mg/m³

Absorption Coefficient

5.489 mm⁻¹

F(000)

1336

Data Collection

Diffractometer Used

Siemens R3m/V

Radiation

MoK_α (λ = 0.71073 Å)

Temperature (K)

298

Monochromator

Highly oriented graphite crystal

2θ Range

3.5 to 45.0°

Scan Type

Wyckoff

Scan Speed

Variable; 3.97 to 19.53°/min. in w

Scan Range (w)

0.60°

Background Measurement

Stationary crystal and stationary counter at beginning and end of scan, each for 25.0% of total scan time

Standard Reflections

3 measured every 300 reflections

Index Ranges

0 ≤ h ≤ 14, 0 ≤ k ≤ 26, -15 ≤ l ≤ 15

Reflections Collected

6375

Independent Reflections

6055 (R_{int} = 1.45%)

Observed Reflections

5630 (F > 3.0σ(F))

Absorption Correction

Semi-empirical

Min./Max. Transmission

0.6175 / 1.0000

Solution and Refinement

System Used

Siemens SHELXTL PLUS (VMS)

Solution

Direct Methods

Refinement Method

Full-Matrix Least-Squares

Quantity Minimized

Σw(F_o-F_c)²

Absolute Structure

h = 1.11(4)

Extinction Correction

c = 0.00020(3), where

F* = F[1 + 0.002cF²/sin(2q)]^{-1/4}

Hydrogen Atoms

Riding model, fixed isotropic U

Weighting Scheme

w⁻¹ = s²(F) + 0.0007F²

Number of Parameters refined

506

Final R indices (obs. data)

R = 3.29 %, wR = 3.92 %

R Indices (all data)

R = 3.70 %, wR = 4.01 %

Goodness-of-Fit

1.06

Largest and Mean D/s

0.382, 0.017

Data-to-Parameter Ratio

11.1:1

Largest Difference Peak

1.07 eÅ⁻³

Largest Difference Hole

-1.10 eÅ⁻³

Table 1. Atomic coordinates ($\times 10^4$) and equivalent isotropic displacement coefficients ($\text{\AA}^2 \times 10^3$)

	x	y	z	U(eq)
Ir	4261(1)	9983	4283(1)	41(1)
P(1)	3672(3)	8922(2)	3689(2)	65(1)
P(2)	3189(2)	10552(2)	2954(3)	59(1)
P(3)	4534(3)	10864(2)	5578(3)	65(1)
O(1)	5344(7)	9470(4)	5516(6)	61(3)
N(1)	6070(6)	9981(4)	3448(5)	43(2)
O(2)	7231(7)	9197(5)	6040(6)	69(3)
C(1)	6484(11)	9400(6)	5318(8)	60(4)
C(2)	6963(8)	9563(5)	4165(8)	48(3)
C(3)	8195(10)	9945(8)	4152(9)	74(4)
C(4)	8085(10)	10408(8)	3117(10)	76(5)
C(5)	6721(9)	10595(7)	3129(10)	63(4)
C(11)	2213(20)	8814(10)	3064(20)	174(12)
C(12)	4576(24)	8436(11)	2774(19)	190(14)
C(13)	3519(19)	8387(8)	4881(13)	122(8)
C(21)	1531(11)	10571(10)	3097(13)	96(7)
C(22)	3584(20)	11429(8)	2781(18)	124(9)
C(23)	3385(13)	10235(11)	1526(10)	99(7)
C(31)	3519(29)	11507(18)	5731(24)	432(34)
C(32)	5803(19)	11304(17)	5817(19)	257(21)
C(33)	4418(36)	10510(14)	6948(19)	318(31)
Ir'	9121(1)	8939(1)	9443(1)	34(1)
P(1')	9017(2)	8017(2)	10666(2)	50(1)
P(2')	10255(2)	8413(2)	8143(2)	50(1)
P(3')	9569(2)	10021(2)	8838(2)	52(1)
O(1')	7953(6)	9397(3)	10630(5)	45(2)
N(1')	7314(6)	8906(4)	8530(5)	34(2)
O(2')	6017(7)	9511(4)	11121(6)	63(3)
C(1')	6779(8)	9407(5)	10435(8)	43(3)
C(2')	6379(8)	9291(6)	9207(8)	49(3)
C(3')	5153(10)	8926(9)	9058(12)	85(5)
C(4')	5337(10)	8460(7)	8101(9)	64(4)
C(5')	6691(10)	8260(6)	8247(10)	56(3)
C(11')	8517(18)	8282(9)	12046(10)	126(8)
C(12')	8031(14)	7292(9)	10458(14)	103(7)
C(13')	10508(11)	7642(6)	10966(9)	67(4)
C(21')	11916(10)	8400(9)	8340(12)	82(5)
C(22')	9925(14)	7525(7)	7937(12)	82(5)
C(23')	10091(12)	8727(8)	6737(8)	82(5)
C(31')	11115(11)	10196(8)	8423(15)	99(6)
C(32')	9348(16)	10594(6)	10027(12)	88(6)
C(33')	8655(15)	10387(7)	7726(13)	98(6)
P(4)	4081(3)	6776(2)	325(3)	73(1)
F(1)	5044(16)	6891(11)	-509(14)	211(10)
F(2)	5038(12)	6857(8)	1310(12)	183(7)
F(3)	3163(15)	6689(12)	1278(11)	221(11)
F(4)	3123(17)	6768(9)	-635(13)	209(9)
F(5)	3864(18)	7548(7)	321(12)	185(8)
F(6)	4163(18)	6046(7)	280(19)	231(11)
P(4')	-332(3)	1962(2)	5527(2)	65(1)
F(1')	-174(11)	2730(5)	5653(11)	123(5)
F(2')	764(10)	1983(8)	4672(8)	135(5)
F(3')	-432(17)	1200(5)	5392(9)	170(7)

F(4')	-1419(9)	1958(7)	6383(7)	126(5)
F(5')	-1308(9)	2090(8)	4534(6)	125(5)
F(6')	599(9)	1847(5)	6559(7)	110(4)

* Equivalent isotropic U defined as one third of the trace of the orthogonalized U_{ij} tensor

Table 2. Bond lengths (Å)

Ir-P(1)	2.323	(4)
Ir-P(2)	2.245	(3)
Ir-P(3)	2.351	(4)
Ir-O(1)	2.118	(7)
Ir-N(1)	2.211	(7)
P(1)-C(11)	1.743	(22)
P(1)-C(12)	1.766	(24)
P(1)-C(13)	1.780	(16)
P(2)-C(21)	1.806	(13)
P(2)-C(22)	1.819	(17)
P(2)-C(23)	1.821	(14)
P(3)-C(31)	1.704	(34)
P(3)-C(32)	1.650	(25)
P(3)-C(33)	1.775	(24)
O(1)-C(1)	1.269	(14)
N(1)-C(2)	1.523	(12)
N(1)-C(5)	1.469	(15)
O(2)-C(1)	1.232	(13)
C(1)-C(2)	1.506	(14)
C(2)-C(3)	1.538	(16)
C(3)-C(4)	1.537	(18)
C(4)-C(5)	1.523	(15)
Ir'-P(1')	2.349	(3)
Ir'-P(2')	2.249	(3)
Ir'-P(3')	2.336	(3)
Ir'-O(1')	2.116	(6)
Ir'-N(1')	2.215	(6)
P(1')-C(11')	1.810	(14)
P(1')-C(12')	1.815	(17)
P(1')-C(13')	1.810	(13)
P(2')-C(21')	1.809	(11)
P(2')-C(22')	1.828	(14)
P(2')-C(23')	1.782	(11)
P(3')-C(31')	1.788	(13)
P(3')-C(32')	1.834	(13)
P(3')-C(33')	1.787	(15)
O(1')-C(1')	1.287	(11)
N(1')-C(2')	1.514	(11)
N(1')-C(5')	1.494	(13)
O(2')-C(1')	1.187	(12)
C(1')-C(2')	1.525	(13)
C(2')-C(3')	1.521	(16)
C(3')-C(4')	1.483	(19)
C(4')-C(5')	1.525	(16)
P(4)-F(1)	1.467	(17)
P(4)-F(2)	1.551	(14)
P(4)-F(3)	1.527	(15)
P(4)-F(4)	1.522	(17)
P(4)-F(5)	1.562	(14)

P(4)-F(6)	1.465 (14)
P(4')-F(1')	1.553 (10)
P(4')-F(2')	1.575 (11)
P(4')-F(3')	1.538 (12)
P(4')-F(4')	1.568 (10)
P(4')-F(5')	1.585 (9)
P(4')-F(6')	1.584 (10)

Table 3. Bond angles (°)

P(1)-Ir-P(2)	96.8(1)
P(1)-Ir-P(3)	156.0(1)
P(2)-Ir-P(3)	97.6(1)
P(1)-Ir-O(1)	84.8(2)
P(2)-Ir-O(1)	177.5(2)
P(3)-Ir-O(1)	81.6(2)
P(1)-Ir-N(1)	95.9(2)
P(2)-Ir-N(1)	98.0(2)
P(3)-Ir-N(1)	101.1(2)
O(1)-Ir-N(1)	79.8(3)
Ir-P(1)-C(11)	118.8(7)
Ir-P(1)-C(12)	122.5(8)
C(11)-P(1)-C(12)	100.4(11)
Ir-P(1)-C(13)	109.9(5)
C(11)-P(1)-C(13)	99.4(10)
C(12)-P(1)-C(13)	102.4(9)
Ir-P(2)-C(21)	116.5(6)
Ir-P(2)-C(22)	116.7(7)
C(21)-P(2)-C(22)	103.1(9)
Ir-P(2)-C(23)	113.8(6)
C(21)-P(2)-C(23)	103.2(7)
C(22)-P(2)-C(23)	101.6(9)
Ir-P(3)-C(31)	124.2(10)
Ir-P(3)-C(32)	127.2(9)
C(31)-P(3)-C(32)	96.6(15)
Ir-P(3)-C(33)	106.5(9)
C(31)-P(3)-C(33)	98.5(15)
C(32)-P(3)-C(33)	97.6(14)
Ir-O(1)-C(1)	117.0(6)
Ir-N(1)-C(2)	108.1(5)
Ir-N(1)-C(5)	123.1(6)
C(2)-N(1)-C(5)	107.5(7)
O(1)-C(1)-O(2)	122.5(9)
O(1)-C(1)-C(2)	119.7(9)
O(2)-C(1)-C(2)	117.8(10)
N(1)-C(2)-C(1)	113.5(8)
N(1)-C(2)-C(3)	105.2(8)
C(1)-C(2)-C(3)	115.6(8)
C(2)-C(3)-C(4)	104.7(8)
C(3)-C(4)-C(5)	101.6(9)
N(1)-C(5)-C(4)	105.5(10)
P(1')-Ir'-P(2')	94.9(1)
P(1')-Ir'-P(3')	158.5(1)
P(2')-Ir'-P(3')	96.0(1)
P(1')-Ir'-O(1')	84.0(2)
P(2')-Ir'-O(1')	176.3(2)
P(3')-Ir'-O(1')	86.1(2)

P(1')-Ir'-N(1')	103.0(2)
P(2')-Ir'-N(1')	98.1(2)
P(3')-Ir'-N(1')	93.7(2)
O(1')-Ir'-N(1')	78.7(2)
Ir'-P(1')-C(11')	110.1(6)
Ir'-P(1')-C(12')	125.5(5)
C(11')-P(1')-C(12')	99.9(8)
Ir'-P(1')-C(13')	113.2(4)
C(11')-P(1')-C(13')	103.1(7)
C(12')-P(1')-C(13')	102.4(7)
Ir'-P(2')-C(21')	118.3(5)
Ir'-P(2')-C(22')	116.0(5)
C(21')-P(2')-C(22')	101.2(7)
Ir'-P(2')-C(23')	115.3(5)
C(21')-P(2')-C(23')	101.9(6)
C(22')-P(2')-C(23')	101.7(7)
Ir'-P(3')-C(31')	117.9(5)
Ir'-P(3')-C(32')	108.3(4)
C(31')-P(3')-C(32')	103.0(8)
Ir'-P(3')-C(33')	119.4(5)
C(31')-P(3')-C(33')	103.0(7)
C(32')-P(3')-C(33')	103.2(7)
Ir'-O(1')-C(1')	119.2(5)
Ir'-N(1')-C(2')	108.7(5)
Ir'-N(1')-C(5')	121.7(6)
C(2')-N(1')-C(5')	104.8(7)
O(1')-C(1')-O(2')	125.2(8)
O(1')-C(1')-C(2')	115.4(7)
O(2')-C(1')-C(2')	119.3(8)
N(1')-C(2')-C(1')	113.6(7)
N(1')-C(2')-C(3')	106.6(9)
C(1')-C(2')-C(3')	114.4(9)
C(2')-C(3')-C(4')	105.0(9)
C(3')-C(4')-C(5')	102.9(9)
N(1')-C(5')-C(4')	103.1(9)
F(1)-P(4)-F(2)	90.9(8)
F(1)-P(4)-F(3)	174.4(9)
F(2)-P(4)-F(3)	83.8(8)
F(1)-P(4)-F(4)	89.0(9)
F(2)-P(4)-F(4)	174.6(10)
F(3)-P(4)-F(4)	96.0(9)
F(1)-P(4)-F(5)	87.3(11)
F(2)-P(4)-F(5)	89.8(9)
F(3)-P(4)-F(5)	90.8(11)
F(4)-P(4)-F(5)	84.8(9)
F(1)-P(4)-F(6)	95.0(12)
F(2)-P(4)-F(6)	95.2(10)
F(3)-P(4)-F(6)	87.4(12)
F(4)-P(4)-F(6)	90.2(11)
F(5)-P(4)-F(6)	174.4(11)
F(1')-P(4')-F(2')	87.3(7)
F(1')-P(4')-F(3')	177.6(9)
F(2')-P(4')-F(3')	90.7(8)
F(1')-P(4')-F(4')	91.5(7)
F(2')-P(4')-F(4')	178.7(8)
F(3')-P(4')-F(4')	90.6(8)
F(1')-P(4')-F(5')	89.0(7)
F(2')-P(4')-F(5')	91.1(5)

F(3')-P(4')-F(5')	92.2(8)
F(4')-P(4')-F(5')	88.9(5)
F(1')-P(4')-F(6')	90.2(6)
F(2')-P(4')-F(6')	91.3(5)
F(3')-P(4')-F(6')	88.7(7)
F(4')-P(4')-F(6')	88.6(5)
F(5')-P(4')-F(6')	177.4(5)

Table 4. Anisotropic displacement coefficients ($\text{\AA}^2 \times 10^3$)

	U ₁₁	U ₂₂	U ₃₃	U ₁₂	U ₁₃	U ₂₃
Ir	35(1)	54(1)	35(1)	-4(1)	0(1)	-4(1)
P(1)	75(2)	64(2)	56(1)	-26(2)	-4(1)	-5(2)
P(2)	45(1)	76(2)	54(1)	14(1)	-3(1)	2(1)
P(3)	49(1)	81(2)	65(2)	1(1)	0(1)	-31(2)
O(1)	48(4)	93(6)	42(3)	4(4)	3(3)	15(4)
N(1)	49(4)	52(4)	29(3)	-7(4)	3(3)	0(3)
O(2)	59(4)	95(6)	51(4)	18(4)	-9(3)	15(4)
C(1)	77(7)	63(7)	38(5)	13(6)	-6(5)	-2(5)
C(2)	41(4)	63(6)	41(5)	-3(4)	2(4)	-4(4)
C(3)	54(6)	124(11)	44(5)	6(7)	-7(4)	-7(7)
C(4)	53(6)	115(10)	61(7)	-20(7)	5(5)	-4(7)
C(5)	48(5)	80(8)	61(6)	-4(5)	11(5)	6(6)
C(11)	195(22)	114(16)	208(24)	-108(16)	-96(19)	33(15)
C(12)	278(32)	106(15)	192(23)	-55(18)	154(23)	-77(16)
C(13)	193(20)	82(11)	90(11)	-59(13)	30(12)	0(9)
C(21)	49(6)	158(16)	81(9)	20(8)	-5(6)	-4(10)
C(22)	150(17)	79(10)	143(16)	13(11)	0(14)	34(11)
C(23)	79(8)	171(17)	47(6)	28(10)	-2(6)	-15(8)
C(31)	435(57)	547(72)	304(41)	413(57)	-266(42)	-340(49)
C(32)	168(22)	413(54)	195(24)	-188(29)	105(20)	-223(32)
C(33)	643(86)	176(28)	136(22)	-53(42)	-19(36)	-123(22)
Ir'	32(1)	41(1)	30(1)	1(1)	-2(1)	-1(1)
P(1')	52(1)	53(1)	44(1)	12(1)	3(1)	12(1)
P(2')	38(1)	71(2)	39(1)	9(1)	5(1)	-4(1)
P(3')	56(1)	50(1)	48(1)	-11(1)	-2(1)	3(1)
O(1')	53(4)	52(4)	29(3)	9(3)	-5(3)	-2(3)
N(1')	41(3)	39(3)	21(2)	-2(3)	0(2)	5(3)
O(2')	60(4)	89(5)	41(3)	12(4)	10(3)	-8(4)
C(1')	45(5)	42(5)	42(4)	7(4)	10(4)	-1(4)
C(2')	34(4)	63(6)	49(5)	11(4)	2(4)	5(4)
C(3')	43(5)	126(11)	87(8)	-23(8)	12(5)	-15(10)
C(4')	60(6)	79(7)	53(6)	-17(6)	-10(5)	-2(6)
C(5')	63(6)	51(6)	55(6)	-8(5)	-15(5)	-11(5)
C(11')	211(20)	114(13)	56(8)	88(13)	49(10)	38(8)
C(12')	86(10)	104(12)	119(13)	-10(9)	-18(9)	57(10)
C(13')	86(8)	63(7)	52(6)	14(6)	-9(6)	16(5)
C(21')	37(5)	120(12)	89(9)	20(6)	5(5)	10(9)
C(22')	97(10)	73(8)	76(8)	23(7)	14(7)	-18(7)
C(23')	76(8)	135(13)	36(5)	26(8)	4(5)	-6(6)
C(31')	64(7)	77(9)	158(15)	-22(7)	18(9)	3(9)
C(32')	147(13)	38(6)	78(8)	-19(7)	-7(9)	-4(6)
C(33')	124(13)	74(9)	92(10)	-24(9)	-51(10)	43(8)
P(4)	79(2)	71(2)	68(2)	-10(2)	7(2)	7(2)
F(1)	183(14)	277(23)	177(14)	-35(15)	108(12)	28(14)

F(2)	142(10)	223(15)	180(12)	-42(11)	-80(10)	60(12)
F(3)	172(13)	374(28)	119(10)	-49(15)	44(9)	56(13)
F(4)	250(18)	212(17)	161(12)	-34(14)	-101(13)	24(12)
F(5)	319(21)	87(7)	147(11)	-6(10)	-21(12)	25(8)
F(6)	276(21)	73(8)	346(24)	21(11)	65(18)	14(12)
P(4')	90(2)	63(2)	43(1)	-7(2)	5(1)	-2(1)
F(1')	151(9)	68(6)	151(10)	-11(6)	4(7)	1(5)
F(2')	116(7)	211(13)	80(6)	39(9)	37(5)	28(7)
F(3')	327(20)	79(7)	105(8)	-52(9)	26(10)	-24(6)
F(4')	111(7)	200(11)	67(5)	-17(8)	24(5)	18(6)
F(5')	113(7)	204(12)	59(4)	-11(8)	-18(5)	5(6)
F(6')	127(7)	130(8)	72(5)	45(6)	-21(5)	-21(5)

3The anisotropic displacement exponent takes the form:

$$-2p^2(h^2a^2U_{11} + \dots + 2hka*b*U_{12})$$

Table 5. H-Atom coordinates ($\times 10^4$) and isotropic displacement coefficients ($\text{\AA}^2 \times 10^3$)

	x	y	z	U
H(1)	3161	10012	5132	80
H(1A)	5940	9763	2791	80
H(2A)	7109	9145	3793	80
H(3A)	8918	9668	4141	80
H(3B)	8240	10232	4803	80
H(4A)	8218	10138	2461	80
H(4B)	8633	10785	3111	80
H(5A)	6623	10920	3717	80
H(5B)	6425	10781	2426	80
H(11A)	2100	8353	2867	80
H(11B)	1576	8949	3569	80
H(11C)	2170	9082	2392	80
H(12A)	4184	8014	2624	80
H(12B)	4668	8675	2078	80
H(12C)	5375	8361	3118	80
H(13A)	3275	7944	4660	80
H(13B)	4314	8372	5254	80
H(13C)	2922	8568	5387	80
H(21A)	1171	10822	2482	80
H(21B)	1217	10123	3078	80
H(21C)	1324	10778	3801	80
H(22A)	3087	11632	2194	80
H(22B)	3449	11655	3483	80
H(22C)	4441	11462	2592	80
H(23A)	2902	10496	1000	80
H(23B)	4240	10256	1329	80
H(23C)	3110	9779	1500	80
H(31A)	3813	11843	6249	80
H(31B)	3102	11717	5101	80
H(31C)	2956	11216	6108	80
H(32A)	5662	11656	6350	80
H(32B)	6312	10966	6165	80
H(32C)	6210	11481	5169	80
H(33A)	4513	10834	7541	80
H(33B)	3602	10322	6966	80
H(33C)	5018	10161	7054	80
H(1')	10115	8977	10199	80

H(1'A)	7426	9117	7867	80
H(2'A)	6246	9721	8868	80
H(3'A)	4428	9199	8969	80
H(3'B)	5069	8644	9708	80
H(4'A)	5274	8734	7435	80
H(4'B)	4773	8092	8028	80
H(5'A)	6753	7959	8877	80
H(5'B)	7019	8051	7587	80
H(11D)	8481	7899	12532	80
H(11E)	9117	8593	12344	80
H(11F)	7721	8494	12007	80
H(12D)	8169	6995	11085	80
H(12E)	7173	7414	10416	80
H(12F)	8255	7073	9770	80
H(13D)	10375	7272	11466	80
H(13E)	10869	7483	10281	80
H(13F)	11057	7957	11326	80
H(21D)	12273	8161	7722	80
H(21E)	12240	8846	8363	80
H(21F)	12118	8176	9037	80
H(22D)	10443	7336	7371	80
H(22E)	10039	7285	8633	80
H(22F)	9076	7495	7691	80
H(23D)	10606	8468	6251	80
H(23E)	9247	8696	6478	80
H(23F)	10350	9185	6725	80
H(31D)	11172	10655	8198	80
H(31E)	11701	10109	9025	80
H(31F)	11290	9914	7790	80
H(32D)	9523	11043	9794	80
H(32E)	8524	10573	10311	80
H(32F)	9926	10462	10612	80
H(33D)	8946	10830	7574	80
H(33E)	8723	10118	7057	80
H(33F)	7807	10406	7945	80

STRUCTURE DETERMINATION SUMMARY OF [Ir(val)(H)(PMe₃)₃]PF₆**Crystal Data**

Empirical Formula	C ₁₄ H ₃₈ F ₆ IrNO ₂ P ₄
Color; Habit	Clear rectangular prism
Crystal Size (mm)	0.2 x 0.2 x 0.4
Crystal System	Tetragonal
Space Group	P4 ₃
Unit Cell Dimensions	a = 14.327(3) Å c = 14.397(4) Å

Volume	2955.3(16) Å ³
Z	4
Formula weight	682.5
Density(calc.)	1.534 Mg/m ³
Absorption Coefficient	4.759 mm ⁻¹
F(000)	1344

Data Collection

Diffractometer Used	Siemens R3m/V
Radiation	MoK _α (λ = 0.71073 Å)
Temperature (K)	298
Monochromator	Highly oriented graphite crystal
2θ Range	3.5 to 45.0°
Scan Type	Wyckoff
Scan Speed	Variable; 3.00 to 19.53°/min. in ω
Scan Range (ω)	0.60°
Background Measurement	Stationary crystal and stationary counter at beginning and end of scan, each for 25.0% of total scan time

Standard Reflections	2 measured every 300 reflections
Index Ranges	0 ≤ h ≤ 15, 0 ≤ k ≤ 15, -15 ≤ l ≤ 15
Reflections Collected	4250
Independent Reflections	3870 (R _{int} = 2.63%)
Observed Reflections	3264 (F > 4.0σ(F))
Absorption Correction	Semi-empirical
Min./Max. Transmission	0.5122 / 1.0000

Solution and Refinement

System Used	Siemens SHELXTL PLUS (VMS)
Solution	Direct Methods
Refinement Method	Full-Matrix Least-Squares
Quantity Minimized	Σw(F _o -F _c) ²
Absolute Structure	η = 1.04(3)
Extinction Correction	χ = 0.00015(4), where F* = F [1 + 0.002χF ² /sin(2θ)] ^{-1/4} Riding model, fixed isotropic U
Hydrogen Atoms	w ⁻¹ = σ ² (F) + 0.0008F ²
Weighting Scheme	254
Number of Parameters refined	R = 4.33 %, wR = 5.06 %
Final R indices (obs. data)	R = 5.60 %, wR = 5.80 %
R Indices (all data)	1.26
Goodness-of-Fit	0.071, 0.007
Largest and Mean Δ/σ	12.9:1
Data-to-Parameter Ratio	

Largest Difference Peak
Largest Difference Hole

$2.00 \text{ e}\text{\AA}^{-3}$
 $-1.19 \text{ e}\text{\AA}^{-3}$

Table 1. Atomic coordinates ($\times 10^4$) and equivalent isotropic displacement coefficients ($\text{\AA}^2 \times 10^3$)

	x	y	z	U(eq)
Ir(1)	617(1)	3477(1)	1206	43(1)
P(1)	-588(3)	2882(3)	2136(3)	53(1)
P(2)	-276(3)	4412(3)	316(3)	55(1)
P(3)	2025(3)	4217(3)	811(3)	60(1)
O(1)	1509(7)	2547(7)	1937(6)	53(4)
N(1)	761(8)	2316(8)	227(7)	46(4)
C(1)	1590(9)	1722(11)	1590(9)	46(5)
C(2)	1048(9)	1443(9)	732(9)	44(4)
C(3)	1535(10)	712(10)	142(10)	52(5)
C(4)	2445(12)	1044(12)	-289(11)	77(7)
C(5)	895(13)	300(12)	-600(13)	85(7)
O(2)	2077(8)	1117(7)	1988(7)	66(4)
C(11)	-1451(13)	2069(14)	1707(13)	91(8)
C(12)	-120(14)	2277(15)	3123(12)	93(8)
C(13)	-1291(14)	3743(14)	2695(14)	98(9)
C(21)	-53(13)	4232(11)	-904(11)	72(6)
C(22)	-154(14)	5676(12)	458(13)	83(8)
C(23)	-1531(11)	4291(13)	354(14)	79(7)
C(31)	2979(12)	3436(15)	691(18)	109(10)
C(32)	2204(15)	4861(14)	-288(14)	99(9)
C(33)	2378(15)	5010(19)	1692(16)	132(12)
P(4)	2180(3)	2958(3)	-2671(3)	67(2)
F(1)	1536(13)	2715(12)	-1840(12)	184(9)
F(2)	2909(14)	3248(14)	-1963(15)	214(11)
F(3)	2804(15)	3166(12)	-3506(12)	202(10)
F(4)	1454(12)	2648(13)	-3395(12)	177(9)
F(5)	2580(12)	1948(9)	-2643(10)	147(7)
F(6)	1792(12)	3966(8)	-2694(11)	144(7)

* Equivalent isotropic U defined as one third of the trace of the orthogonalized U_{ij} tensor

Table 2. Bond lengths (Å)

Ir(1)-P(1)	2.345 (4)
Ir(1)-P(2)	2.252 (4)
Ir(1)-P(3)	2.349 (4)
Ir(1)-O(1)	2.126 (10)
Ir(1)-N(1)	2.190 (11)
P(1)-C(11)	1.807 (20)
P(1)-C(12)	1.795 (19)
P(1)-C(13)	1.784 (20)
P(2)-C(21)	1.804 (16)
P(2)-C(22)	1.832 (17)
P(2)-C(23)	1.807 (16)
P(3)-C(31)	1.775 (19)
P(3)-C(32)	1.849 (21)
P(3)-C(33)	1.776 (25)
O(1)-C(1)	1.288 (18)
N(1)-C(2)	1.504 (17)
C(1)-C(2)	1.514 (19)
C(1)-O(2)	1.251 (18)
C(2)-C(3)	1.517 (19)
C(3)-C(4)	1.520 (22)
C(3)-C(5)	1.527 (23)
P(4)-F(1)	1.551 (18)
P(4)-F(2)	1.517 (21)
P(4)-F(3)	1.527 (19)
P(4)-F(4)	1.538 (18)
P(4)-F(5)	1.557 (14)
P(4)-F(6)	1.548 (14)

Table 3. Bond angles (°)

P(1)-Ir(1)-P(2)	97.1(2)
P(1)-Ir(1)-P(3)	159.1(1)
P(2)-Ir(1)-P(3)	94.7(2)
P(1)-Ir(1)-O(1)	86.1(3)
P(2)-Ir(1)-O(1)	175.0(3)
P(3)-Ir(1)-O(1)	83.5(3)
P(1)-Ir(1)-N(1)	99.3(3)
P(2)-Ir(1)-N(1)	98.0(3)
P(3)-Ir(1)-N(1)	96.1(3)
O(1)-Ir(1)-N(1)	77.6(4)
Ir(1)-P(1)-C(11)	122.9(6)
Ir(1)-P(1)-C(12)	110.6(7)
C(11)-P(1)-C(12)	102.4(9)
Ir(1)-P(1)-C(13)	115.0(7)
C(11)-P(1)-C(13)	102.4(9)
C(12)-P(1)-C(13)	100.8(9)
Ir(1)-P(2)-C(21)	111.6(6)
Ir(1)-P(2)-C(22)	118.1(6)
C(21)-P(2)-C(22)	103.5(8)
Ir(1)-P(2)-C(23)	119.4(6)
C(21)-P(2)-C(23)	101.1(9)
C(22)-P(2)-C(23)	100.7(9)
Ir(1)-P(3)-C(31)	113.6(7)
Ir(1)-P(3)-C(32)	123.4(7)
C(31)-P(3)-C(32)	97.1(10)
Ir(1)-P(3)-C(33)	111.1(7)
C(31)-P(3)-C(33)	104.7(11)
C(32)-P(3)-C(33)	104.6(10)
Ir(1)-O(1)-C(1)	116.0(8)
Ir(1)-N(1)-C(2)	110.3(7)
O(1)-C(1)-C(2)	120.8(12)
O(1)-C(1)-O(2)	120.6(12)
C(2)-C(1)-O(2)	118.5(13)
N(1)-C(2)-C(1)	108.4(11)
N(1)-C(2)-C(3)	115.4(11)
C(1)-C(2)-C(3)	113.7(11)
C(2)-C(3)-C(4)	114.0(12)
C(2)-C(3)-C(5)	112.4(12)
C(4)-C(3)-C(5)	110.5(13)
F(1)-P(4)-F(2)	87.3(11)
F(1)-P(4)-F(3)	178.0(10)
F(2)-P(4)-F(3)	94.1(11)
F(1)-P(4)-F(4)	93.2(10)
F(2)-P(4)-F(4)	178.8(11)
F(3)-P(4)-F(4)	85.4(10)
F(1)-P(4)-F(5)	89.4(9)
F(2)-P(4)-F(5)	89.1(10)
F(3)-P(4)-F(5)	89.2(9)
F(4)-P(4)-F(5)	89.8(9)
F(1)-P(4)-F(6)	90.8(9)
F(2)-P(4)-F(6)	90.4(10)
F(3)-P(4)-F(6)	90.6(9)

F(4)-P(4)-F(6) 90.7(9)
 F(5)-P(4)-F(6) 179.4(7)

Table 4. Anisotropic displacement coefficients ($\text{\AA}^2 \times 10^3$)

	U ₁₁	U ₂₂	U ₃₃	U ₁₂	U ₁₃	U ₂₃
Ir(1)	47(1)	35(1)	47(1)	1(1)	1(1)	-5(1)
P(1)	57(3)	52(2)	51(2)	-1(2)	9(2)	-5(2)
P(2)	63(3)	42(2)	58(2)	5(2)	1(2)	-1(2)
P(3)	54(3)	49(2)	78(3)	-9(2)	-1(2)	-7(2)
O(1)	58(6)	51(7)	50(6)	5(5)	-10(5)	-3(5)
N(1)	48(7)	53(7)	37(6)	0(6)	4(5)	2(5)
C(1)	26(7)	51(9)	60(9)	3(7)	-9(6)	17(7)
C(2)	35(8)	46(8)	50(7)	-4(6)	-5(6)	12(6)
C(3)	45(9)	51(9)	58(8)	22(7)	0(7)	-3(7)
C(4)	91(14)	71(12)	69(10)	51(10)	19(10)	2(9)
C(5)	102(15)	44(10)	110(14)	28(9)	-35(11)	-23(9)
O(2)	73(8)	60(7)	67(7)	11(6)	-14(6)	2(5)
C(11)	89(14)	111(16)	73(11)	-31(12)	23(10)	-33(11)
C(12)	96(15)	113(16)	70(12)	-12(12)	11(10)	27(11)
C(13)	118(17)	80(14)	96(14)	9(12)	54(13)	-15(11)
C(21)	87(13)	49(10)	79(11)	22(9)	-3(9)	6(8)
C(22)	86(14)	63(12)	99(14)	4(10)	-11(11)	-5(10)
C(23)	49(10)	91(14)	98(13)	7(9)	0(9)	30(11)
C(31)	45(11)	103(16)	178(22)	-9(10)	43(12)	13(14)
C(32)	102(16)	82(14)	114(16)	-19(12)	17(13)	11(12)
C(33)	67(14)	182(25)	146(21)	-43(15)	10(13)	-62(18)
P(4)	68(3)	69(3)	62(3)	8(2)	6(2)	0(2)
F(1)	215(18)	155(13)	183(15)	94(12)	125(13)	65(11)
F(2)	181(17)	207(19)	254(21)	64(15)	-129(16)	-81(16)
F(3)	295(23)	148(13)	163(16)	-9(14)	142(17)	14(11)
F(4)	156(14)	172(15)	202(18)	-19(11)	-87(12)	-34(12)
F(5)	213(16)	91(9)	137(11)	74(10)	-4(11)	-18(8)
F(6)	223(17)	69(8)	139(11)	50(9)	15(11)	12(7)

The anisotropic displacement exponent takes the form: $-2\pi^2(h^2a^2U_{11} + \dots + 2hka^*b^*U_{12})$

Table 5. H-Atom coordinates ($\times 10^4$) and isotropic displacement coefficients ($\text{\AA}^2 \times 10^3$)

	x	y	z	U
H(1A)	1194	2450	-207	80
H(1B)	211	2224	-61	80
H(2A)	484	1156	950	80
H(3A)	1690	203	547	80
H(4A)	2724	546	-638	80
H(4B)	2315	1559	-695	80
H(4C)	2868	1242	190	80
H(5A)	1219	-158	-964	80
H(5B)	360	18	-313	80
H(5C)	696	803	-994	80

H(11A)	-1882	1910	2192	80
H(11B)	-1783	2353	1202	80
H(11C)	-1144	1514	1492	80
H(12A)	-621	2040	3497	80
H(12B)	261	1768	2913	80
H(12C)	252	2698	3486	80
H(13A)	-1768	3451	3063	80
H(13B)	-899	4116	3089	80
H(13C)	-1576	4134	2234	80
H(21A)	-444	4641	-1262	80
H(21B)	591	4369	-1032	80
H(21C)	-183	3596	-1068	80
H(22A)	-571	5997	45	80
H(22B)	-295	5846	1088	80
H(22C)	478	5848	317	80
H(23A)	-1818	4735	-56	80
H(23B)	-1690	3670	160	80
H(23C)	-1750	4392	976	80
H(31A)	3532	3778	530	80
H(31B)	3072	3127	1276	80
H(31C)	2851	2980	219	80
H(32A)	2827	5106	-305	80
H(32B)	2111	4451	-807	80
H(32C)	1764	5365	-318	80
H(33A)	2953	5305	1516	80
H(33B)	1897	5474	1746	80
H(33C)	2457	4700	2278	80

STRUCTURE DETERMINATION SUMMARY OF [Ir(COD)(DMPE)]Cl rearranged product

Crystal Data

Empirical Formula	C ₁₄ H ₂₈ ClIrP ₂
Color; Habit	Clear irregular prism
Crystal Size (mm)	0.2 x 0.3 x 0.4
Crystal System	Monoclinic
Space Group	P2 ₁ /m
Unit Cell Dimensions	a = 7.100(2) Å b = 15.295(5) Å c = 8.784(4) Å β = 112.72(3)°
Volume	880.0(5) Å ³
Z	2
Formula Weight	486.0
Density(calc.)	1.834 Mg/m ³
Absorption Coefficient	7.904 mm ⁻¹
F(000)	472
Data Collection	
Diffractionmeter Used	Siemens R3m/V
Radiation	MoKα (λ = 0.71073 Å)
Temperature (K)	298
Monochromator	Highly oriented graphite crystal
2θ Range	3.5 to 55.0°
Scan Type	Wyckoff
Scan Speed	Variable; 3.91 to 19.53°/min. in ω
Scan Range (ω)	0.60°
Background Measurement	Stationary crystal and stationary counter at beginning and end of scan, each for 25.0% of total scan time
Standard Reflections	3 measured every 300 reflections
Index Ranges	0 ≤ h ≤ 9, 0 ≤ k ≤ 19, -11 ≤ l ≤ 10
Reflections Collected	1930
Independent Reflections	1791 (R _{int} = 2.44%)
Observed Reflections	1536 (F > 3.0σ(F))
Absorption Correction	Semi-empirical
Min./Max. Transmission	0.0977 / 0.5595
Solution and Refinement	
System Used	Siemens SHELXTL PLUS (VMS)
Solution	Direct Methods
Refinement Method	Full-Matrix Least-Squares
Quantity Minimized	Σw(F _o -F _c) ²
Extinction Correction	χ = -0.00003(11), where F* = F [1 + 0.002χF ² /sin(2θ)] ^{-1/4}
Hydrogen Atoms	Riding model, fixed isotropic U
Weighting Scheme	w ⁻¹ = σ ² (F) + 0.0003F ²
Number of Parameters Refined	89
Final R Indices (obs. data)	R = 4.77 %, wR = 5.61 %
R Indices (all data)	R = 5.58 %, wR = 5.71 %
Goodness-of-Fit	2.13
Largest and Mean Δ/σ	0.266, 0.005

Data-to-Parameter Ratio
 Largest Difference Peak
 Largest Difference Hole

17.3:1
 1.39 eÅ⁻³
 -1.15 eÅ⁻³

Table 1. Atomic coordinates ($\times 10^4$) and equivalent isotropic displacement coefficients ($\text{\AA}^2 \times 10^3$)

	x	y	z	U(eq)
Ir(1)	1897(1)	2500	5629(1)	60(1)
Cl(1)	-332(6)	2500	7282(6)	164(4)
P(1)	3833(4)	3499(2)	7491(3)	69(1)
C(1)	3696(18)	2500	4246(15)	66(5)
C(2)	3312(16)	3362(8)	3206(14)	90(5)
C(3)	1047(18)	3562(12)	2376(16)	115(7)
C(4)	-102(15)	3296(12)	3529(13)	106(6)
C(5)	-983(22)	2500	3608(27)	126(12)
C(11)	2516(26)	4335(14)	8039(28)	218(16)
C(12)	5837(23)	4102(10)	7133(20)	137(10)
C(13)	5308(21)	2944(10)	9361(15)	124(6)

* Equivalent isotropic U defined as one third of the trace of the orthogonalized U_{ij} tensor

Table 2. Bond lengths (\AA)

Ir(1)-Cl(1)	2.527 (6)
Ir(1)-P(1)	2.272 (3)
Ir(1)-C(1)	2.076 (15)
Ir(1)-C(4)	2.209 (13)
Ir(1)-C(5)	2.128 (15)
Ir(1)-P(1A)	2.272 (3)
Ir(1)-C(4A)	2.209 (13)
P(1)-C(11)	1.758 (23)
P(1)-C(12)	1.822 (18)
P(1)-C(13)	1.785 (12)
C(1)-C(2)	1.566 (14)
C(1)-C(2A)	1.566 (14)
C(2)-C(3)	1.519 (16)
C(3)-C(4)	1.580 (21)
C(4)-C(5)	1.383 (19)
C(5)-C(4A)	1.383 (19)
C(13)-C(13A)	1.357 (29)

Table 3. Bond angles ($^\circ$)

Cl(1)-Ir(1)-P(1)	85.7(1)
Cl(1)-Ir(1)-C(1)	179.3(3)
P(1)-Ir(1)-C(1)	94.8(2)
Cl(1)-Ir(1)-C(4)	97.9(3)
P(1)-Ir(1)-C(4)	104.2(4)
C(1)-Ir(1)-C(4)	81.6(4)

Cl(1)-Ir(1)-C(5)	82.3(6)
P(1)-Ir(1)-C(5)	136.1(2)
C(1)-Ir(1)-C(5)	97.0(7)
C(4)-Ir(1)-C(5)	37.1(5)
Cl(1)-Ir(1)-P(1A)	85.7(1)
P(1)-Ir(1)-P(1A)	84.5(1)
C(1)-Ir(1)-P(1A)	94.8(2)
C(4)-Ir(1)-P(1A)	170.8(4)
C(5)-Ir(1)-P(1A)	136.1(2)
Cl(1)-Ir(1)-C(4A)	97.9(3)
P(1)-Ir(1)-C(4A)	170.8(4)
C(1)-Ir(1)-C(4A)	81.6(4)
C(4)-Ir(1)-C(4A)	66.9(8)
C(5)-Ir(1)-C(4A)	37.1(5)
P(1A)-Ir(1)-C(4A)	104.2(4)
Ir(1)-P(1)-C(11)	116.6(6)
Ir(1)-P(1)-C(12)	120.8(5)
C(11)-P(1)-C(12)	102.3(9)
Ir(1)-P(1)-C(13)	108.6(5)
C(11)-P(1)-C(13)	106.2(9)
C(12)-P(1)-C(13)	100.4(7)
Ir(1)-C(1)-C(2)	109.5(7)
Ir(1)-C(1)-C(2A)	109.5(7)
C(2)-C(1)-C(2A)	114.6(12)
C(1)-C(2)-C(3)	111.4(11)
C(2)-C(3)-C(4)	110.7(10)
Ir(1)-C(4)-C(3)	110.7(7)
Ir(1)-C(4)-C(5)	68.3(9)
C(3)-C(4)-C(5)	127.9(16)
Ir(1)-C(5)-C(4)	74.6(7)
Ir(1)-C(5)-C(4A)	74.6(7)
C(4)-C(5)-C(4A)	123.5(18)
P(1)-C(13)-C(13A)	118.4(5)

Table 4. Anisotropic displacement coefficients ($\text{\AA}^2 \times 10^3$)

	U ₁₁	U ₂₂	U ₃₃	U ₁₂	U ₁₃	U ₂₃
Ir(1)	36(1)	101(1)	43(1)	0	15(1)	0
Cl(1)	52(2)	374(11)	76(3)	0	35(2)	0
P(1)	65(1)	83(2)	59(1)	12(1)	25(1)	-9(1)
C(1)	43(5)	113(11)	41(6)	0	15(4)	0
C(2)	96(7)	115(9)	72(6)	21(7)	45(6)	38(7)
C(3)	99(8)	169(14)	79(8)	40(9)	35(7)	40(9)
C(4)	63(6)	193(15)	53(5)	44(7)	13(5)	4(8)
C(5)	36(7)	240(29)	83(13)	0	1(7)	0
C(11)	130(13)	279(28)	214(27)	56(17)	33(15)	-147(24)
C(12)	198(17)	105(10)	129(15)	-68(11)	86(13)	-16(10)
C(13)	148(10)	121(10)	55(6)	-36(8)	-16(7)	5(6)

The anisotropic displacement factor exponent takes the form: $-2\pi^2(h^2a^2U_{11} + \dots + 2hka^*b^*U_{12})$

Table 5. H-Atom coordinates ($\times 10^4$) and isotropic displacement coefficients ($\text{\AA}^2 \times 10^3$)

	x	y	z	U
H(1A)	5096	2500	5008	80
H(2A)	3853	3295	2366	80
H(2B)	4007	3841	3902	80
H(3A)	456	3234	1371	80
H(3B)	853	4172	2101	80
H(4A)	-670	3793	3868	80
H(5A)	-2174	2500	3872	80
H(11A)	3489	4719	8812	80
H(11B)	1608	4669	7125	80
H(11C)	1746	4040	8573	80
H(12A)	6466	4479	8066	80
H(12B)	6853	3726	7011	80
H(12C)	5220	4448	6154	80
H(13A)	4867	3137	10210	80
H(13C)	6692	3137	9665	80

STRUCTURE DETERMINATION SUMMARY OF [Ir(thiourea)(H)(PMe₃)₃]PF₆**Crystal Data**

Empirical Formula	C ₁₀ H ₃₁ F ₆ IrN ₂ P ₄ S
Color; Habit	clear orange plates
Crystal size (mm)	0.2 x 0.4 x 0.4
Crystal System	Monoclinic
Space Group	Cc
Unit Cell Dimensions	a = 12.834(4) Å b = 15.287(4) Å c = 13.433(4) Å β = 117.800(0)°
Volume	2331.4(12) Å ³
Z	4
Formula weight	641.5
Density(calc.)	1.828 Mg/m ³
Absorption Coefficient	6.134 mm ⁻¹
F(000)	1248
Data Collection	
Diffractometer Used	Siemens R3m/V
Radiation	MoK _α (λ = 0.71073 Å)
Temperature (K)	298
Monochromator	Highly oriented graphite crystal
2θ Range	3.5 to 45.0°
Scan Type	Wyckoff
Scan Speed	Variable; 6.00 to 20.00°/min. in ω
Scan Range (ω)	1.00°
Background Measurement	Stationary crystal and stationary counter at beginning and end of scan, each for 0.5% of total scan time
Standard Reflections	2 measured every 300 reflections
Index Ranges	0 ≤ h ≤ 13, 0 ≤ k ≤ 16, -14 ≤ l ≤ 12
Reflections Collected	1615
Independent Reflections	1615 (R _{int} = 0.00%)
Observed Reflections	1188 (F > 2.0σ(F))
Solution and Refinement	
System Used	Siemens SHELXTL PLUS (PC Version)
Solution	Direct Methods
Refinement Method	Full-Matrix Least-Squares
Quantity Minimized	Σw(F _o -F _c) ²
Absolute Structure	η = 1.17(10)
Extinction Correction	χ = 0.000048(8), where F* = F [1 + 0.002χF ² /sin(2θ)] ^{-1/4} Riding model, fixed isotropic U
Hydrogen Atoms	w ⁻¹ = σ ² (F) + 0.0001F ²
Weighting Scheme	142
Number of Parameters Refined	R = 5.40 %, wR = 4.05 %
Final R Indices (obs. data)	R = 7.59 %, wR = 4.24 %
R Indices (all data)	0.93
Goodness-of-Fit	0.295, 0.035
Largest and Mean Δ/σ	8.4:1
Data-to-Parameter Ratio	

Largest Difference Peak
Largest Difference Hole

1.57 eÅ⁻³
-1.62 eÅ⁻³

Table 1. Atomic coordinates ($\times 10^4$) and equivalent isotropic displacement coefficients ($\text{\AA}^2 \times 10^3$)

	x	y	z	U(eq)
Ir(1)	2810	974(1)	176	42(1)
P(1)	4352(10)	228(7)	275(8)	60(5)
P(2)	3090(10)	2281(7)	-639(9)	66(6)
P(3)	1424(9)	302(6)	-1383(7)	46(5)
S(1)	3728(9)	1742(6)	2005(7)	56(5)
N(1)	1584(26)	1558(21)	593(24)	68(19)
C(1)	2241(36)	1917(22)	1564(34)	56(25)
N(2)	1817(27)	2389(18)	2145(23)	78(18)
C(11)	4898(30)	377(22)	-750(26)	84(12)
C(12)	5740(30)	467(23)	1552(26)	94(13)
C(13)	4211(31)	-961(24)	238(29)	96(11)
C(21)	2231(27)	3207(21)	-531(26)	82(12)
C(22)	2858(35)	2324(27)	-2073(29)	89(14)
C(23)	4516(29)	2725(24)	42(29)	96(14)
C(31)	957(30)	-706(21)	-1099(27)	90(13)
C(32)	79(24)	940(24)	-2039(24)	74(10)
C(33)	1667(28)	51(20)	-2581(24)	60(10)
P(4)	3245(10)	6394(9)	170(11)	70(7)
F(1)	4233(20)	6723(15)	1247(19)	105(8)
F(2)	2761(34)	5784(22)	848(28)	142(13)
F(3)	2234(23)	5960(19)	-949(19)	114(9)
F(4)	3730(19)	6872(14)	-536(18)	95(7)
F(5)	2460(29)	7123(22)	235(27)	164(15)
F(6)	4212(26)	5648(16)	321(22)	140(10)

* Equivalent isotropic U defined as one third of the trace of the orthogonalized U_{ij} tensor

Table 2. Bond lengths (\AA)

Ir(1)-P(1)	2.234 (13)
Ir(1)-P(2)	2.385 (12)
Ir(1)-P(3)	2.266 (8)
Ir(1)-S(1)	2.470 (9)
Ir(1)-N(1)	2.100 (37)
P(1)-C(11)	1.826 (46)
P(1)-C(12)	1.844 (28)
P(1)-C(13)	1.824 (38)
P(2)-C(21)	1.842 (38)
P(2)-C(22)	1.808 (43)
P(2)-C(23)	1.756 (35)
P(3)-C(31)	1.759 (37)
P(3)-C(32)	1.813 (31)
P(3)-C(33)	1.817 (39)
S(1)-C(1)	1.735 (45)

N(1)-C(1)	1.299	(45)
C(1)-N(2)	1.349	(62)
P(4)-F(1)	1.497	(22)
P(4)-F(2)	1.615	(47)
P(4)-F(3)	1.602	(25)
P(4)-F(4)	1.541	(32)
P(4)-F(5)	1.532	(40)
P(4)-F(6)	1.626	(33)

Table 3. Bond angles (°)

P(1)-Ir(1)-P(2)	97.8	(5)
P(1)-Ir(1)-P(3)	96.6	(4)
P(2)-Ir(1)-P(3)	100.2	(3)
P(1)-Ir(1)-S(1)	100.7	(3)
P(2)-Ir(1)-S(1)	87.4	(4)
P(3)-Ir(1)-S(1)	160.0	(4)
P(1)-Ir(1)-N(1)	162.7	(8)
P(2)-Ir(1)-N(1)	93.4	(10)
P(3)-Ir(1)-N(1)	94.4	(8)
S(1)-Ir(1)-N(1)	66.5	(7)
Ir(1)-P(1)-C(11)	122.2	(11)
Ir(1)-P(1)-C(12)	113.5	(14)
C(11)-P(1)-C(12)	97.6	(18)
Ir(1)-P(1)-C(13)	115.7	(15)
C(11)-P(1)-C(13)	99.9	(19)
C(12)-P(1)-C(13)	105.3	(15)
Ir(1)-P(2)-C(21)	112.6	(14)
Ir(1)-P(2)-C(22)	122.3	(14)
C(21)-P(2)-C(22)	104.4	(18)
Ir(1)-P(2)-C(23)	115.4	(13)
C(21)-P(2)-C(23)	100.3	(17)
C(22)-P(2)-C(23)	98.9	(21)
Ir(1)-P(3)-C(31)	113.4	(10)
Ir(1)-P(3)-C(32)	111.3	(11)
C(31)-P(3)-C(32)	103.5	(17)
Ir(1)-P(3)-C(33)	122.0	(11)
C(31)-P(3)-C(33)	102.9	(17)
C(32)-P(3)-C(33)	101.6	(15)
Ir(1)-S(1)-C(1)	78.2	(14)
Ir(1)-N(1)-C(1)	103.4	(28)
S(1)-C(1)-N(1)	111.9	(37)
S(1)-C(1)-N(2)	124.1	(26)
N(1)-C(1)-N(2)	124.0	(38)
F(1)-P(4)-F(2)	91.4	(17)
F(1)-P(4)-F(3)	175.1	(16)
F(2)-P(4)-F(3)	86.2	(17)
F(1)-P(4)-F(4)	91.8	(15)
F(2)-P(4)-F(4)	173.1	(19)
F(3)-P(4)-F(4)	90.1	(15)
F(1)-P(4)-F(5)	89.1	(16)
F(2)-P(4)-F(5)	87.3	(22)
F(3)-P(4)-F(5)	95.1	(16)
F(4)-P(4)-F(5)	98.9	(19)

F(1)-P(4)-F(6)	82.1(14)
F(2)-P(4)-F(6)	89.8(20)
F(3)-P(4)-F(6)	93.6(15)
F(4)-P(4)-F(6)	84.6(17)
F(5)-P(4)-F(6)	170.6(16)

Table 4. Anisotropic displacement coefficients ($\text{\AA}^2 \times 10^3$)

	U ₁₁	U ₂₂	U ₃₃	U ₁₂	U ₁₃	U ₂₃
Ir(1)	53(1)	39(1)	37(1)	-6(2)	24(1)	-2(2)
P(1)	52(7)	66(8)	60(6)	-8(6)	24(6)	-7(6)
P(2)	60(8)	71(8)	54(7)	-22(7)	14(7)	14(6)
P(3)	43(6)	52(6)	35(5)	-6(5)	12(5)	-5(5)
S(1)	52(7)	70(7)	48(6)	-11(6)	25(6)	-5(5)
N(1)	52(24)	110(29)	57(22)	-22(20)	39(20)	19(21)
C(1)	88(37)	39(25)	70(28)	-17(24)	60(31)	3(23)
N(2)	85(25)	104(26)	68(20)	-29(21)	55(20)	-41(20)
P(4)	48(10)	110(10)	38(6)	-8(7)	10(8)	23(8)

The anisotropic displacement exponent takes the form: $-2\pi^2(h^2a^*2U_{11} + \dots + 2hka^*b^*U_{12})$

Table 5. H-Atom coordinates ($\times 10^4$) and isotropic displacement coefficients ($\text{\AA}^2 \times 10^3$)

	x	y	z	U
H(1A)	797	1600	177	80
H(2A)	2341	2621	2805	80
H(2B)	1041	2474	1893	80
H(11A)	5553	-10	-562	80
H(11B)	4290	247	-1496	80
H(11C)	5151	971	-720	80
H(12A)	6380	131	1568	80
H(12B)	5912	1079	1562	80
H(12C)	5640	325	2198	80
H(13A)	4915	-1221	288	80
H(13B)	4082	-1168	846	80
H(13C)	3552	-1118	-466	80
H(21A)	2377	3717	-862	80
H(21B)	1407	3065	-921	80
H(21C)	2458	3320	247	80
H(22A)	3004	2905	-2247	80
H(22B)	3403	1925	-2134	80
H(22C)	2067	2155	-2592	80
H(23A)	4524	3250	-346	80
H(23B)	4739	2860	813	80
H(23C)	5062	2312	10	80
H(31A)	368	-985	-1764	80
H(31B)	1647	-1069	-765	80
H(31C)	657	-622	-572	80
H(32A)	-502	646	-2694	80
H(32B)	-219	1023	-1510	80
H(32C)	255	1499	-2252	80
H(33A)	982	-236	-3151	80
H(33B)	1804	584	-2879	80
H(33C)	2338	-327	-2351	80

STRUCTURE DETERMINATION SUMMARY OF [Ir(thioacetamide)(H)(PMe₃)₃]PF₆**Crystal Data**

Empirical Formula C₁₁H₃₃F₆IrNP₄S
 Color; Habit Clear orange rectangular prism
 Crystal size (mm) 0.3 x 0.3 x 0.4
 Crystal System Orthorhombic
 Space Group Pnma
 Unit Cell Dimensions a = 13.299(3) Å
 b = 12.002(4) Å
 c = 14.958(4) Å

Volume 2387.5(11) Å³

Z 4

Formula weight 641.5

Density(calc.) 1.785 Mg/m³

Absorption Coefficient 5.989 mm⁻¹

F(000) 1252

Data Collection

Diffractometer Used Siemens R3m/V

Radiation MoK_α (λ = 0.71073 Å)

Temperature (K) 298

Monochromator Highly oriented graphite crystal

2θ Range 3.5 to 50.0°

Scan Type ω

Scan Speed Variable; 7.32 to 29.30°/min. in ω

Scan Range (ω) 1.00°

Background Measurement Stationary crystal and stationary counter at beginning and end of scan, each for 0.5% of total scan time

Standard Reflections 2 measured every 300 reflections

Index Ranges 0 ≤ h ≤ 15, 0 ≤ k ≤ 14, -17 ≤ l ≤ 0

Reflections Collected 2200

Independent Reflections 2200 (R_{int} = 0.00%)

Observed Reflections 1356 (F > 3.0σ(F))

Solution and Refinement

System Used Siemens SHELXTL PLUS (PC Version)

Solution Direct Methods

Refinement Method Full-Matrix Least-Squares

Quantity Minimized Σw(F_o-F_c)²

Extinction Correction χ = 0.00096(5), where

F* = F [1 + 0.002χF²/sin(2θ)]^{-1/4}

Riding model, fixed isotropic U

w⁻¹ = σ²(F) + 0.0001F²

Number of Parameters Refined 111

Final R Indices (obs. data) R = 4.66 %, wR = 4.85 %

R Indices (all data) R = 8.00 %, wR = 5.07 %

Goodness-of-Fit 1.39

Largest and Mean Δ/σ 0.371, 0.025

Data-to-Parameter Ratio 12.2:1

Largest Difference Peak 1.62 eÅ⁻³

Largest Difference Hole -1.06 eÅ⁻³

Table 1. Atomic coordinates ($\times 10^4$) and equivalent isotropic displacement coefficients ($\text{\AA}^2 \times 10^{-3}$)

	x	y	z	U(eq)
Ir(1)	2961(1)	2500	3316(1)	38(1)
S(1)	4597(4)	2500	4123(4)	63(3)
N(1)	2855(13)	2500	4734(11)	45(7)
C(1)	3718(20)	2500	4981(19)	48(9)
C(2)	3963(20)	2500	5903(25)	161(27)
P(1)	2742(3)	576(3)	3408(3)	54(2)
P(2)	3478(5)	2500	1873(4)	54(3)
C(11)	3839(14)	-277(14)	3585(14)	103(10)
C(12)	1935(14)	217(14)	4330(12)	89(8)
C(13)	2093(15)	-107(15)	2491(12)	92(8)
C(21)	2539(17)	2500	1038(17)	84(12)
C(22)	4291(13)	1342(16)	1582(12)	105(9)
P(4)	5290(6)	2500	-1312(5)	66(3)
F(1)	5071(28)	2500	-2329(33)	310(19)
F(2)	4135(15)	2500	-1037(15)	145(8)
F(3)	5582(24)	2500	-332(27)	268(16)
F(4)	6409(19)	2500	-1463(17)	177(9)
F(5)	5234(16)	1253(21)	-1291(15)	236(9)

* Equivalent isotropic U defined as one third of the trace of the orthogonalized U_{ij} tensor

Table 2. Bond lengths (\AA)

Ir(1)-S(1)	2.487 (6)
Ir(1)-N(1)	2.126 (17)
Ir(1)-P(1)	2.332 (4)
Ir(1)-P(2)	2.266 (7)
Ir(1)-P(1A)	2.332 (4)
S(1)-C(1)	1.736 (28)
N(1)-C(1)	1.206 (32)
C(1)-C(2)	1.417 (46)
P(1)-C(11)	1.802 (18)
P(1)-C(12)	1.800 (18)
P(1)-C(13)	1.815 (19)
P(2)-C(21)	1.766 (25)
P(2)-C(22)	1.814 (19)
P(2)-C(22A)	1.814 (19)
P(4)-F(1)	1.548 (50)
P(4)-F(2)	1.590 (22)
P(4)-F(3)	1.517 (41)
P(4)-F(4)	1.505 (27)
P(4)-F(5)	1.499 (25)
P(4)-F(5A)	1.499 (25)

Table 3. Bond angles (°)

S(1)-Ir(1)-N(1)	64.8(5)
S(1)-Ir(1)-P(1)	94.6(1)
N(1)-Ir(1)-P(1)	86.2(1)
S(1)-Ir(1)-P(2)	101.4(2)
N(1)-Ir(1)-P(2)	166.2(5)
P(1)-Ir(1)-P(2)	95.4(1)
S(1)-Ir(1)-P(1A)	94.6(1)
N(1)-Ir(1)-P(1A)	86.2(1)
P(1)-Ir(1)-P(1A)	164.1(2)
P(2)-Ir(1)-P(1A)	95.4(1)
Ir(1)-S(1)-C(1)	76.7(9)
Ir(1)-N(1)-C(1)	104.0(17)
S(1)-C(1)-N(1)	114.5(21)
S(1)-C(1)-C(2)	124.4(20)
N(1)-C(1)-C(2)	121.1(25)
Ir(1)-P(1)-C(11)	118.0(6)
Ir(1)-P(1)-C(12)	110.9(6)
C(11)-P(1)-C(12)	103.5(9)
Ir(1)-P(1)-C(13)	117.5(6)
C(11)-P(1)-C(13)	103.9(9)
C(12)-P(1)-C(13)	100.8(8)
Ir(1)-P(2)-C(21)	117.3(8)
Ir(1)-P(2)-C(22)	114.1(6)
C(21)-P(2)-C(22)	104.6(8)
Ir(1)-P(2)-C(22A)	114.1(6)
C(21)-P(2)-C(22A)	104.6(8)
C(22)-P(2)-C(22A)	100.0(12)
F(1)-P(4)-F(2)	94.2(17)
F(1)-P(4)-F(3)	176.0(20)
F(2)-P(4)-F(3)	89.8(15)
F(1)-P(4)-F(4)	92.2(18)
F(2)-P(4)-F(4)	173.6(14)
F(3)-P(4)-F(4)	83.8(16)
F(1)-P(4)-F(5)	90.7(9)
F(2)-P(4)-F(5)	86.9(8)
F(3)-P(4)-F(5)	89.5(9)
F(4)-P(4)-F(5)	93.0(8)
F(1)-P(4)-F(5A)	90.7(9)
F(2)-P(4)-F(5A)	86.9(8)
F(3)-P(4)-F(5A)	89.5(9)
F(4)-P(4)-F(5A)	93.0(8)
F(5)-P(4)-F(5A)	173.7(17)

Table 4. Anisotropic displacement coefficients ($\text{\AA}^2 \times 10^3$)

	U ₁₁	U ₂₂	U ₃₃	U ₁₂	U ₁₃	U ₂₃
Ir(1)	38(1)	39(1)	39(1)	0	6(1)	0
S(1)	40(3)	90(6)	60(5)	0	-2(3)	0

N(1)	29(11)	59(12)	47(11)	0	7(10)	0
C(1)	52(16)	40(15)	54(17)	0	-16(14)	0
C(2)	64(22)	79(26)	339(74)	0	-88(33)	0
P(1)	66(3)	41(2)	54(3)	0(2)	8(3)	-3(2)
P(2)	52(4)	61(4)	48(5)	0	8(3)	0
C(11)	111(15)	46(11)	153(23)	36(12)	20(15)	8(14)
C(12)	125(16)	47(11)	95(14)	-40(13)	51(14)	-2(10)
C(13)	122(16)	62(12)	91(14)	-27(15)	42(15)	-21(12)
C(21)	70(17)	110(25)	71(21)	0	-3(16)	0
C(22)	120(16)	115(17)	79(14)	41(14)	91(14)	27(14)
P(4)	74(5)	63(5)	61(5)	0	-9(4)	0

The anisotropic displacement exponent takes the form: $-2\pi^2(h^2a^2U_{11} + \dots + 2hka*b*U_{12})$

Table 5. H-Atom coordinates (x104) and isotropic displacement coefficients ($\text{\AA}^2 \times 10^3$)

	x	y	z	U
H(1A)	2294	2500	5071	80
H(2A)	3356	2500	6250	80
H(2B)	4350	1847	6041	80
H(2C)	4350	3153	6041	80
H(11A)	3650	-1048	3609	80
H(11B)	4306	-165	3104	80
H(11C)	4148	-65	4139	80
H(12A)	1851	-577	4360	80
H(12B)	2229	480	4877	80
H(12C)	1292	564	4245	80
H(13A)	2047	-893	2602	80
H(13B)	1430	200	2435	80
H(13C)	2461	19	1948	80
H(21A)	2852	2500	460	80
H(21B)	2128	1847	1100	80
H(22A)	4482	1390	964	80
H(22B)	4882	1376	1950	80
H(22C)	3948	651	1686	80

STRUCTURE DETERMINATION SUMMARY OF [Ir(2-Amino-4-Pentenoic)(PMe₃)₃]Cl

Crystal Data

Empirical Formula C₁₅H₃₆Cl₄IrNO₂P₃
 Color; Habit orange flat plate
 Crystal Size (mm) 0.2 x 0.5 x 0.5
 Crystal System Monoclinic
 Space Group P2₁/c
 Unit Cell Dimensions a = 9.317(2) Å
 b = 17.028(5) Å
 c = 16.855(8) Å
 β = 102.91(3)°

Volume 2607(2) Å³
 Z 4

Formula Weight 689.4
 Density(calc.) 1.757 Mg/m³
 Absorption Coefficient 5.727 mm⁻¹
 F(000) 1356

Data Collection

Diffractometer Used Siemens R3m/V
 Radiation MoK_α (λ = 0.71073 Å)
 Temperature (K) 298
 Monochromator Highly oriented graphite crystal
 2θ Range 3.5 to 50.0°
 Scan Type Wyckoff
 Scan Speed Variable; 3.97 to 19.53°/min. in ω
 Scan Range (ω) 0.60°
 Background Measurement Stationary crystal and stationary counter at beginning and end of scan, each for 25.0% of total scan time

Standard Reflections 3 measured every 300 reflections
 Index Ranges 0 ≤ h ≤ 8, 0 ≤ k ≤ 20, -20 ≤ l ≤ 19
 Reflections Collected 4500
 Independent Reflections 4045 (R_{int} = 2.72%)
 Observed Reflections 3058 (F > 3.0σ(F))

Solution and Refinement

System Used Siemens SHELXTL PLUS (VMS)
 Solution Direct Methods
 Refinement Method Full-Matrix Least-Squares
 Quantity Minimized Σw(F_o-F_c)²
 Extinction Correction χ = 0.00006(3), where
 F* = F [1 + 0.002χF²/sin(2θ)]^{-1/4}
 Riding model, fixed isotropic U
 w⁻¹ = σ²(F) + 0.0010F²
 Hydrogen Atoms 236
 Weighting Scheme R = 4.60 %, wR = 5.24 %
 Number of Parameters Refined R = 6.65 %, wR = 5.64 %
 Final R Indices (obs. data) 1.09
 R Indices (all data) 0.697, 0.026
 Goodness-of-Fit 13.0:1
 Largest and Mean Δ/σ
 Data-to-Parameter Ratio

Largest Difference Peak
Largest Difference Hole

1.11 eÅ⁻³
-1.43 eÅ⁻³

Table 1. Atomic coordinates ($\times 10^4$) and equivalent isotropic displacement coefficients ($\text{\AA}^2 \times 10^3$)

	x	y	z	U(eq)
Ir(1)	760(1)	855(1)	7715(1)	36(1)
C(1)	-1505(13)	1204(8)	7483(7)	61(5)
C(2)	-1888(17)	1886(8)	7964(8)	78(6)
C(3)	-1504(14)	1735(7)	8872(7)	63(5)
C(4)	52(13)	1480(6)	9205(6)	45(4)
C(5)	1072(13)	2083(7)	8960(6)	46(4)
N(1)	332(10)	676(4)	8907(5)	40(3)
O(1)	1445(8)	1939(4)	8283(4)	45(3)
O(2)	1441(9)	2675(4)	9371(5)	63(3)
P(1)	-83(4)	-298(2)	7139(2)	49(1)
P(2)	1131(4)	1417(2)	6551(2)	55(1)
P(3)	3224(4)	405(2)	8212(2)	46(1)
C(11)	-1706(15)	-255(8)	6323(8)	83(6)
C(12)	-611(17)	-980(7)	7828(8)	79(6)
C(13)	1114(15)	-904(7)	6680(7)	64(5)
C(21)	1608(19)	855(8)	5736(7)	90(7)
C(22)	-370(18)	2006(9)	5996(8)	91(7)
C(23)	2623(17)	2126(7)	6747(8)	80(6)
C(31)	4513(14)	233(9)	7547(7)	73(6)
C(32)	3393(15)	-508(7)	8776(7)	67(5)
C(33)	4296(15)	1066(8)	8962(7)	69(5)
Cl(1)	2439(4)	330(2)	10652(2)	68(1)
Cl(3)	5279(13)	1660(5)	3726(10)	294(8)
Cl(2)	5428(12)	1022(7)	5044(11)	356(10)
Cl(1)	5678(22)	2237(20)	5535(15)	581(24)
C(20)	4778(30)	1897(14)	4584(14)	155(13)

* Equivalent isotropic U defined as one third of the trace of the orthogonalized U_{ij} tensor

Table 2. Bond lengths (\AA)

Ir(1)-C(1)	2.143 (12)
Ir(1)-N(1)	2.156 (9)
Ir(1)-O(1)	2.110 (6)
Ir(1)-P(1)	2.253 (3)
Ir(1)-P(2)	2.279 (3)
Ir(1)-P(3)	2.387 (3)
C(1)-C(2)	1.505 (19)
C(2)-C(3)	1.513 (18)
C(3)-C(4)	1.497 (17)
C(4)-C(5)	1.518 (16)
C(4)-N(1)	1.500 (13)
C(5)-O(1)	1.288 (14)

C(5)-O(2)	1.228	(13)
P(1)-C(11)	1.804	(13)
P(1)-C(12)	1.787	(15)
P(1)-C(13)	1.815	(14)
P(2)-C(21)	1.809	(14)
P(2)-C(22)	1.804	(15)
P(2)-C(23)	1.815	(15)
P(3)-C(31)	1.841	(15)
P(3)-C(32)	1.810	(12)
P(3)-C(33)	1.816	(12)
Cl(3)-Cl(2)	2.449	(23)
Cl(3)-C(20)	1.665	(30)
Cl(2)-Cl(1)	2.220	(35)
Cl(2)-C(20)	1.726	(27)
Cl(1)-C(20)	1.734	(33)

Table 3. Bond angles (°)

C(1)-Ir(1)-N(1)	80.2(4)
C(1)-Ir(1)-O(1)	91.5(4)
N(1)-Ir(1)-O(1)	78.5(3)
C(1)-Ir(1)-P(1)	85.9(3)
N(1)-Ir(1)-P(1)	99.2(2)
O(1)-Ir(1)-P(1)	176.8(2)
C(1)-Ir(1)-P(2)	93.4(4)
N(1)-Ir(1)-P(2)	163.3(2)
O(1)-Ir(1)-P(2)	86.3(2)
P(1)-Ir(1)-P(2)	95.7(1)
C(1)-Ir(1)-P(3)	169.6(3)
N(1)-Ir(1)-P(3)	89.5(2)
O(1)-Ir(1)-P(3)	87.3(2)
P(1)-Ir(1)-P(3)	95.0(1)
P(2)-Ir(1)-P(3)	96.8(1)
Ir(1)-C(1)-C(2)	117.2(8)
C(1)-C(2)-C(3)	112.4(11)
C(2)-C(3)-C(4)	114.8(12)
C(3)-C(4)-C(5)	108.3(9)
C(3)-C(4)-N(1)	111.4(8)
C(5)-C(4)-N(1)	111.1(10)
C(4)-C(5)-O(1)	114.9(9)
C(4)-C(5)-O(2)	121.0(10)
O(1)-C(5)-O(2)	124.0(11)
Ir(1)-N(1)-C(4)	105.4(6)
Ir(1)-O(1)-C(5)	117.0(7)
Ir(1)-P(1)-C(11)	116.5(5)
Ir(1)-P(1)-C(12)	114.0(4)
C(11)-P(1)-C(12)	102.5(7)
Ir(1)-P(1)-C(13)	119.4(4)
C(11)-P(1)-C(13)	100.8(6)
C(12)-P(1)-C(13)	101.1(6)
Ir(1)-P(2)-C(21)	122.9(4)
Ir(1)-P(2)-C(22)	115.5(6)
C(21)-P(2)-C(22)	101.2(7)
Ir(1)-P(2)-C(23)	112.3(4)

C(21)-P(2)-C(23)	100.5(7)
C(22)-P(2)-C(23)	101.4(7)
Ir(1)-P(3)-C(31)	123.0(4)
Ir(1)-P(3)-C(32)	115.1(5)
C(31)-P(3)-C(32)	101.0(7)
Ir(1)-P(3)-C(33)	112.4(4)
C(31)-P(3)-C(33)	100.9(6)
C(32)-P(3)-C(33)	101.4(6)
Cl(2)-Cl(3)-C(20)	44.7(9)
Cl(3)-Cl(2)-Cl(1)	84.5(9)
Cl(3)-Cl(2)-C(20)	42.8(10)
Cl(1)-Cl(2)-C(20)	50.2(10)
Cl(2)-Cl(1)-C(20)	49.9(12)
Cl(3)-C(20)-Cl(2)	92.5(15)
Cl(3)-C(20)-Cl(1)	135.4(19)
Cl(2)-C(20)-Cl(1)	79.8(15)

Table 4. Anisotropic displacement coefficients ($\text{\AA}^2 \times 10^3$)

	U ₁₁	U ₂₂	U ₃₃	U ₁₂	U ₁₃	U ₂₃
Ir(1)	52(1)	30(1)	27(1)	1(1)	9(1)	-1(1)
C(1)	50(9)	71(8)	54(7)	17(7)	-2(6)	-12(6)
C(2)	83(11)	65(9)	76(9)	0(8)	-4(8)	-12(7)
C(3)	68(10)	59(8)	63(8)	16(7)	20(7)	-3(6)
C(4)	53(8)	46(6)	36(5)	8(6)	10(5)	-11(5)
C(5)	46(8)	51(7)	39(6)	0(6)	2(5)	-10(5)
N(1)	47(6)	37(5)	38(5)	0(4)	14(4)	-7(3)
O(1)	74(6)	26(3)	39(4)	-4(4)	18(4)	-2(3)
O(2)	79(6)	48(5)	62(5)	-10(4)	12(4)	-24(4)
P(1)	64(2)	40(2)	44(2)	-8(2)	13(1)	-8(1)
P(2)	91(3)	42(2)	35(1)	2(2)	20(2)	7(1)
P(3)	51(2)	47(2)	40(1)	4(1)	11(1)	-2(1)
C(11)	103(12)	67(9)	70(9)	-9(8)	2(8)	-37(7)
C(12)	113(13)	65(9)	67(9)	-25(8)	36(9)	-9(7)
C(13)	84(10)	49(7)	59(7)	-1(7)	18(7)	-21(6)
C(21)	172(16)	69(9)	41(7)	2(10)	50(9)	3(6)
C(22)	125(14)	76(10)	74(10)	19(10)	29(9)	39(8)
C(23)	140(14)	51(7)	56(8)	-19(8)	35(8)	0(6)
C(31)	76(11)	92(10)	56(7)	16(8)	24(7)	2(7)
C(32)	85(11)	50(7)	62(8)	15(7)	8(7)	12(6)
C(33)	75(10)	71(9)	58(7)	-7(7)	8(7)	-6(6)
Cl(1)	61(2)	97(3)	45(2)	-3(2)	8(1)	17(2)
Cl(3)	288(11)	183(9)	478(18)	0(8)	227(12)	-60(10)
Cl(2)	199(10)	220(11)	567(24)	8(8)	-91(12)	179(14)
Cl(1)	357(27)	823(53)	577(35)	117(30)	133(24)	-104(36)
C(20)	211(27)	135(19)	107(15)	73(18)	9(17)	14(14)

The anisotropic displacement factor exponent takes the form:

$$-2\pi^2(h^2a^2U_{11} + \dots + 2hka^*b^*U_{12})$$

Table 5. H-Atom coordinates ($\times 10^4$) and isotropic displacement coefficients ($\text{\AA}^2 \times 10^3$)

	x	y	z	U
H(1A)	-2055	759	7603	80
H(1C)	-1831	1308	6912	80
H(2A)	-2924	1986	7787	80
H(2B)	-1367	2344	7851	80
H(3A)	-2152	1333	8985	80
H(3B)	-1685	2200	9156	80
H(4A)	240	1462	9788	80
H(1B)	1107	446	9241	80
H(1D)	-463	367	8872	80
H(11A)	-1965	-777	6125	80
H(11B)	-2505	-31	6520	80
H(11C)	-1510	63	5889	80
H(12A)	-955	-1453	7537	80
H(12B)	232	-1096	8255	80
H(12C)	-1378	-765	8059	80
H(13A)	606	-1375	6464	80
H(13B)	1387	-615	6248	80
H(13C)	1982	-1040	7082	80
H(21A)	1711	1194	5296	80
H(21B)	2527	594	5949	80
H(21C)	859	471	5539	80
H(22A)	-103	2211	5518	80
H(22B)	-1248	1695	5838	80
H(22C)	-546	2432	6334	80
H(23A)	2752	2353	6247	80
H(23B)	2427	2534	7101	80
H(23C)	3503	1851	7006	80
H(31A)	5447	54	7859	80
H(31B)	4099	-159	7152	80
H(31C)	4647	712	7273	80
H(32A)	4419	-638	8947	80
H(32B)	2982	-442	9246	80
H(32C)	2885	-924	8443	80
H(33A)	5275	861	9143	80
H(33B)	4342	1578	8730	80
H(33C)	3833	1103	9415	80

VITA

The author was born in Concord, New Hampshire, on December 22, 1967, to Alfred and Marie Roy. He graduated from Essex Junction High School in the spring of 1985. In the fall of that year he entered the University of Vermont, where he was an IBM Watson Scholar and a Vermont Scholar. He received his B.S. in Chemistry in the spring of 1989. He began graduate studies in the fall of 1989 and after finding himself in 1990, joined the Merola group in the beginning of 1991.

Christopher F. Roy